SYNTHETIC HYDROGELS RECAPITULATE EPITHELIAL MORPHOGENESIS PROGRAMS

A Dissertation
Presented to
The Academic Faculty

by

Ricardo Cruz-Acuña

In Partial Fulfillment
of the Requirements for the Degree
Doctor of Philosophy in the
BioEngineering Interdisciplinary Program

Georgia Institute of Technology
August 2018

SYNTHETIC HYDROGELS RECAPITULATE EPITHELIAL MORPHOGENESIS PROGRAMS

Approved by:

Dr. Andrés J. García, Advisor
School of George W. Woodruff School of
Mechanical Engineering
Georgia Institute of Technology

Dr. Johnna S. Temenoff
Wallace H. Coulter Department of
Biomedical Engineering
Georgia Institute of Technology

Dr. Asma Nusrat
Department of Pathology
University of Michigan

Dr. Alberto Fernández-Nieves
School of Physics
Georgia Institute of Technology

Dr. Krishnendu Roy
Wallace H. Coulter Department of
Biomedical Engineering
Georgia Institute of Technology

Date Approved: 5/18/18

To my family, friends and beloved Puerto Rico

ACKNOWLEDGEMENTS

I would like to first start off with thanking my family for their continuous love, support and encouragement throughout my graduate training thus far. Thank you Mom, Dad, and Abu (grandma) for always giving me the freedom to seek opportunities even (and specially) when they have been far away from home. Your prayers and words of wisdom have been a guide along my road ahead. Thank you to my sister Melissa; my best friend and my confidant. I have no words to describe how essential you have always been in my life, my PhD journey, and in every stage in my life. Since we were kids you have always been the one I would look up to and the first person I run to for advice.

To my close friends, Arnaldo Negrón, Legna Figueroa, Ángel Santiago, Melanie Santos and Ricardo Bonilla. You have been there every day during my life at Georgia Tech making it all feel a little easier and bearable. I am incredibly grateful to you for all the time you have spent with me, all the complaints you had to listen to about my day to day life, and all the emotions you have shared with me during my time in Atlanta. You are my family away from home, and I will forever be grateful for the incredible support you have been.

To my advisor, Andrés, for being the best mentor I could have ever asked for. You have been a fantastic mentor, both personally and professionally, and what I have learned from you will continue to influence my own mentorship style throughout my career. You always provided me with anything I needed to complete my work, and most importantly, listened to me and took my opinions seriously. You have taught me to be critical and meticulous in my research work and to be persistent and to not give up easy. You have

always believed in me and motivated me to do my best, and always had my back as I endeavor in my PhD journey and future plans.

Thank you to my thesis committee and collaborators. You have been great advisors throughout my graduate training and have provided critical feedback to make this thesis better. Many thanks to Asma Nusrat for our collaboration and for welcoming me into your lab. We have been collaborating since day one, and since then you have been extremely supportive, an excellent host in Michigan, and always believed in our work.

A big thank you to everyone, past and present, in the Garcia Lab. You made my training a great experience, and I actually looked forward to coming into lab and working with you every day. I need to especially thank Woojin Han, Lina Mancipe and Rachit Agarwal for making my days in the lab very enjoyable. Our research discussions and your critical opinions about my work have definitely contributed to the development of my thesis. Thank you for sharing so many laughs and great talks during our frequent lunches together, hiking trips, nights out, coffee breaks, and just random breaks during the day.

Finally, and most importantly, many thanks to my beloved Puerto Rico, my beautiful home, and the University of Puerto Rico at Mayaguez, as you are the foundation of where I am today. I will forever be in debt and will always hold you in my heart, proudly, wherever I am.

TABLE OF CONTENTS

LIST OF TABLES

LIST OF FIGURES

LIST OF SYMBOLS AND ABBREVIATIONS

PEG   poly (ethylene glycol)

PEG-4MAL   4-arm poly(ethylene glycol) with terminal maleimide groups

ECM   extracellular matrix

RGD   GRGDSPC adhesive peptide

GFOGER   GYGGGP(GPP)5GFOGER(GPP)5GPC adhesive peptide

IKVAV   CGGAASIKVAVSADR adhesive peptide

YIGSR   CGGEGYGEGYIGSR adhesive peptide

RDG   GRDGSPC inactive scrambled peptide

GPQ-W   GCRDGPQGIWGQDRCG; MMP-sensitive crosslinking peptide

IPES   GCRDIPESLRAGDRCG; MT1-MMP-sensitive crosslinking peptide

DTT   1,4-dithiothreitol; non-degradable crosslinking agent

MMP   matrix metalloproteinase

MT1-MMP   membrane-type matrix metalloproteinase-1

hESC   human embryonic stem cell

hiPSC   human induced pluripotent stem cell

HO   human organoiod

HIO   human intestinal organoid

HLO   human lung organoid

EHS   Engelbreth-Holm-Swarm

IMCD   inner medullary collecting duct

MDCK   Madin-Darby canine kidney

HEPES	4-(2-hydroxyethyl)piperazine-1-ethanesulfonic acid buffer
NSG	NOD-scid IL2Rg-null mice
ISH	in situ hydridization
EdU	5-ethynyl-2′-deoxyuridine
CFTR	cystic fibrosis transmembrane conductance regulator
DAPI	4',6-Diamidino-2-Phenylindole
DMSO	dimethyl sulfoxide
G'	storage modulus
G"	loss modulus
ANOVA	analysis of variance
χ^2	chi-squared test
wt./vol.	weight per volume
IACUC	institutional animal care and use committee
USDA	U.S. Department of Agriculture
NIH	National Institutes of Health

SUMMARY

Understanding the contributions of the ECM biophysical and biochemical properties to epithelial cell responses has been a major goal for biomaterials scientists in order to engineer materials that can recapitulate ECM-mediated epithelial morphogenesis programs. Although 3D natural matrices have been found suitable for the study of many cellular processes, they are limited by lot-to-lot compositional and structural variability, inability to decouple mechanical and biochemical properties, and in some cases, their tumor-derived nature limits their clinical translational potential. Therefore, there is a significant need for a biomaterial matrix that can recapitulate epithelial morphogenetic programs while overcoming these limitations.

This project aims to develop an engineered synthetic hydrogel matrix that presents independently-tunable basement membrane-like bioactivity and mechanical properties, and can support epithelial cell survival, proliferation, polarization, and assembly into 3D multicellular structures recapitulating different epithelial morphogenesis program. This synthetic material has the capacity to present adhesive peptides and protease-degradable crosslinks that support cell functions and promote cell engraftment in vivo. As part of this project, we have developed an engineered synthetic hydrogel platform that recapitulates the morphogenetic program of human pluripotent stem cell (hPSC)-derived intestinal organoids (HIOs), and has been established as a delivery vehicle for HIOs to mucosal intestinal wounds in mice. Furthermore, in order to prove the versatility of our hydrogel platform, we aim to engineer a synthetic hydrogel that recapitulates the mouse inner medullary collecting duct (IMCD) cell morphogenetic program. We hypothesize that these

engineered hydrogels will be superior to naturally-derived materials by supporting these different epithelial morphogenetic programs while overcoming the imitations of natural and other synthetic materials. This synthetic hydrogel technology is significant as it allows the study of the independent contributions of ECM properties to different epithelial morphogenetic programs, and will form a basis for the adaptation to in vitro generation and in vivo delivery of human PSC-derived organoids for regenerative medicine.

CHAPTER 1.   INTRODUCTION AND SPECIFIC AIMS

1.1   Introduction

Cell-extracellular matrix (ECM) interactions transduce mechanical and biochemical signals that regulate epithelial morphogenesis[1-3]. Understanding these interactions has been a major goal for biomaterials scientists in order to engineer materials that can recapitulate complex ECM-mediated cellular responses[4]. Bissell, Mostov and others have pioneered the use of 3D collagen and laminin (i.e., Matrigel™) gels in organotypic cultures that recreate the epithelial morphogenetic developmental programs observed in the organism[5-7]. Although 3D natural matrices have been found suitable for the study of many cellular processes, they are limited by lot-to-lot compositional and structural variability[8] which decreases their reliability. Additionally, these matrices are limited by the inability to decouple mechanical and biochemical properties. Furthermore, as Matrigel™ is a tumor-derived matrix, its clinical translational potential is limited for regenerative medicine applications. Therefore, our lab has developed an engineered synthetic hydrogel matrix that presents independently-tunable basement membrane-like bioactivity and mechanical properties, and can support epithelial cell survival, proliferation, polarization, and assembly into 3D multicellular structures recapitulating the epithelial morphogenesis program[9]. These engineered polymer networks are based on a four-arm poly(ethylene glycol) (PEG) macromer with maleimide groups at each terminus (PEG-4MAL), and have the capacity to present adhesive peptides, protease-degradable cross-links, and growth factors that support cell functions and promote cell engraftment and tissue repair *in vivo* [10-14].   Importantly, PEG-4MAL hydrogels exhibit high cytocompatibility, and minimal

toxicity and inflammation *in vivo* while offering significant advantages due to its well-defined structure, stoichiometric incorporation of biofunctional groups, and tunable reaction time scales for *in situ* gelation for *in vivo* applications[10,11]. These engineered, synthetic materials offer a highly significant and disruptive opportunity to establish supportive microenvironments for different epithelial multicellular systems and robust delivery vehicles for *in vivo* applications.

The **objective** of my project is to develop an engineered PEG-4MAL hydrogel platform with independently tunable physicochemical properties that can recapitulate different epithelial morphogenesis programs and serves as a delivery vehicle for regenerative medicine applications. This synthetic hydrogel platform will be engineered to recapitulate the morphogenetic program of human pluripotent stem cell (hPSC)-derived intestinal organoids (HIOs) and mouse inner medullary collecting duct (IMCD) cells. Additionally, the engineered hydrogel will be established as a delivery vehicle for HIOs to mucosal intestinal wounds in mice. I **hypothesize** that these engineered hydrogels will be superior to naturally-derived materials by supporting these different epithelial morphogenetic programs while overcoming the imitations of natural and other synthetic materials. This synthetic hydrogel technology is **significant** as it allows the study of the independent contributions of ECM properties to different epithelial morphogenetic programs, and will form a basis for the adaptation to *in vitro* generation and *in vivo* delivery of human PSC-derived organoids for regenerative medicine. The objective of the project will be achieved through the following specific aims:

1.2   Specific Aim 1

Engineer a PEG-4MAL hydrogel that supports the generation of hPSC-derived intestinal organoids and serves as an injectable vehicle via colonoscope resulting in HIOs survival and engraftment into healing colonic wounds in mice.

We will engineer a completely synthetic hydrogel that supports *in vitro* generation of intestinal organoids from hPSC-derived spheroids without the use of Matrigel™. We will study the contributions of the mechanical and biochemical properties of the synthetic ECM to intestinal organoid formation to identify an optimal formulation that supports intestinal spheroid survival, expansion and epithelial differentiation into HIOs and differentiation into mature intestinal tissue *in vivo* to similar levels as Matrigel™. We will also inject hydrogel liquid precursors and HIOs to murine intestinal mucosal wounds using a murine colonoscope in order to establish the use of the engineered hydrogel as a delivery vehicle for HIOs. This study will demonstrate that the modular nature of this hydrogel platform allows for the adaptation to *in vitro* generation and *in vivo* delivery of hPSC-derived intestinal organoids for regenerative medicine.

1.3   Specific Aim 2

Engineer a PEG-4MAL hydrogel that can recapitulate the tubulogenesis program of murine inner medullary collecting duct cells.

We will engineer a PEG-4MAL hydrogel system that supports *in vitro* development of a tubular epithelial system using murine inner medullary collecting duct cells without the use of type I collagen gels. We will study the contributions of the biophysical and biochemical properties of the synthetic ECM to epithelial tubular system formation to identify an optimal formulation that supports epithelial cell survival, proliferation, polarization, and

3

assembly into 3D tubular structures to similar levels as type I collagen gels. This study will reveal the independent contributions of the physicochemical matrix properties to *in vitro* recapitulation of tubular epithelial morphological programs validating the modular nature of this hydrogel platform.

1.4   Significance and Innovation

The proposed project is **innovative** as it will use a synthetic material that overcomes the major limitations of naturally-derived materials by allowing the study of the independent contributions of ECM properties to different epithelial morphogenetic programs. Additionally, it will form a basis for the development of HIO-based therapies to treat gastrointestinal diseases in humans involving intestinal epithelial wounds (e.g., intestinal bowel disease, IBD), and for the adaptation to *in vitro* generation and *in vivo* delivery of other human PSC-derived organoids (e.g., lung, kidney) for regenerative medicine.

CHAPTER 2.   LITERATURE REVIEW[1]

Synthetic Hydrogels Mimicking Basement Membrane Matrices to Promote Cell-Matrix Interactions[1]

Naturally-derived materials have been extensively used as 3D cellular matrices as their inherent bioactivity makes them suitable for the study of many cellular processes. Nevertheless, lot-to-lot variability, inability to decouple biochemical and biophysical properties and, in some types, their tumor-derived nature limits their translational potential and reliability. One innovative approach to overcome these limitations has focused on incorporating bioactivity into cytocompatible, synthetic hydrogels that present tunable physicochemical properties. Incorporation of adhesive peptides, protease-degradable crosslinkers and growth factor binding domains to the polymer backbone are the most successful approaches to promote bioactivity in synthetic hydrogel matrices in order to recapitulate epithelial morphogenetic programs. Furthermore, the tunable physicochemical properties of these materials can be exploited to study the separate contributions of biochemical and biophysical matrix properties to different epithelial cellular processes.

2.1   Basement Membrane-like Natural 3D Matrices

In an attempt to create materials that mimic the native BM environment, matrices consisting of extracts or purified proteins (e.g. Matrigel™, type I collagen) have been developed. These 3D natural matrices have been used for a wide range of studies to model

---

[1] Adapted from Cruz-Acuña, R. & García, A. J. Synthetic hydrogels mimicking basement membrane matrices to promote cell-matrix interactions. Matrix Biology, DOI: http://dx.doi.org/10.1016/j.matbio.2016.06.002 (2016).

epithelial cell migration[15], cancer invasion[16] and metastasis[17], as well as many epithelial morphogenetic programs[18,19] due to their inherent bioactivity. The characteristics of some of these materials are highlighted below.

2.1.1 Matrigel™

Matrigel™ is the commercial name for a BM extract secreted by Engelbrecht-Holm-Swarm (EHS) mouse sarcoma cells. Matrigel™ is a complex mixture of over 1,000 proteins[8]. It primarily consists of type IV collagen, laminin and nidogen, which makes it the most BM-like natural matrix model[8,20]. Epithelial morphogenesis[21] and oncogenesis[22], as well as intestinal organoid generation[23-25] are current major areas that involve 3D cultures in Matrigel™. A study by Sato et al (2009)[26] exemplifies the potential of Matrigel™ by establishing a 3D culture condition that generates intestinal crypt organoids from single intestinal stem cells in the absence of a cellular niche. After 4 days of encapsulation in Matrigel™, and supplemented with soluble proteins essential for crypt proliferation (R-spondin 1 and epidermal growth factor) and expansion (Noggin), the resulting multi-cellular structures comprise approximately 100 cells, which is consistent with the 12-hour cell cycle of proliferative crypt cells. Additionally, the presence of stem cells at the crypt bottom as well as four major differentiated epithelial cell types are present, demonstrating the ability of Matrigel™ to support intestinal epithelial expansion reminiscent of normal gut[25].

2.1.2 Laminin

Laminins are highly biologically active molecules that can act as strong adhesive substrates for many cell types, and have been found to promote cell adhesion, migration,

protease activity, proliferation, tumor growth, angiogenesis, and metastasis[27-29]. Among the more of a dozen laminin isoforms, laminin-111 (also known as laminin-1; composed of α1-, β1-, and γ1-chains) is the most widely used for 2D and 3D culture systems as it can be isolated from EHS mouse tumors and it is commercially available[27,30]. The use of laminin-111 as a culture substrate has helped identify specific peptide motifs that promote malignant phenotypes by increasing tumor adhesion and migration, as well as tumor cell metastasis through induction of protease production[28,30,31]. Although laminin-111 is the most prominent and studied form of laminin, studies have provided insights into the importance of other laminin isoforms in the morphogenesis of different epithelial organs[32-34].

2.1.3 Other Naturally-derived 3D Matrices

Other naturally derived materials that have been used as cellular matrices include fibrin, alginate and hyaluronic acid gels. Fibrin gels, which are products of the polymerization of fibrinogen by the proteolytic activity of thrombin, started as one of the first biomaterials used to prevent bleeding and promote wound healing[35], and transitioned to a variety of biomedical applications including islet transplantation[36]. Alginate and hyaluronic acid gels, which are derived from marine brown algae and vertebrate connective tissues, respectively[37], are polysaccharides that have been extensively used as biomaterials for controlled release of drugs and tissue engineering applications[38-40].

2.2 Limitations of Natural Matrices

Although 3D natural matrices have been found suitable for the study of many cellular processes, they are limited by lot-to-lot compositional and structural variability[8]

which decrease their reliability. Additionally, these matrices are limited by the inability to decouple mechanical and biochemical properties. For instance, a common approach to vary the mechanical properties is to change the bulk concentration (e.g., increase matrix density). However, these changes in bulk concentration inevitably alter other matrix properties, such as adhesive ligand density and fiber density/structure. Furthermore, as Matrigel™ is a tumor-derived matrix, its clinical translational potential is limited for regenerative medicine applications. For these reasons, approaches have been pursued to overcome these limitations, including the combination of purified natural BM proteins with biocompatible synthetic hydrogels that exhibit defined mechanical properties[41,42]. However, although these materials have decoupled mechanical and biochemical properties, they still have limited translational potential. Therefore, as the field of biomaterials continues to advance, novel engineered synthetic hydrogel matrices that present independently-tunable BM-like bioactivity and mechanical properties have been developed, overcoming each of the aforementioned limitations of natural matrices.

2.3 Synthetic Hydrogel Matrices

Hydrogels are water-swollen crosslinked polymer networks that can be considered synthetic equivalents of ECM matrices. Commonly used hydrogel polymers for biomedical applications include poly(acrylic acid) (PAA), poly(ethylene glycol) (PEG), poly(vinyl alcohol) (PVA), polyacrylamide (PAAm), and polypeptides[43]. These mesh-like structures are held together by either covalent crosslinks or non-covalent interactions that include ionic interactions, hydrogen bonds, affinity and hydrophobic interactions, polymer crystallites, physical entanglements, or a combination of the above[44].

8

2.3.1 Physical Properties of Hydrogels

Hydrogel stiffness and swelling behavior are two important physical characteristics that are inversely related and are primarily controlled by polymer density[45,46]. The swelling behavior of hydrogels involves a swelling force produced by the thermodynamic compatibility of the polymer chains and water, which is counterbalanced by the retractive forces exerted by its crosslinks[44,45]. Swelling equilibrium is reached when these two forces are equal[44]. Consequently, a hydrogel with high (low) polymer density has a greater (smaller) number of crosslinks that cause increased (decreased) retractive forces that will result in less (more) swelling. Moreover, an opposite effect is followed in hydrogel stiffness, as polymer density is proportional to the matrix stiffness; a high polymer density would produce a denser (thus, stiffer) polymer network. Hydrogel elastic modulus is an important physical parameter to consider in the design of a synthetic cellular matrix as many studies demonstrate matrix stiffness-dependent cellular responses, such as extent of cell migration and differentiation[47,48].

2.3.2 Synthesis of Hydrogels

Among several methods to produce synthetic hydrogels matrices, photo-polymerization and chemical reaction crosslinking stand out as two of the most widely used for biomedical applications[43,49]. Photo-polymerization involves the crosslinking of two water-soluble polymers (Fig. 1a), or copolymerization between one or more monomers and one multi-functional monomer (Fig. 1b), via photo-ionization of the monomers using light, often in the UV range. The high reactivity of the photo-ionized polymer components induces crosslinking reactions that produce a crosslinked network. As the polymerization

is light-dependent, this technique grants *in situ* spatiotemporal control over the mechanical properties of the hydrogel and presentation of incorporated ligands[43,50-52].
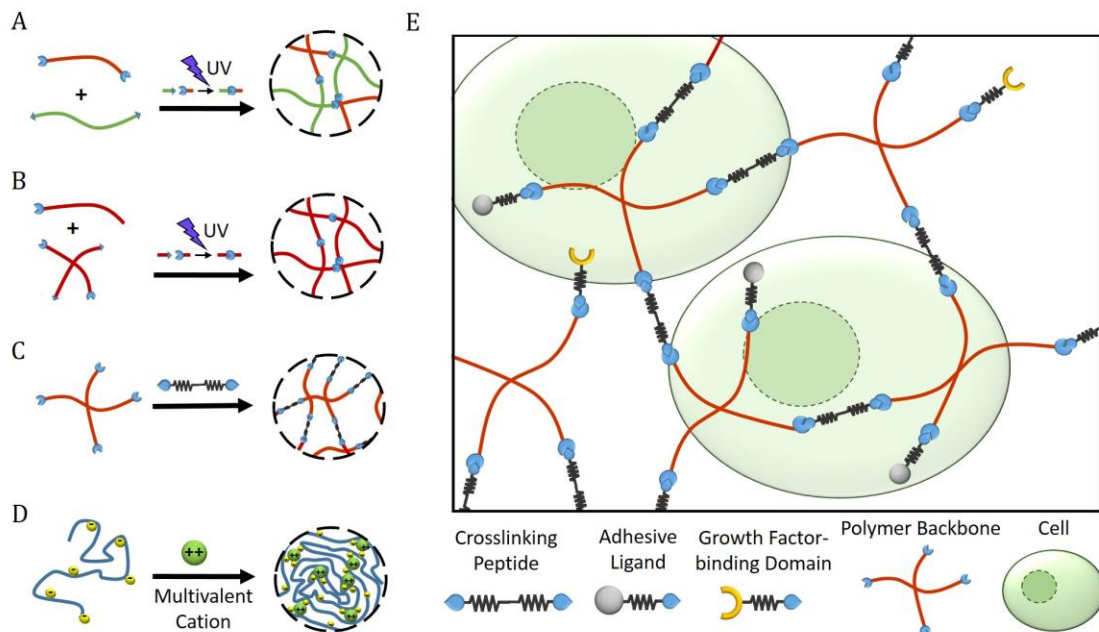
Figure 1: Synthesis methods of engineered synthetic hydrogels. Photo-polymerization of two water-soluble polymers (A) and copolymerization of one monomer and one multi-functional monomer (B) via covalent reaction after UV irradiation. (C) Direct chemical reaction of a branched polymer with a di-functional crosslinking agent. (D) Electrostatic interactions of an anionic polymer with divalent cations yields an "ionotropic" hydrogel. (E) Encapsulated cells in an engineered biofunctionalized hydrogel exhibiting adhesive ligand, growth factor-binding domain and MMP-degradable crosslinks.

Chemical reaction crosslinking involves a direct chemical reaction between linear or branched polymer macromolecules (macromers) with a di-functional or multi-functional crosslinking agent. Each agent, which has a smaller molecular weight, crosslinks two or more macromers together forming a mesh-like structured hydrogel[49] (Fig. 1c). Examples of chemical reactions used to produce hydrogels are chemical ligation[53], click chemistry[54] and Michael-type addition reaction[10].

These two general hydrogel synthesis methods have been widely used for generating artificial 3D cellular matrices as they allow easy incorporation of BM-like biochemical properties, which will be discussed in the next section. Although these synthesis techniques are based on covalently crosslinking the synthetic hydrogel constituents, there are other synthesis methods that involve crosslinking by non-covalent interactions which are common in naturally-derived hydrogels, such as alginate "ionotropic" hydrogels which are formed based on electrostatic interactions[49] (Figure 1d).

2.4 Incorporation of BM-like Properties to Synthetic Hydrogels

The BM contains key biophysical and biochemical characteristics that are essential for epithelial and endothelial cell attachment and viability as well as numerous cellular processes that include proliferation, differentiation, and migration. These cellular processes are primarily mediated by cell-matrix interactions via integrins, the ability of cells to remodel their supporting matrix via degradation of their microenvironment, and by presentation of growth factors[55]. Consequently, in order to incorporate bioactivity into artificial hydrogel matrices, successful approaches have focused on incorporating bioactive peptides derived from natural ECM. Three common themes explored in biofunctional hydrogels are (1) cell adhesive peptides, (2) protease-degradable crosslinkers, and (3) growth factor-binding domains in order to mimic native cell-BM interactions (Fig. 1e).

2.4.1 Cell Adhesive Peptides

Integrin binding to short peptide sequences present in BM proteins such as collagen and laminin provides cellular attachment and triggers signals that direct cell function, cell-cycle progression and expression of differentiated phenotypes[56-59]. Therefore,

11

incorporating biofunctional short peptide sequences into 3D artificial hydrogel systems has been an effective method to promote integrin-mediated cellular functions. These peptide motifs have the advantage of being relatively stable, and can be covalently tethered to the hydrogel polymer backbone at tunable densities via integration of reactive groups, yielding a biofunctionalized hydrogel[43]. The most widely used cell-adhesive motif is the short peptide arginine-glycine-aspartic acid (RGD); this oligopeptide was originally identified in fibronectin but is also present in many other ECM proteins including laminin and collagen[60]. Presentation of RGD on synthetic matrices supports cell adhesion by targeting integrins, such as $\alpha_v\beta_3$. Many studies have demonstrated successful BM-like bioactivity of RGD-functionalized hydrogels, as compared to non-functionalized matrices, by directing essential cellular processes such as attachment and spreading[61], migration and invasion[62,63], and stem cell support[64] and differentiation[65]. Furthermore, other peptides like IKVAV and YIGSR, which are derived from laminin, can also be incorporated into hydrogels together with RGD to orchestrate ligand density-dependent signal presentation independently of the mechanical characteristics of the matrix[65,66]. This demonstrates the potential of engineered hydrogels as matrices that can elucidate tunable biochemical signals that direct complex cellular processes via presentation of cell adhesion peptides.

2.4.2   Protease-Degradable Crosslinkers

The capacity of cells to modify their microenvironment via matrix degradation is essential for their ability to migrate and proliferate, as well as for tissue remodeling and homeostasis[55]. ECM remodeling involves degradation and modification of its protein components, most significantly by cell-secreted or membrane-bound matrix metalloproteinases (MMPs)[67]. Therefore, crosslinking hydrogel matrices with MMP-

12

cleavable peptides has been a widely used strategy to allow for cell-directed modifications of the matrix biophysical characteristics. These short peptide sequences are derived from ECM proteins, such as type I or type IV collagen, and incorporation into synthetic hydrogel matrices conveys sensitivity to MMP-dependent degradation[47,68]. Moreover, studies show that mutations to, or combinations of, different MMP-sensitive crosslinking peptides can yield hydrogels with different degradability rates that result in variations of cellular responses within the hydrogel, such as extent of cell invasion[47] and determination of stem cell fate[48,69]. This demonstrates that artificial hydrogel matrices with tunable degradability rates present BM-like bioactivity that can direct a wide range of cellular responses independent of their cell adhesive peptide density.

2.4.3   Growth Factor-binding Domains

The BM hosts a wide variety of signaling molecules such as growth factors (GFs), which reside in the matrix by non-covalent interactions with heparan sulfate proteoglycans such as perlecan and other minor BM components (agrin and type XVIII collagen)[70,71]. GFs play significant roles in tissue development by eliciting a variety of essential cellular responses such as cell proliferation, stem cell differentiation, and vascular and organ morphogenesis[72]. Therefore, presentation of specific GF types and densities to cells through the use of artificial hydrogel matrices has been an effective approach to orchestrate desired cellular responses. The traditional method for GF incorporation into hydrogels is direct encapsulation, which involves physical entrapment of GFs within the matrix which will be released as the hydrogel degrades and/or will diffuse out of the hydrogel network[73]. Nevertheless, as this method may not provide long-term control over GF presentation, another approach has been to covalently tether GFs to the hydrogel backbone[70,74].

13

However, as covalent linkage may compromise GF activity by alterations to its conformation or masking its active sites, strategies focus on incorporating GF-binding domains into hydrogel matrices by covalently tethering heparan sulfate-containing molecules to the polymer backbone that interact with GFs[75-77]. This method, compared to previous approaches, has gained popularity as it mimics native BM-GF non-covalent interactions within artificial hydrogel matrices. Consequently, investigations have demonstrated inherent GF-directed cellular responses via presentation of GF-binding domains within synthetic hydrogels, such as in vivo neovascularization[78,79] and wound healing[75].

2.5   Exemplary Applications of BM-mimicking Hydrogels

As the fields of cell and matrix biology progress, our understanding of what biological cues are essential for specific cellular processes becomes clearer, and thus, more robust synthetic hydrogels that present these essential biological signals have been engineered. In order to construct such materials, it is critical to understand how changes in the chemical and physical characteristics of hydrogels translate into changes in the local microenvironment of encapsulated cells. The establishment of an artificial hydrogel microenvironment that directs epithelial morphogenesis, controls cell fate, and provides insights into cancer progression are among the most recent advances in the field of biomaterials, and various studies are highlighted below.

2.5.1   *Epithelial Morphogenesis*

Epithelial morphogenesis is part of the organogenesis program of multicellular organisms where the epithelia form transient structures, such as tubules and hollow

spherical systems (cysts), that further develop into more complex organs[80]. During this process, epithelial cells establish tight junctions among neighboring epithelial cells through their lateral membranes, and connections to their supporting BM via integrin receptors in their basal membranes[81], which contribute to their distinctive cellular polarity[21,81]. Studies using 3D collagen and laminin gel cultures have demonstrated that the epithelial morphogenesis developmental program is regulated by biochemical and mechanical signals that result from cell-BM interactions[18,81,82]. In these studies, single-cell encapsulation of epithelial cells, such as MDCK cells, results in cell proliferation into a multicellular aggregate and further development of cysts composed of a polarized epithelial monolayer that recreates the morphogenesis of epithelial organs[83]. Although these natural matrices have been able to recapitulate the epithelial morphogenesis program of MDCK cells, they do not offer the capacity to study individual contributions of the mechanical and biochemical properties of the ECM towards epithelial morphogenesis. Therefore, Enemchukwu et al (2016)[9] established an engineered ECM-mimetic PEG hydrogel system with independent control over ligand density and presentation, proteolytic degradation and mechanical properties to independently study the effects of ECM biochemical and biophysical properties on MDCK cell morphogenesis. In this study, normal cyst growth, polarization, and lumen formation were restricted to a narrow range of hydrogel elasticity that was controlled by the polymer density. Additionally, RGD density dramatically regulated apicobasal polarity and lumenogenesis independently of cell proliferation, and a threshold level of MMP-directed hydrogel degradation rate was required to regulate these critical epithelial characteristics. This study offers new insights into how ECM biochemical and biophysical properties independently regulate epithelial morphogenetic behaviors, as

well as present a platform technology that could potentially be adopted in developmental cell and tumor biology fields to study ECM-directed processes.

2.5.2 3D iPSCs Generation

Since the discovery of induced pluripotent stem cells (iPSCs), reprogramming of somatic cells has been considered a multi-step process that is initiated by cytoskeletal and epigenetic alterations[84-86]. Some of these alterations are related to effects of the ECM on cells, for example, iPSC generation can be influenced by biophysical parameters in 2D culture[87]. In order to better understand the role of the microenvironment on somatic-cell reprogramming, a synthetic 3D ECM-like hydrogel culture system that supports the initiation of reprogramming was developed by Lutolf[86]. These PEG hydrogels allow for precise control of the physiochemical characteristics of the cellular microenvironment which is not possible in 2D culture. In order to take full advantage of the tunable nature of this hydrogel, a high-throughput imaging system was used to detect pluripotency levels as a function of hydrogel stiffness, susceptibility to MMP degradation, and functionalization with different proteins previously shown to play a role in regulating pluripotency. This analysis yielded an engineered 3D PEG hydrogel that demonstrated a 2.5-fold higher reprogramming efficiency of human fibroblasts into iPSCs as compared to 2D culture. The accelerated reprogramming was attributed to hydrogel matrix selection of colony-forming iPSCs by limiting proliferation of non-colony-forming cells, and to the pronounced morphological changes that may cause the key events for the initiation of iPSC generation. These findings provide the first proof of principle for 3D reprogramming in synthetic matrices, and demonstrate the capacity of an engineered ECM-like hydrogel system to

reveal the influence of the physiochemical characteristics of the cellular microenvironment in cell fate regulation.

2.6 Outlook for BM-like Synthetic Hydrogel Matrices

Although the studies discussed in here have developed novel artificial hydrogel matrices that present BM-like properties, several challenges need to be addressed in order to continue engineering synthetic matrices that recapitulate and direct complex cellular processes. For instance, there is a need for hydrogels that can recapitulate the in vivo microenvironment by presentation of multiple adhesive ligand types at specific densities that can orchestrate complex cellular responses. Such artificial matrix designs are important for the support of complex cellular systems (e.g. primary and stem cells) that still represent a challenge due to their increased sensitivity, and to further direct innate cellular functions. Furthermore, as different studies have demonstrated successful culture of complex cellular systems using Matrigel™, future developments of BM-like synthetic hydrogels should move towards designing hydrogels that recapitulate mechanical and structural (e.g., fibrillar structure) properties of Matrigel™ and collagen gels. Consequently, designing artificial matrices that present combinations of biochemical signals by functionalization with multiple adhesive ligand types, and possess biophysical characteristics of Matrigel™, may lead to hydrogels that reiterate the in vivo microenvironment of complex cellular systems and can, thus, further expand their application as cell-delivery vehicles for in vivo studies. Therefore, as new ways of integrating bioactivity into hydrogel matrices are designed, these novel engineered synthetic materials will continue to offer new developments in regenerative medicine and

tissue engineering fields, and promise innovative therapeutic options that naturally derived materials cannot provide.

CHAPTER 3. SYNTHETIC HYDROGELS FOR HUMAN INTESTINAL ORGANOID GENERATION AND COLONIC WOUND REPAIR[2]

3.1 Abstract

In vitro differentiation of human intestinal organoids (HIOs) from pluripotent stem cells is an unparalleled system for creating complex, multi-cellular 3D structures capable of giving rise to tissue analogous to native human tissue. Current methods for generating HIOs rely on growth in an undefined tumor-derived extracellular matrix (ECM), which severely limits use of organoid technologies for regenerative and translational medicine. Here, we developed a fully defined, synthetic hydrogel based on a four-armed, maleimide-terminated poly(ethylene glycol) macromer that supports robust and highly reproducible *in vitro* growth and expansion of HIOs such that 3D structures are never embedded in tumor-derived ECM. We also demonstrate that the hydrogel serves as an injectable HIO vehicle that can be delivered into injured intestinal mucosa resulting in HIO engraftment and improved colonic wound repair. Together, these studies show proof-of-concept that HIOs may be used therapeutically to treat intestinal injury.

3.2 Introduction

Human pluripotent stem cells (hPSCs), such as embryonic stem cells (ESCs)[88] and induced pluripotent stem cells (iPSCs)[89], are important cell sources for regenerative

---

therapies and modeling of human diseases[90-92]. *In vitro* generation of human organoids from hPSCs offers unparalleled strategies for generating multi-cellular 3D structures recapitulating important features of epithelial and mesenchymal tissues[24,25,93,94]. For example, human intestinal organoid (HIO) technology provides a powerful platform for functional modeling and repair of genetic defects in human intestinal development[95,96] and the establishment of chronic disease models, such as inflammatory bowel disease[97].

In order to generate HIOs, hPSCs were cultured and differentiated using growth factors in a Matrigel^TM-coated substrate, giving rise to 3D intestinal spheroids which were collected and encapsulated within Matrigel^TM for expansion into HIOs[98]. Matrigel^TM is a heterogeneous, complex mixture of ECM proteins, proteoglycans, and growth factors secreted by Engelbreth-Holm-Swarm mouse sarcoma cells[99], which is required for 3D growth and expansion of HIOs. However, Matrigel^TM suffers from lot-to-lot compositional and structural variability and, importantly, this tumor-derived matrix has limited clinical translational potential[100]. Indeed, a synthetic alternative to Matrigel^TM that supports murine intestinal stem cell expansion and organoid formation has been recently reported[100].

Here, we describe a completely synthetic hydrogel that supports *in vitro* generation of intestinal organoids from human ESC- and iPSC-derived 3D spheroids without Matrigel^TM encapsulation and promotes their engraftment and healing of murine colonic mucosal wounds. Hydrogel mechanical properties and adhesive ligand type were key parameters in engineering a synthetic ECM mimic that supported HIO viability, expansion and development. Additionally, this synthetic hydrogel served as an injectable vehicle to deliver HIOs to intestinal wounds via a colonoscope resulting in organoid survival, engraftment, and wound repair. The modular design of this synthetic matrix and ability to

deliver via endoscopic techniques support the translational potential of this delivery platform for regenerative medicine and overcomes limitations associated with the use of Matrigel[TM] for hPSC-based organoid technologies.

3.3   Results

3.3.1   Engineered hydrogels support HIO viability

We selected a hydrogel platform based on a four-arm poly(ethylene glycol) (PEG) macromer with maleimide groups at each terminus (PEG-4MAL) (Fig. 2a), which exhibits high cytocompatibility and minimal toxicity and inflammation *in vivo*[10,11]. Moreover, this hydrogel system offers significant advantages due to its well-defined structure, stoichiometric incorporation of biofunctional groups, and tunable reaction time scales for *in situ* gelation for *in vivo* applications[10,11].

PEG-4MAL macromers were functionalized with adhesive peptides and crosslinked in the presence of cells to generate PEG-4MAL hydrogels (Fig. 2a,b). The mechanical properties of the hydrogel were tuned by varying polymer density (Fig. 2c,d). We explored hydrogel formulations that supported the viability of ESC-derived HIOs that were first generated in Matrigel[TM]. After HIOs were grown in Matrigel[TM], they were retrieved and encapsulated in PEG-4MAL hydrogel formulations (Fig. 2e). Because ECM mechanical properties influence epithelial cell behaviors[9], we investigated the influence of hydrogel polymer density (3.5-6.0% wt/vol), which controls hydrogel mechanical properties (Fig. 2c,d), on HIO viability at day 7 post-encapsulation (Fig. 3a). For reference, the mechanical properties of Matrigel™ (G' = 78 Pa, G'' = 5.8 Pa) are in the range of the 3.5-4.0% PEG-4MAL formulations. These synthetic hydrogels were engineered to present

a constant 2.0 mM RGD adhesive peptide (GRGDSPC) density and crosslinked with the protease-degradable peptide GPQ-W (GCRDGPQGIWGQDRCG). This adhesive peptide type and density were chosen as they have been shown to support high epithelial cell viability and cyst formation in PEG-4MAL hydrogels[9]. The protease-degradable crosslinking peptide is necessary for cell-dependent matrix remodeling, cell migration and growth[9,86]. HIOs embedded in 3.5% and 4.0% PEG-4MAL gels grew as cysts with an epithelium and central lumen, and maintained high viability for at least 7 d in culture comparable with growth and viability of HIOs in Matrigel[TM] (Fig. 3a). Quantification of organoid viability area demonstrated no significant differences between HIOs embedded in 3.5% or 4.0% PEG-4MAL gels and HIOs in Matrigel (Fig. 3b). In contrast, organoids encapsulated in 5.0% or 6.0% PEG-4MAL hydrogels exhibited a significantly reduced viability at day 7 after encapsulation as compared to HIOs embedded in 3.5%, 4.0% PEG-4MAL gels or Matrigel (Fig. 3a,b). These results suggest polymer density-dependent effects on HIO survival within PEG-4MAL hydrogels. Although 3.5% PEG-4MAL hydrogels supported high HIO viability, this formulation was less mechanically stable compared to 4.0% PEG-4MAL hydrogels by 7 days in culture. We therefore selected 4.0% PEG-MAL hydrogels for subsequent studies.
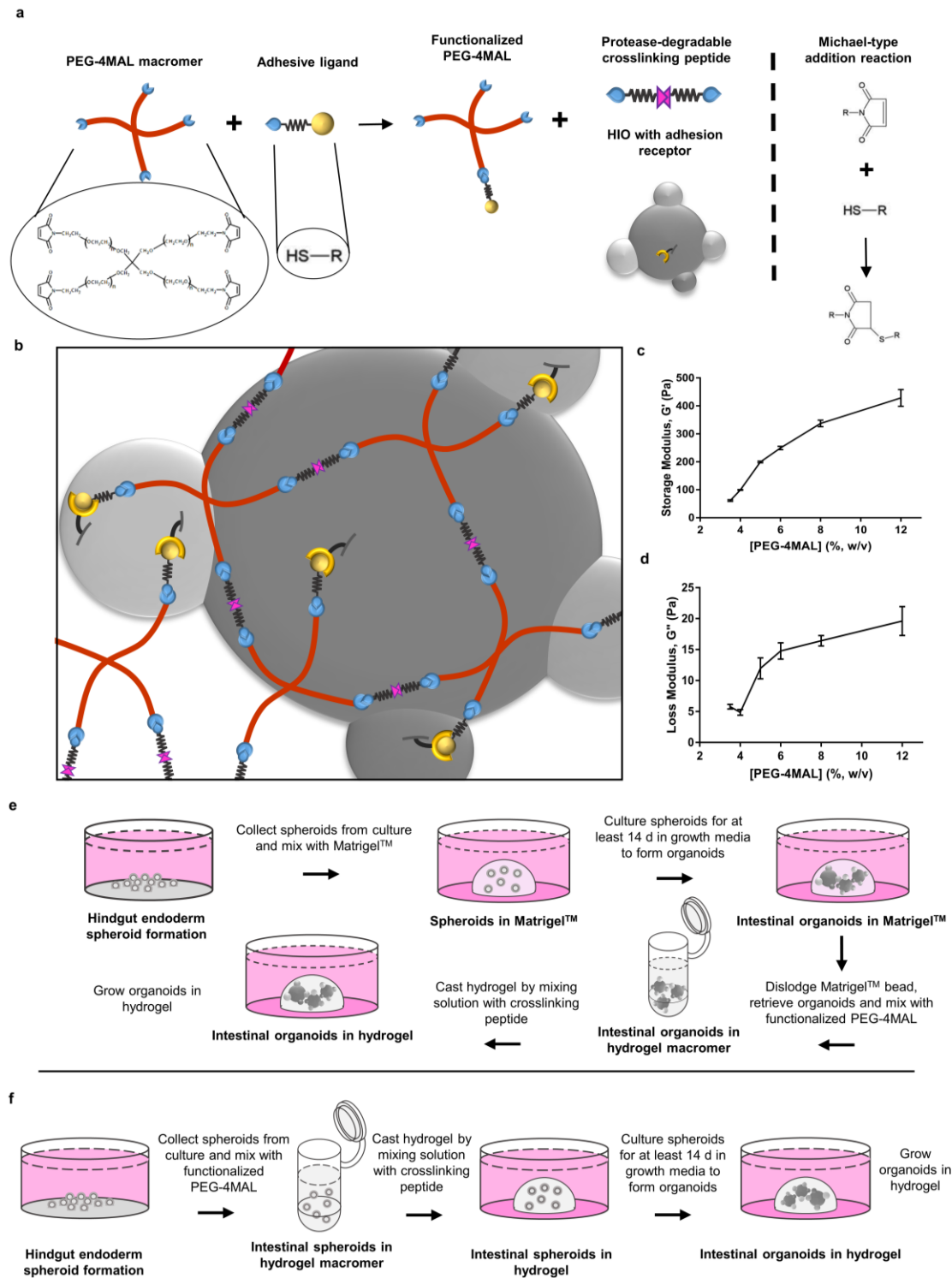
Figure 2: PEG-4MAL hydrogel preparation and mechanical properties. (a) PEG-4MAL macromers are conjugated with thiol-containing adhesive peptide to produce a functionalized PEG-4MAL macromer, which is then crosslinked in the presence of HIOs

using protease-cleavable peptides containing terminal cysteines to form a (b) hydrogel network. (c,d) Relationship between polymer density (wt%) and (c) storage modulus or (d) loss modulus (mean ± SEM; n = 10 independently prepared hydrogels per condition). (e) Schematic of spheroid development into HIOs within Matrigel[TM] and further growth within PEG-4MAL hydrogel. (f) Schematic of spheroid development into HIOs within hydrogel. (c,d) Graphs are representative of one experiment.
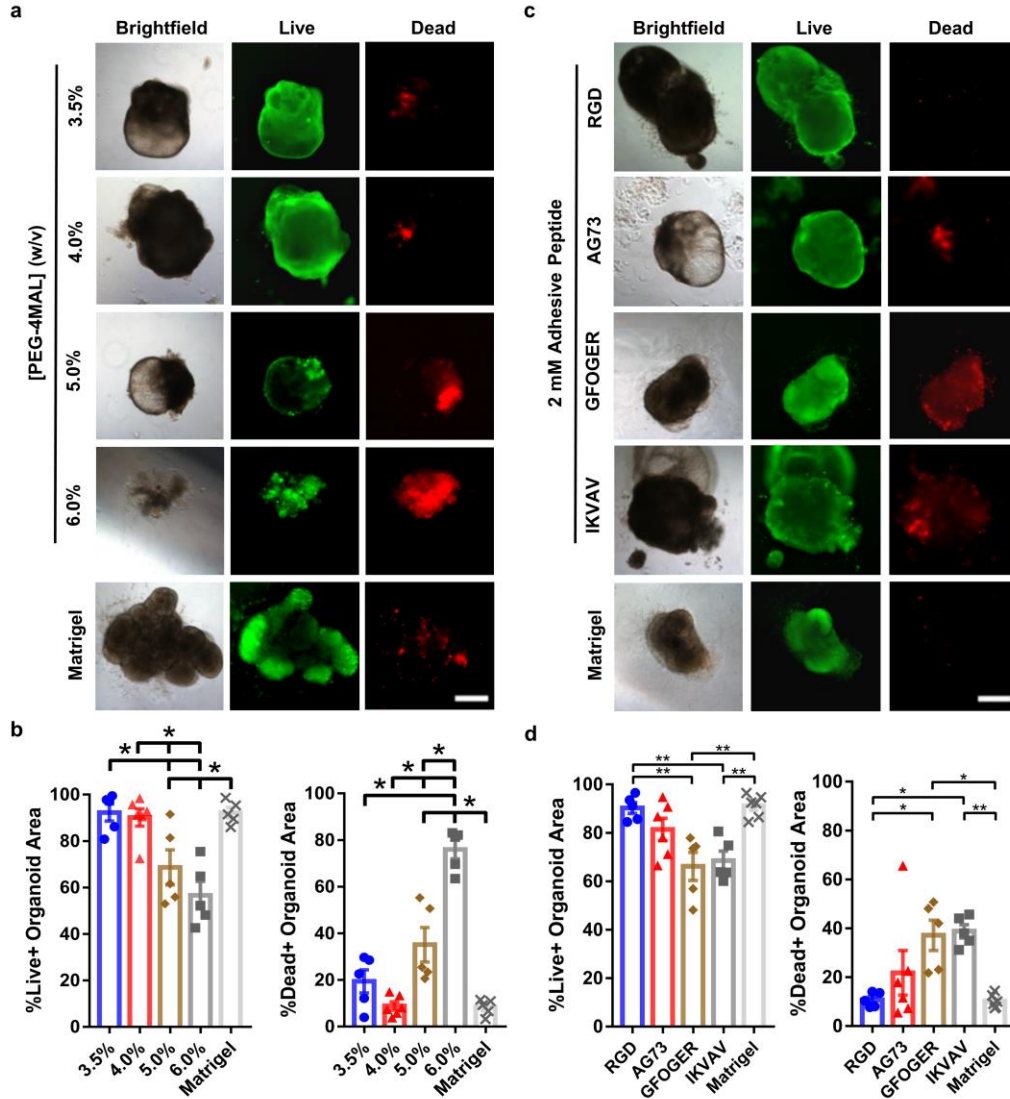
Figure 3: PEG-4MAL polymer density and adhesive ligand type control HIO viability. (a) Transmitted light and fluorescence microscopy images of HIOs cultured in PEG-4MAL hydrogels of different polymer density or Matrigel[TM]. HIO viability was assessed at 7 d after encapsulation. Bar, 500 μm. (b) Percentage of total organoid area stained for live or dead (mean ± SEM) after 7 d of encapsulation (n = 5 organoids analyzed for all groups,

24

except n = 6 organoids analyzed for 4.0% group). (c) Transmitted light and fluorescence microscopy images of HIOs cultured in 4.0% PEG-4MAL hydrogels functionalized with different adhesive peptides or Matrigel[TM]. HIO viability was assessed at 7 d after encapsulation. Bar, 500 μm. (d) Percentage of total organoid area stained for live or dead (mean ± SEM) after 7 d of encapsulation (n = 5 organoids analyzed for all groups, except n = 6 organoids analyzed for AG73 and Matrigel groups). (b,d) One-way ANOVA with Tukey's multiple comparisons test showed significant differences between (b) 4.0% PEG-4MAL or Matrigel[TM] and 5.0 or 6.0% PEG-4MAL, and between (b) PEG-4MAL-RGD or Matrigel[TM] and PEG-4MAL-GFOGER or -IKVAV. (*$P < 0.05$, **$P < 0.01$, ***$P < 0.001$, ****$P < 0.0001$). (a-d) Three independent experiments were performed and data is presented for one of the experiments. All experiments performed with 6 PEG-4MAL/Matrigel[TM] per experimental group.

Interactions between adhesion receptors and ECM provide signals critical for cell survival, proliferation and differentiation[101]. Therefore, we examined whether the adhesive ligand type in the synthetic hydrogel impacts HIO viability. Organoids were embedded within PEG-4MAL formulations of 4.0% polymer density and constant GPQ-W crosslinking peptide density but with different cysteine-terminated adhesive peptides (all at 2.0 mM; Fig. 3c,d): RGD, laminin α1 chain-derived AG73 (CGGRKRLQVQLSIRT)[102], type I collagen-mimetic triple helical GFOGER (GYGGGP(GPP)₅GFOGER(GPP)₅GPC)[103], and laminin α1 chain-derived IKVAV (CGGAASIKVAVSADR)[30]. Since the adhesive peptide-functionalized macromer building blocks of the hydrogel are symmetric and form a regular mesh structure that is fully swollen, the adhesive peptide is uniformly distributed throughout the hydrogel network within the 'statistical average' of the mesh size (30-40 nm). Furthermore, because of the small size of the PEG macromer arms and the swollen state of the gel, the mobility of the adhesive peptide is very limited and there is no effective clustering of the adhesive peptide[9]. Nevertheless, changes in adhesive peptide at the nanoscale cannot be completely ruled out. Organoids encapsulated in RGD-functionalized hydrogels maintained high viability for at least 7 d after encapsulation (Fig. 3c,d; Fig. 4a), similar to viability within

Matrigel^{TM}. In contrast, organoids encapsulated in PEG-4MAL hydrogels functionalized with AG73, GFOGER or IKVAV showed reduced viability at 7 d post-encapsulation (Fig. 3c,d). Adhesion to RGD was required for HIO viability as organoids encapsulated in hydrogels presenting an inactive scrambled peptide (RDG) showed reduced viability at 7 d post-encapsulation (Fig. 4b). Finally, organoids exhibited low viability at 7 d post-encapsulation in hydrogels crosslinked with non-degradable molecules (DTT), demonstrating that prolonged survival of HIO requires a degradable matrix (Fig. 4c). Taken together, these results identify an engineered hydrogel formulation (4.0% polymer density, 2.0 mM RGD adhesive peptide, GPQ-W crosslinking peptide) that supports high viability for established HIOs, and which was used for all subsequent experiments.

3.3.2 Engineered hydrogel supports HIO development

We next examined HIO maintenance during culture in engineered hydrogels. Over several days in culture, established HIOs grew in size, changed shape, maintained a central lumen, and displayed epithelial budding at the interface with the hydrogel (Fig. 4d). Additionally, mesenchymal cells were observed migrating into the hydrogel, similar to HIOs maintained in Matrigel^{TM} (Fig. 4d,e). To further characterize the intestinal epithelium of HIOs, we examined cell proliferation and apicobasal polarity in HIOs generated in Matrigel^{TM} and those transferred to the engineered PEG-4MAL hydrogels. After 7 d in culture, HIOs stained positive for Ki67, indicating cell proliferation, demonstrated appropriate polarization of apical (EZRIN) and basolateral (β-CATENIN) proteins, and localization of an epithelial tight junction protein (ZO-1)[104] (Fig. 4f,g). The staining patterns were similar when comparing HIOs maintained in PEG-4MAL hydrogel and

Matrigel™ (Fig. 4f,g), demonstrating that the engineered PEG-4MAL hydrogel robustly supports HIO maintenance.
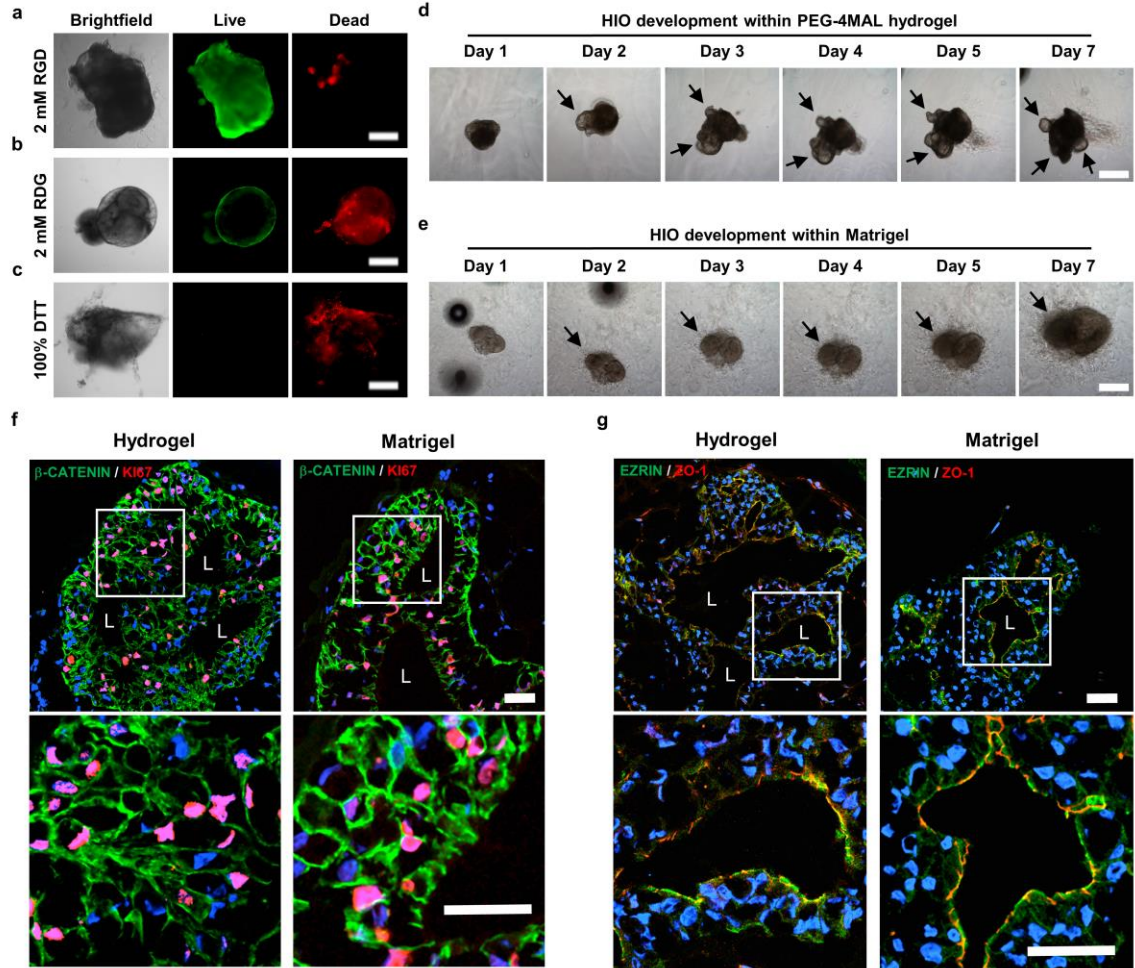
Figure 4: Engineered PEG-4MAL supports HIO development. (a) Transmitted light and fluorescence microscopy images of HIOs cultured in 4.0% PEG-4MAL hydrogels functionalized with (a) RGD, (b) inactive, scrambled RDG peptide, or (c) non-degradable crosslinker (DTT). HIO viability was assessed at 7 d after encapsulation. (d,e) Transmitted light microscopy images of Matrigel™-generated HIOs cultured within (d) 4.0% PEG-4MAL-RGD hydrogel or (e) Matrigel™ over time. Bars, 500 μm. (f,g) Fluorescence microscopy images of a HIO at 7 d after encapsulation in 4.0% PEG-4MAL-RGD hydrogel or Matrigel™, and labeled for (f) β-CATENIN, proliferative cells (KI67), and (g) epithelial apical polarity (EZRIN) and tight junctions (ZO-1). DAPI, counterstain. "L" indicates HIO lumen. Bars, 100 μm. (a-g) Three independent experiments were performed and data is presented for one of the experiments. Experiments performed with (a-c) 4, (f,g) 6 or (d,e) 12 PEG-4MAL/Matrigel™ per experimental group.

3.3.3   *Engineered hydrogel generates HIOs from spheroids*

The use of Matrigel^{TM} to generate HIOs is a fundamental roadblock to the clinical translation of organoid technologies. We therefore examined whether the engineered PEG-4MAL hydrogel supports survival of hESC-derived intestinal spheroids and growth into HIOs without ever embedding in Matrigel^{TM}. After 4-5 days of induction towards the intestinal lineage on a Matrigel^{TM}-coated substrate, small 3D intestinal spheroids self-assemble and bud off from the cultured monolayer losing contact with Matrigel^{TM}. Detached, floating mCherry-expressing intestinal spheroids were collected from the media and encapsulated in PEG-4MAL hydrogels formulated over a range of polymer densities (3.5%-12.0%) (Fig. 2f) to examine a range of mechanical properties (Fig. 2c,d). All these hydrogels were engineered to present 2.0 mM RGD adhesive peptide and crosslinked with GPQ-W. Spheroids embedded in 3.5% and 4.0% PEG-4MAL maintained viability at 2 h after encapsulation and grew into larger structures reminiscent of organoids with high viability at 5 d after encapsulation (Fig. 5a). In contrast, spheroids encapsulated in 8.0% and 12.0% PEG-4MAL hydrogels displayed significantly lower viability at 2 h post-encapsulation when compared to spheroids embedded in 3.5% or 4.0% PEG-4MAL (Fig. 5a). Consistent results were observed between hESC- and hiPSC-derived spheroids (Fig. 6). hiPSC-derived intestinal spheroids encapsulated in 4.0% PEG-4MAL grew into organoids with high viability at 5 d after encapsulation and developed over 3 weeks into HIOs similar to spheroids encapsulated in Matrigel™ (Fig. 6a,b). In contrast, hiPSC-derived spheroids encapsulated in 8.0% PEG-4MAL hydrogels showed very low viability by 1 d post-encapsulation (Fig. 6c).
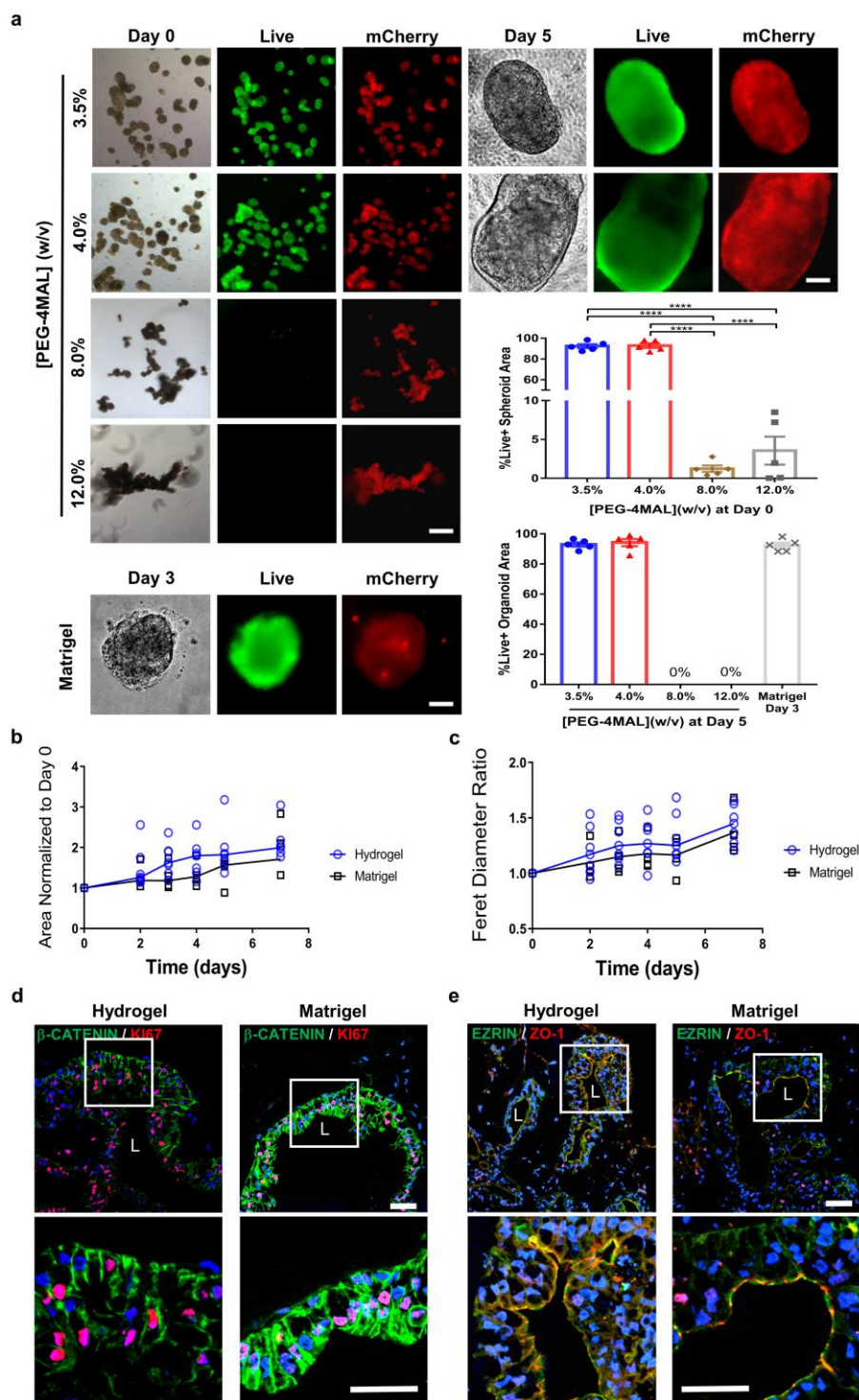
Figure 5: PEG-4MAL polymer density regulates HIO generation from intestinal spheroids in the absence of Matrigel™ embedding. (a) Transmitted light and fluorescence microscopy images of mCherry-spheroids cultured in PEG-4MAL hydrogels of different polymer density or MatrigelTM. Spheroids viability was assessed by Calcein-AM labeling

at 2 hr after encapsulation (day 0) and at day 5 for PEG-4MAL conditions, and at day 3 for MatrigelTM. Bar, 100 µm. Viability is quantified as percentage of total spheroid or organoid area stained for live or dead (mean ± SEM; n = 5 organoids analyzed per condition/time-point). One-way ANOVA with Tukey's multiple comparisons test showed significant differences between 3.5% or 4.0% PEG-4MAL and 8.0% or 12.0% PEG-4MAL at Day 0 (****$P < 0.0001$). (b) HIO projected area and (c) Feret diameter normalized to Day 0 values at different time-points after encapsulation in 4.0% PEG-4MAL-RGD hydrogel (●) or MatrigelTM (■) (n = 6 organoids for PEG-4MAL and n = 4 organoids for MatrigelTM per time-point). Repeated measures two-way ANOVA showed no significant difference between matrix types ($P > 0.05$). Graph line represents the mean of the individual data points at each time-point. (d,e) Fluorescence microscopy images of a HIO at 21 d after encapsulation in 4.0% PEG-4MAL-RGD hydrogel or MatrigelTM and labeled for (d) β-CATENIN, proliferative cells (KI67), and (e) epithelial apical polarity (EZRIN) and tight junctions (ZO-1). DAPI, counterstain. "L" indicates HIO lumen. Bars, 100 µm. Three independent experiments were performed and data is presented for one of the experiments. All experiments performed with 6 PEG-4MAL/MatrigelTM per experimental group.
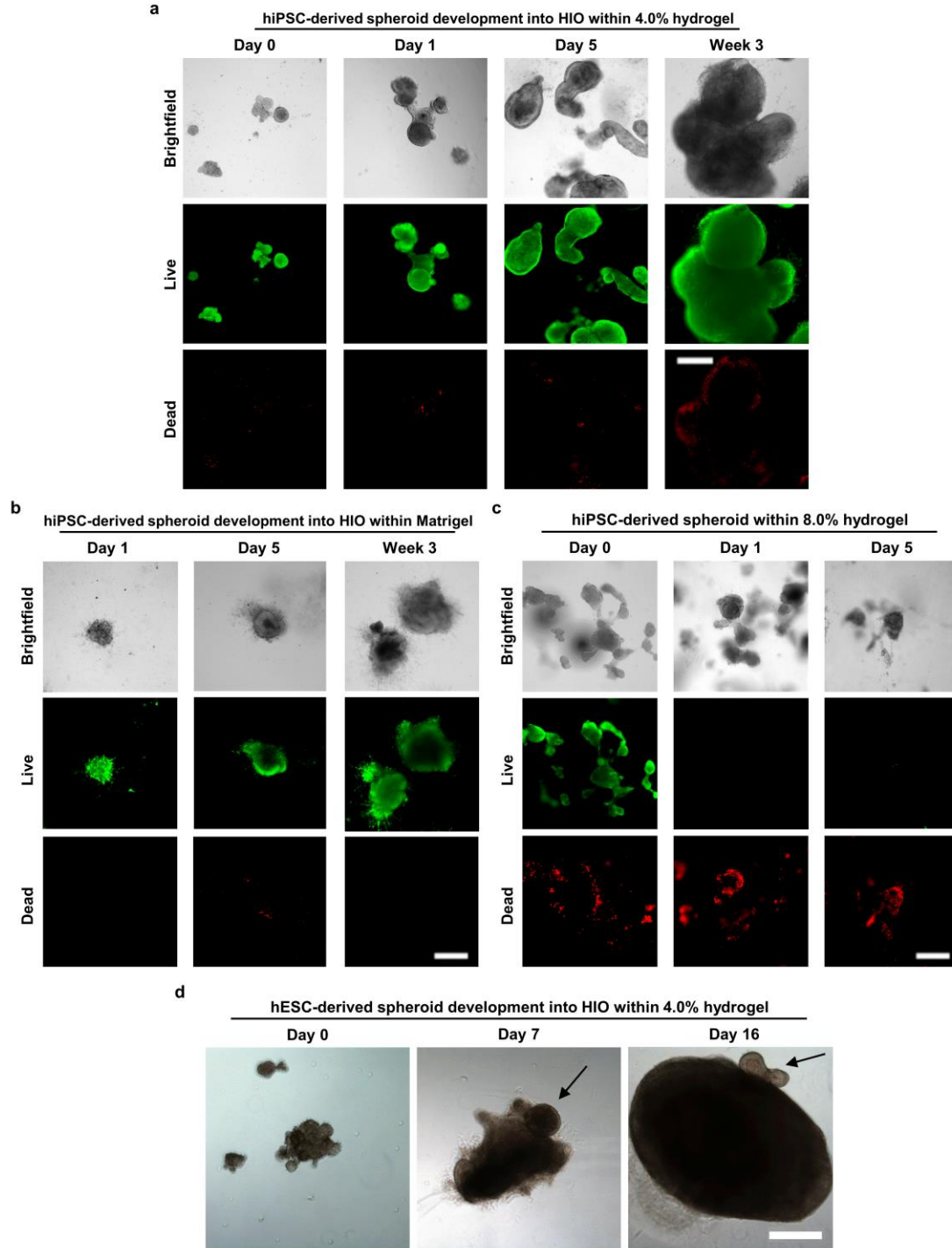
Figure 6: PEG-4MAL hydrogel supports hiPSC-derived intestinal spheroid development into HIOs comparable to hESC-derived spheroids. (a) Transmitted light and fluorescence microscopy images of hiPSC-derived HIO generation within (a) 4.0% PEG-4MAL-RGD hydrogels, (b) Matrigel^{TM}, or (c) 8.0% PEG-4MAL-RGD hydrogels. hiPSC-derived spheroid and HIO viability was assessed at different time-points after encapsulation. (d)

Transmitted light microscopy images of hESC-derived HIO generation within 4.0% PEG-4MAL-RGD hydrogels. (a,c,d) These organoids were never encapsulated within Matrigel[TM]. Black arrows show epithelial budding. Bars, 500 μm. Three independent experiments were performed and data is presented for one of the experiments. All experiments performed with 12 PEG-4MAL/Matrigel[TM] per experimental condition.

The strong dependence of spheroid and HIO viability on hydrogel polymer density suggests that the mechanical properties of these synthetic matrices regulate organoid survival. However, varying polymer density also alters the mesh size for these networks which can impact diffusional properties of the hydrogel. It is not possible to uncouple mechanical properties from diffusional properties over the full range of polymer densities (3.5%-12.0%) examined in this study. However, we compared organoid viability and size in RGD-functionalized hydrogels from different macromer sizes (20 vs. 40 kDa) but different polymer densities (4.0% vs. 8.0%) and engineered to have equivalent crosslinking densities (Fig. 7a-c). These hydrogels exhibit different diffusive characteristics/permeability caused by the differences in macromer arm length but have equivalent mechanical properties due to equivalent crosslinking densities[9]. ESC-derived spheroids developed normally into HIOs after 5 days of encapsulation in either hydrogel formulation showing no differences in HIO viability (Fig. 7a,b), and no differences in projected area and longest distance between two points along the projected area (Feret diameter; Fig. 7c). These results suggest that polymer density-dependent spheroid survival and development into HIOs is related to hydrogel mechanical properties. Furthermore, we evaluated the role of known mechanotransduction pathways on spheroid survival. Inhibition of nuclear translocation of yes-associated protein (YAP), which has been implicated in mechanostransduction and regulation of intestinal stem cell self-renewal[100], using verteporfin resulted in significant cell death for spheroids encapsulated in PEG-

4MAL hydrogels compared to vehicle control (Fig. 7d-f). Treatment with blebbistatin or Y-27632, which inhibit myosin II and Rho-associated kinase[105,106], respectively, resulted in dose-dependent increases in apoptosis and spheroid death at 1 d post-encapsulation (Fig. 7d-f). These results provide a preliminary indication that YAP and cellular contractility are important in the initial stages of human intestinal spheroid survival and development into HIOs.
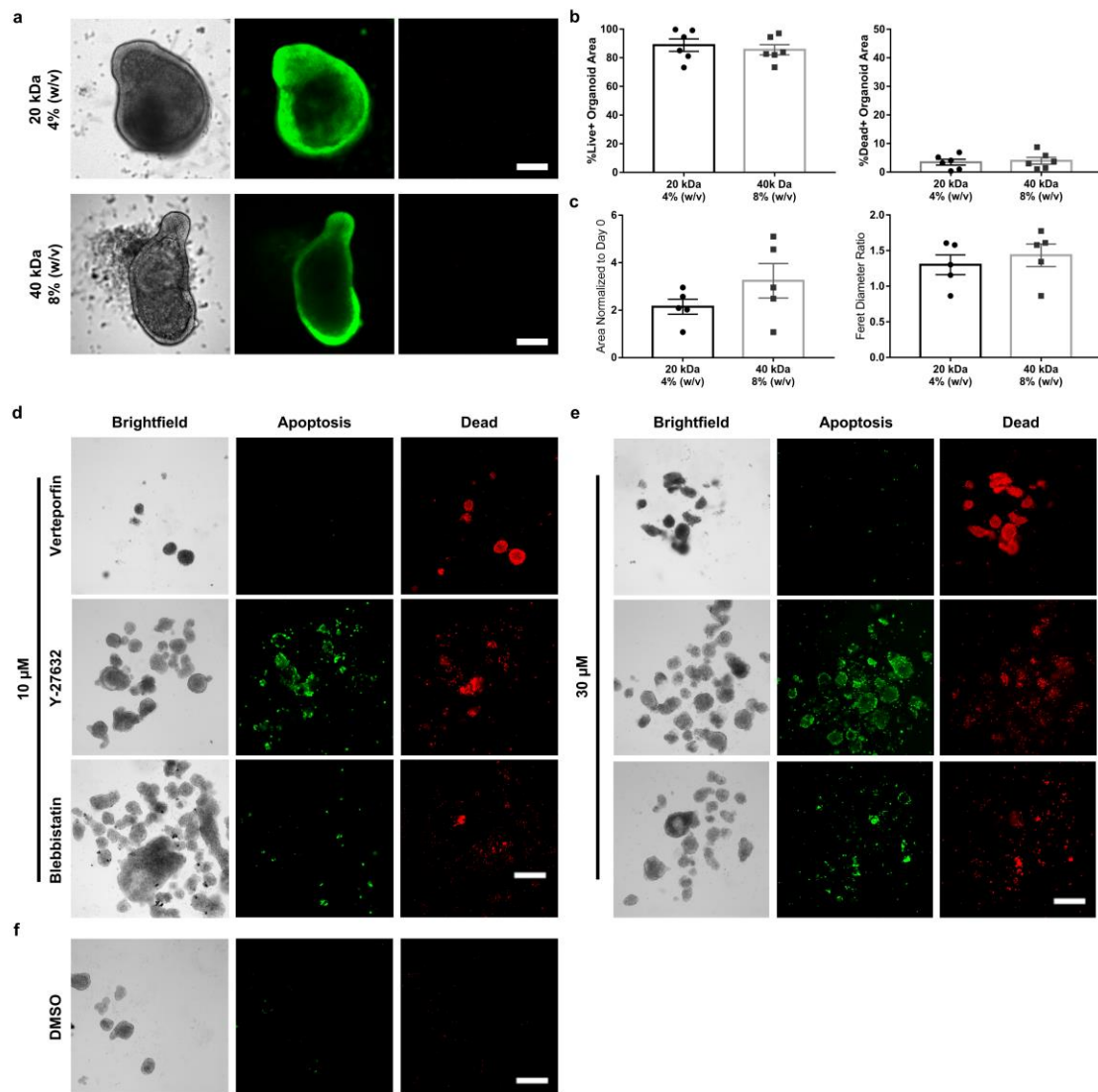
Figure 7: PEG-4MAL hydrogels with different macromer sizes and mediators of mechanotransduction are essential for hESC-derived spheroid survival. (a) Transmitted

light and fluorescence microscopy images of HIO generation within 20 kDa (4.0%) or 40 kDa (8.0%) PEG-4MAL-RGD hydrogels. HIO viability was assessed at 5 d after encapsulation. (b) Percentage of total organoid area stained for live or dead (mean ± SEM) after 5 d of encapsulation (n = 6 organoids analyzed per condition). (c) HIO projected area and Feret diameter normalized to Day 0 values (mean ± SEM) after 5 d of encapsulation (n = 5 organoids analyzed per condition). (b,c) Unpaired two-tailed t-test with Welch's correction showed no significant differences between HIO viability or HIO size parameters within 20 kDa (4.0%) and 40 kDa (8.0%) PEG-4MAL-RGD ($P > 0.05$). (d) Transmitted light and fluorescence microscopy images of spheroids cultured within 4.0% PEG-4MAL-RGD hydrogels supplemented with (d) 10 µM or (e) 30 µM of verteporfin, Y-27632 or blebbistatin, or (f) DMSO (vehicle control). Spheroids death was assessed by annexin-V (apoptosis) and propidium iodide (dead) labeling at 1 d after encapsulation. Bars, 100 µm. One experiment was performed with 12 PEG-4MAL hydrogels per experimental condition.

We next analyzed HIO generation from ESC-derived spheroids cultured within the engineered synthetic matrix (4.0% polymer density, 2.0 mM RGD, GPQ-W crosslinker). Intestinal spheroids cultured within PEG-4MAL hydrogels grew in size over 7 d as shown by a 2-fold increase in projected area (Fig. 5b) and 1.4-fold increase in Feret diameter (Fig. 5c) as compared to the day of encapsulation (Day 0; Fig. 5b,c). There were no differences in spheroid area, diameter, or growth rates between spheroids cultured in PEG-4MAL hydrogels and Matrigel[TM] (Fig. 5b,c). Similar to our observations for established HIOs, spheroids changed shape during expansion and displayed epithelial budding at the interface with the hydrogel and cell outgrowths migrating into the hydrogel (Fig. 6d). During HIO development, spheroids cultured in PEG-4MAL hydrogels were passaged in a similar manner as previously described for Matrigel[98,107]. Immunostaining analyses at 21 d post-encapsulation demonstrated that organoids generated in engineered PEG-4MAL hydrogels were proliferating as shown by Ki67 labeling, had polarized distribution of apical EZRIN and basolateral β-CATENIN, and expressed ZO-1 in the apical junctional complex (Fig. 7d,e). These staining patterns were identical to organoids generated in Matrigel[TM]. Quantitative reverse transcription polymerase chain reaction (RT-qPCR) confirmed that

expression levels of pluripotency (OCT4), endoderm (FOXA2), and epithelial junction (ZO1, ECAD and CLDN2) markers in hydrogel-encapsulated spheroids were comparable to those embedded in Matrigel^{TM} and had similar behaviors during early timepoints while developing into HIOs (Fig. 8). Finally, to test whether these synthetic matrices are suitable for the culture of other human organoids, we embedded human lung organoids (HLOs)[108,109] in engineered PEG-4MAL hydrogels (Fig. 9). HLOs cultured in PEG-4MAL hydrogels maintained high viability 7 d after encapsulation (Fig. 9a), and demonstrated an organized lung epithelium (ECAD), lumen formation, and specific markers for lung epithelium (NKX2.1) and airway basal cells (P63) as assessed by immunostaining analyses (Fig. 9b)[108,109]. Taken together, these results demonstrate that this fully synthetic hydrogel supports the generation of ESC- and iPSC-derived HIOs from the intestinal spheroid stage without the use of Matrigel^{TM}, and has the potential to be adapted for the generation of different human organoids.
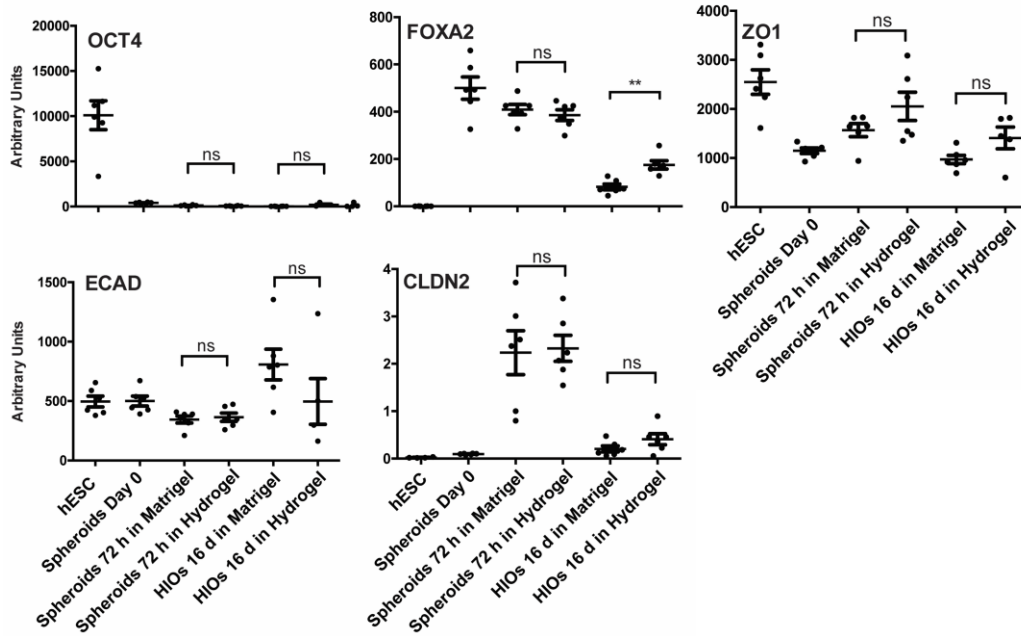
Figure 8: Gene expression levels of PEG-4MAL-encapsulated spheroids are comparable to those embedded in Matrigel™. RNA levels of pluripotency (OCT4), endoderm (FOXA2), and epithelial junction (ZO1, ECAD and CLDN2) genes, as quantified by RT-qPCR (mean ± SEM; n = 6 samples per condition). Unpaired two-tailed t-test was used to identify statistical differences between matrix types (**$P < 0.01$; ns, not significant). One experiment was performed. Primer sequences are provided in Supplementary Table 1.

Primer sequences for RT-qPCR

Human gene	Forward primer	Reverse primer
4-Oct	gtggaggaagctgacaacaa	ggttctcgatactggttcgc
FOXA2	cgactggagcagctactatgc	tacgtgttcatgccgttcat
CDX2	gggctctctgagaggcaggt	ggtgacggtggggtttagca
ECAD	ttgacgccgagagctacac	gaccggtgcaatcttcaaa
CLDN2	aaggctctgcaaagaactgc	ctgccaggctgacttctctc
ZO1	gggaacaacatagagtgacgc	ccccactctgaaaatgagga

Table 1: Primer Sequences for RT-qPCR.
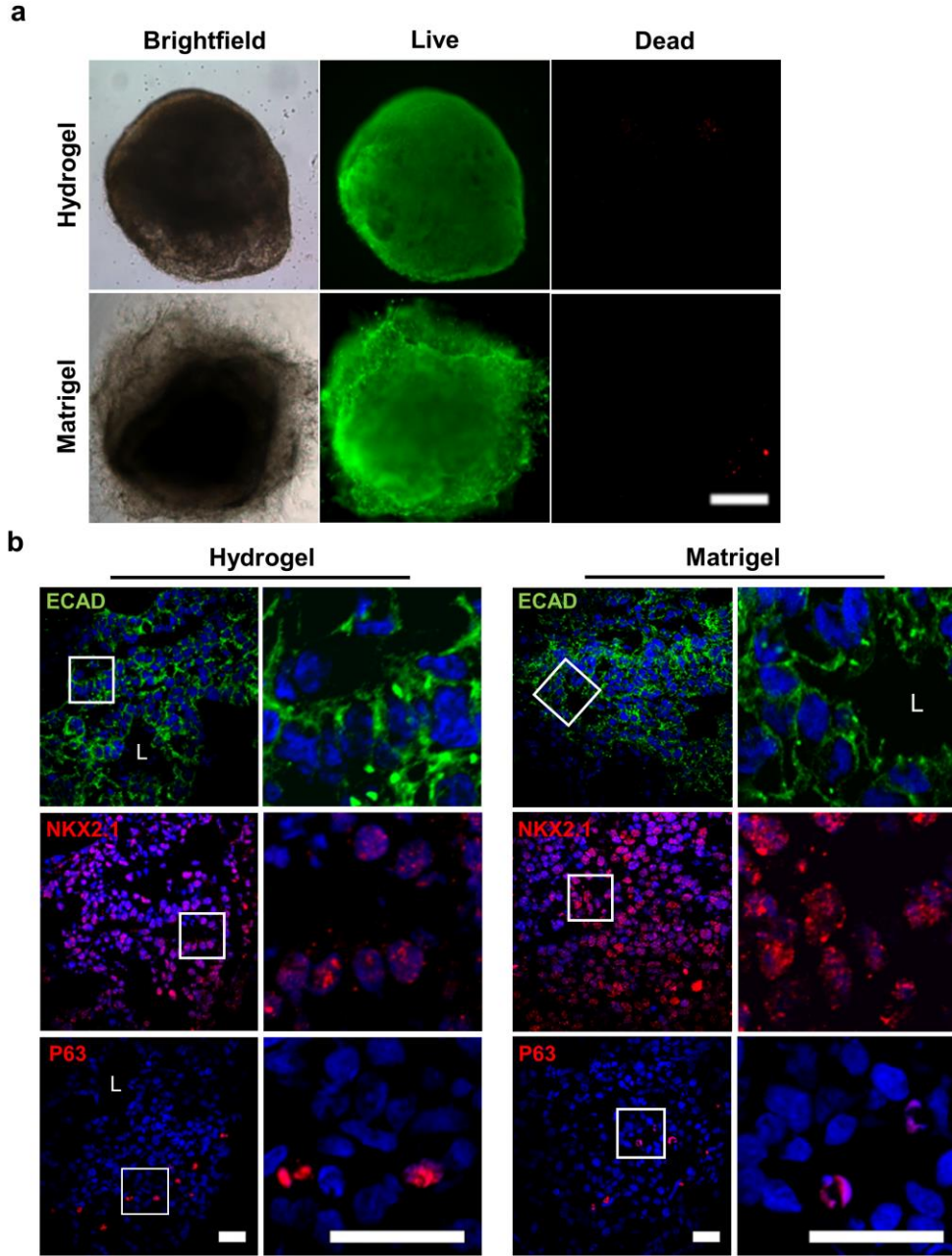
Figure 9: PEG-4MAL hydrogel supports HLO development comparable to Matrigel^{TM}. (a) Transmitted light and fluorescence microscopy images of HIOs cultured in 4.0% PEG-4MAL-RGD hydrogels or Matrigel^{TM}. HIO viability was assessed at 7 d after encapsulation. Bar, 500 μm. (b) Fluorescence microscopy images of HLO at 7 d after encapsulation in 4.0% PEG-4MAL-RGD hydrogel or Matrigel^{TM} and labeled for e-cadherin (ECAD), lung epithelia (NKX2.1), and basal cells (P63). DAPI, counterstain. "L" indicates HLO lumen. Bars, 25 μm. One experiment was performed with 6 PEG-4MAL/Matrigel^{TM} per condition (a,b).

3.3.4   *Hydrogel-generated HIOs differentiate in vivo*

We next examined the potential of hydrogel-grown HIOs to differentiate into mature intestinal tissue *in vivo* as previously demonstrated[104,110]. mCherry-expressing spheroids that were embedded and grown within engineered PEG-4MAL hydrogels or in Matrigel[TM] for 3 weeks were recovered from their respective matrix and implanted under the kidney capsule of immunocompromised NSG mice (Fig. 10). In addition, HIOs grown in Matrigel[TM] for 2 weeks and then transferred and cultured within PEG-4MAL hydrogels for 1 week (Hydrogel-maintained) were implanted under the kidney capsule (Fig. 10a,b,d). After 12 weeks, implanted kidneys contained mCherry-expressing HIOs that were 10- to 40-fold larger in area than at the time of implantation (Fig. 10a,b), consistent with previous reports. Dissected PEG-4MAL-generated HIOs showed differentiated intestinal epithelium that resembled mature human intestine with crypt-villus architecture and underlying lamina propria, muscularis mucosae and submucosa[104], with structured collagen fibers (trichrome) and presence of differentiated goblet cells (alcian blue), comparable to Matrigel[TM]-generated and Hydrogel-maintained organoids (Fig. 10c,d). Polarized epithelial differentiation of PEG-4MAL hydrogel-generated HIOs was demonstrated by immunostaining for β-CATENIN, EZRIN, ZO-1 and ECAD (Fig. 11a). Additionally, PEG-4MAL-generated organoid epithelium showed localized cell proliferation (KI67) at the base of the crypt where the intestinal stem cells reside, and expressed characteristic markers for the intestinal epithelial protein CDX2, enteroendocrine cells (CHGA), goblet cells (MUC2), and tuft cells (DCLK1)[111]. Furthermore, PEG-4MAL-generated HIOs expressed PDX1, demonstrating a duodenum regional identity (Fig. 11a)[98]. Expression was comparable to Matrigel[TM]-generated organoids and Hydrogel-maintained organoids (Fig.

11b). These results demonstrate that HIOs generated in the engineered synthetic matrix can differentiate into mature intestinal tissue in an *in vivo* environment to the same extent as HIOs generated within Matrigel[TM]. These findings establish engineered synthetic PEG-4MAL hydrogels as a robust alternative to Matrigel[TM] with significant implications for translational medicine.
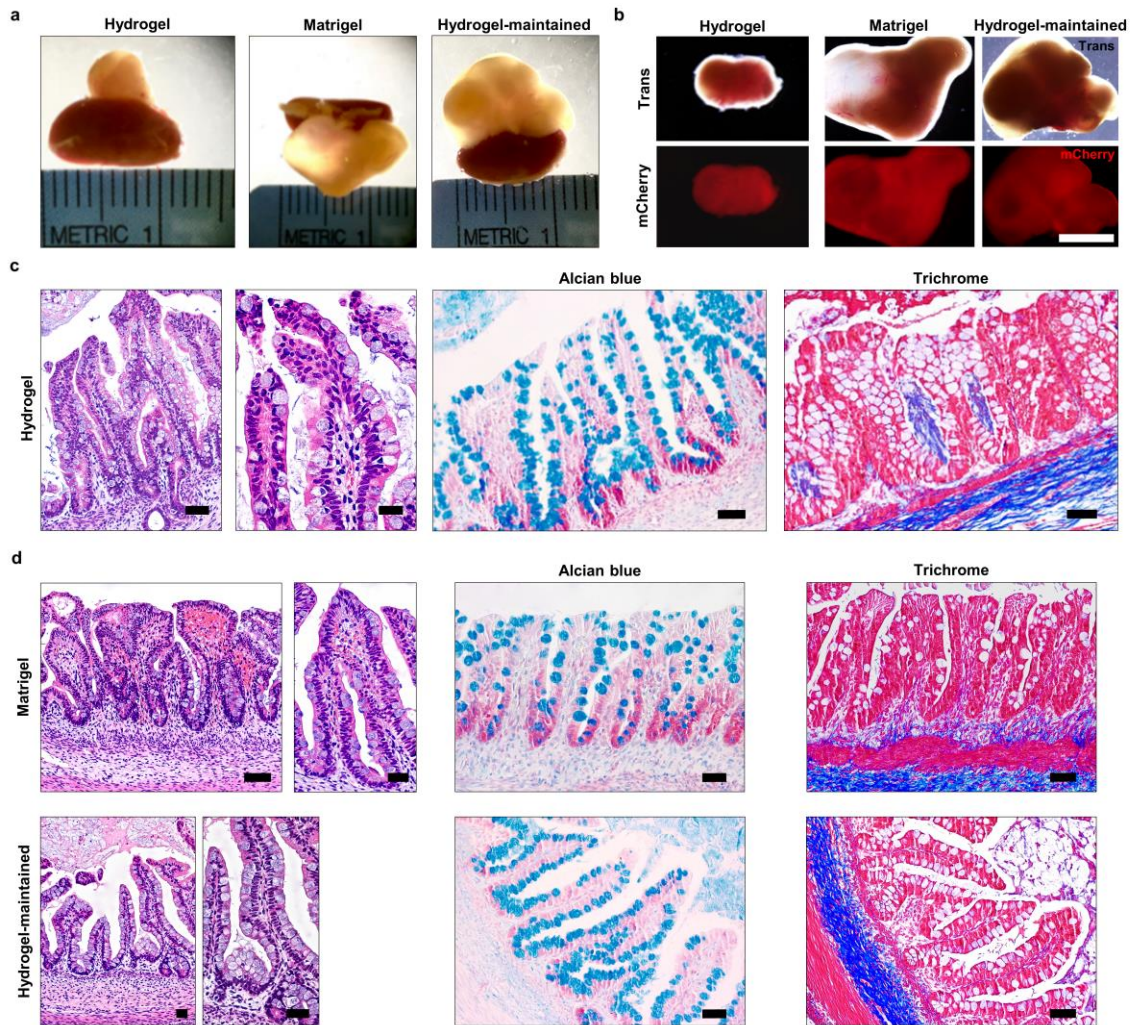
Figure 10: PEG-4MAL-generated HIOs develop a mature intestinal tissue structure *in vivo*. (a) Micrographs of dissected kidneys containing HIOs generated within PEG-4MAL-RGD, Matrigel[TM], or generated within Matrigel[TM] and maintained within PEG-4MAL-RGD. (b) Transmitted light and fluorescence microscopy (mCherry) images of harvested organoids. Bar, 0.5 cm. (c,d) H&E staining demonstrates mature human intestinal crypt-villus structure, and Alcian blue and trichrome staining reveal presence of

differentiated goblet cells and organized collagen fibers. Bar, 100 μm. One experiment was performed using 3 mice per experimental condition.
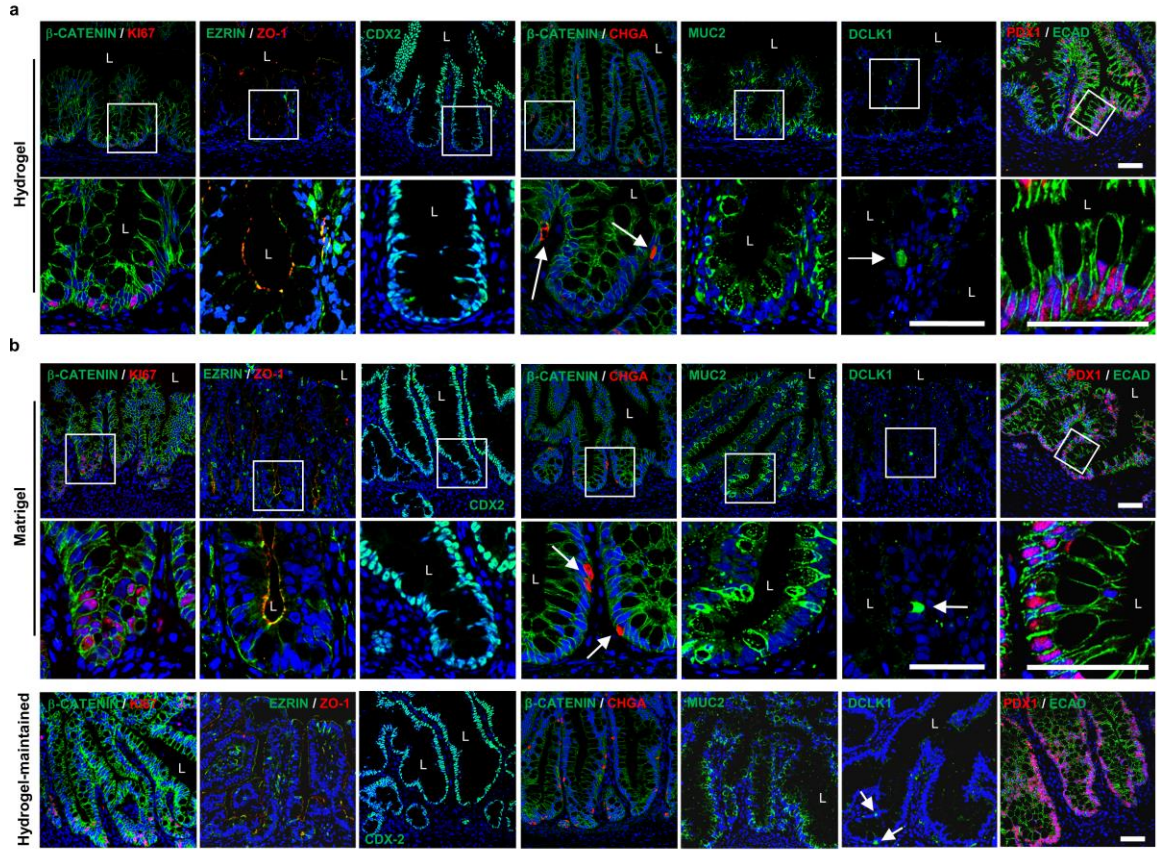
Figure 11: PEG-4MAL-generated HIOs differentiate into mature intestinal tissue *in vivo*. (a,b) Fluorescence microscopy images of HIOs generated within (a) PEG-4MAL-RGD, (b) Matrigel[TM], or generated within Matrigel[TM] and maintained within PEG-4MAL-RGD, and labeled for β-CATENIN, proliferative cells (KI67), epithelial apical polarity (EZRIN) and junctions (ZO-1 and ECAD), intestinal epithelial protein CDX2, enteroendocrine cells (CHGA), goblet cells (MUC2), tuft cells (DCLK1) and small intestinal marker (duodenum; PDX1). DAPI, counterstain. "L" indicates HIO lumen. White arrows show enteroendocrine cells or tuft cells. Bars, 50 μm. One experiment was performed using 3 mice per experimental condition.

3.3.5 Hydrogels as a HIO delivery vehicle to heal colonic wounds

A key advantage of the PEG-4MAL hydrogel system is control over gelling time

so that the hydrogel components can be injected as a solution that gels *in situ*[11]. We

therefore explored the use of the engineered hydrogel as a delivery vehicle for HIOs into murine intestinal mucosal wounds using a murine colonoscope. HIOs generated in PEG-4MAL hydrogels or Matrigel[TM] were recovered from their matrix, mixed with the hydrogel precursor solution, and injected at the site of mechanically-induced mucosal wounds in the distal colon of immunocompromised mice (Fig. 12a, Fig.136a)[112]. Wound closure was evaluated using a colonoscope, and fluorescence imaging showed localized expression of mCherry-positive tissue at the wound site 5 d post-injection (Fig. 12b). Immunostaining at 4 weeks post-injection demonstrated that HIO delivery via the synthetic hydrogel resulted in HIO engraftment into host intestinal epithelial tissue as shown by positive staining for human nuclei (NUMA) to detect either HIOs generated in the PEG-4MAL hydrogel or Matrigel[TM] (Fig. 12c). Importantly, no staining was evident for no-injection control, only hydrogel, and HIOs injected in saline (Fig. 12c), demonstrating that the hydrogel delivery vehicle is required for HIO engraftment and wound repair. Examination of HIO engraftment at the wound edge demonstrated staining for human cells adjacent to host tissue which stained negative for human markers. Engraftment of human cells into the colonic wound was also confirmed by positive staining for human mitochondria (HUMIT; Fig. 13b). Furthermore, colonic wounds treated with HIOs delivered with hydrogel showed positive staining for an *OLFM4* probe specific to human cells at the base of the crypt-like domain (Fig. 12d; Fig. 13c), a pattern consistent with staining in the normal adult human colon (Fig. 13c), which is also consistent with previous reports of human OLFM4 protein and/or mRNA localization[113-115]. Additionally, several negatively stained human crypt-like domains were adjacent to mouse intestinal crypts which stained positive for a mouse-specific *Lgr5* probe (Fig. 13d) via *in situ* hybridization[116]. These observations were

compared to control tissue sections from immunocompromised mice that did not undergo colonic injuries or received HIO injections (Fig. 12d; Fig. 13d).

We also examined whether delivered HIOs promote colonic mucosal wound repair (Fig. 12e). Strikingly, delivery of HIOs to colonic wounds using the hydrogel carrier significantly increased wound closure compared to untreated wounds and wounds treated with hydrogel alone or HIOs without the carrier (Fig. 12e). No differences were observed in wound closure between HIOs generated in the synthetic hydrogels and Matrigel^{TM}. Taken together, these results demonstrate that the engineered PEG-4MAL hydrogel serves as an injectable delivery vehicle that supports localized HIO engraftment in colonic mucosal wounds and enhances wound closure. These findings establish the clinical translational potential of the synthetic hydrogel as an *in vivo* delivery vehicle for hPSC-derived HIOs and provide proof-of-concept that HIOs may be used therapeutically to treat intestinal injury or disease.
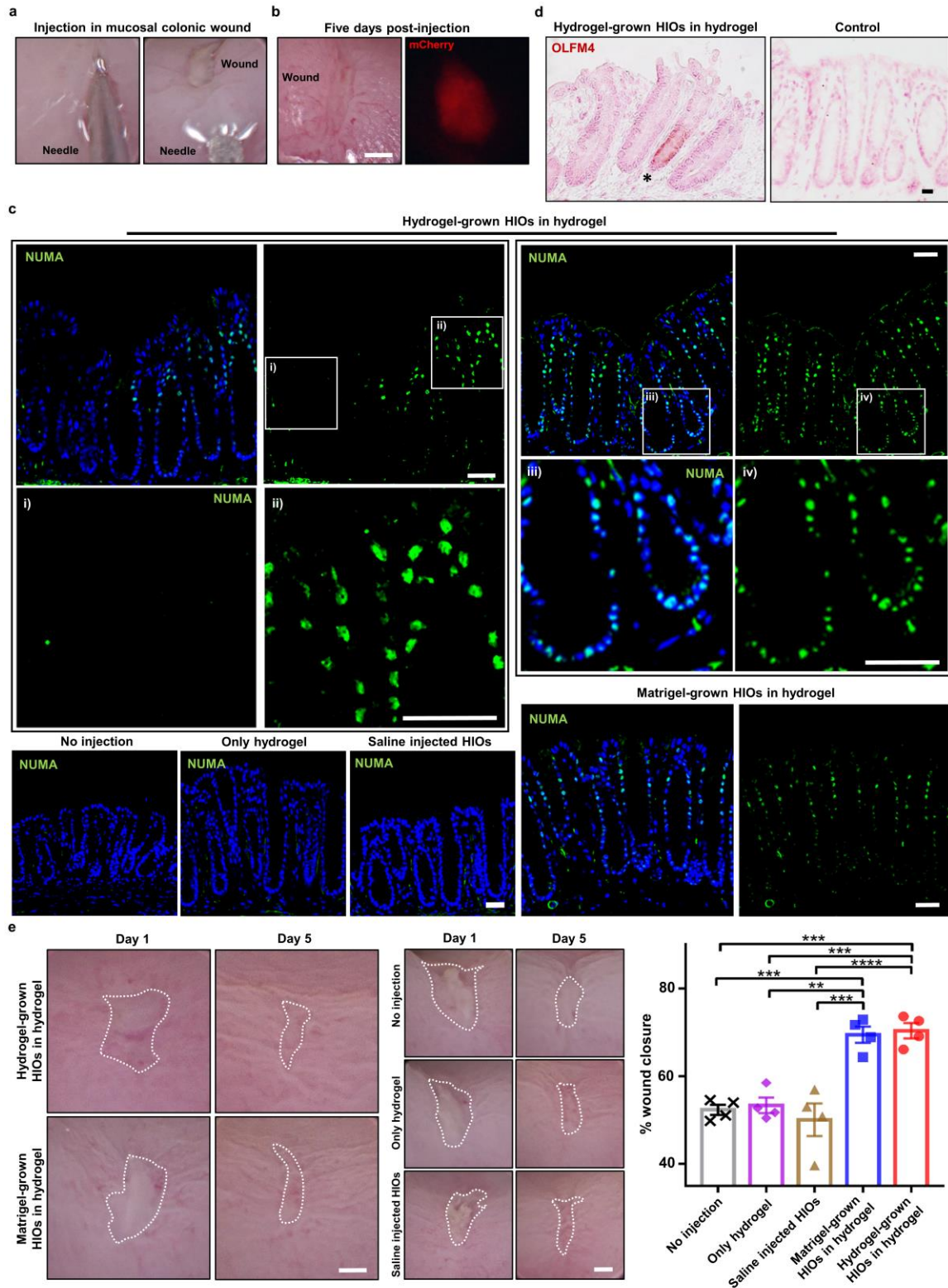
Figure 12: PEG-4MAL serves as an injectable delivery vehicle to promote HIO engraftment and wound closure. (a) PEG-4MAL-generated HIOs mixed with engineered

hydrogel precursor solutions were injected underneath mechanically-induced mucosal wounds, as seen through the colonoscope camera. (b) Mechanically-induced mucosal wound and fluorescence imaging (mCherry) at the wound site at 5 d post-injection. Bar, 500 μm. (c) Fluorescence microscopy images of murine colonic tissue at the wound site labeled for human cell nuclei (NUMA) at 4 weeks post-delivery. Left: Images from wound edge showing insets from i) adjacent host tissue and ii) wound. Right: Images from wound center showing insets at wound site. DAPI, counterstain. Bars, 100 μm. (d) *In situ* hybridization, stained for human OLFM4+ cells. Bar, 50 μm. (e) Images of mucosal wounds at 1 d (prior to injection) or 5 d post-injury in murine colon as seen through the colonoscope camera. Mucosal wound area at 5 d post-injury was normalized to day 1 (prior to injection) values (mean ± SEM). Five colonic wounds per mouse were analyzed and averaged (n = 4 mice per condition). One-way ANOVA with Tukey's multiple comparisons test showed significant difference between Hydrogel-grown HIOs in hydrogel (●) or Matrigel-grown HIOs in hydrogel (■) and Saline injected HIOs (▲) Only hydrogel (♦) or No injection group (X) (**$P < 0.01$, ***$P < 0.001$, ****$P < 0.0001$). Bars, 500 μm. Two independent experiments were performed and data is presented for one of the experiments. Experiments performed with 4 mice per experimental group (five colonic wounds/injections per mouse; a-e).
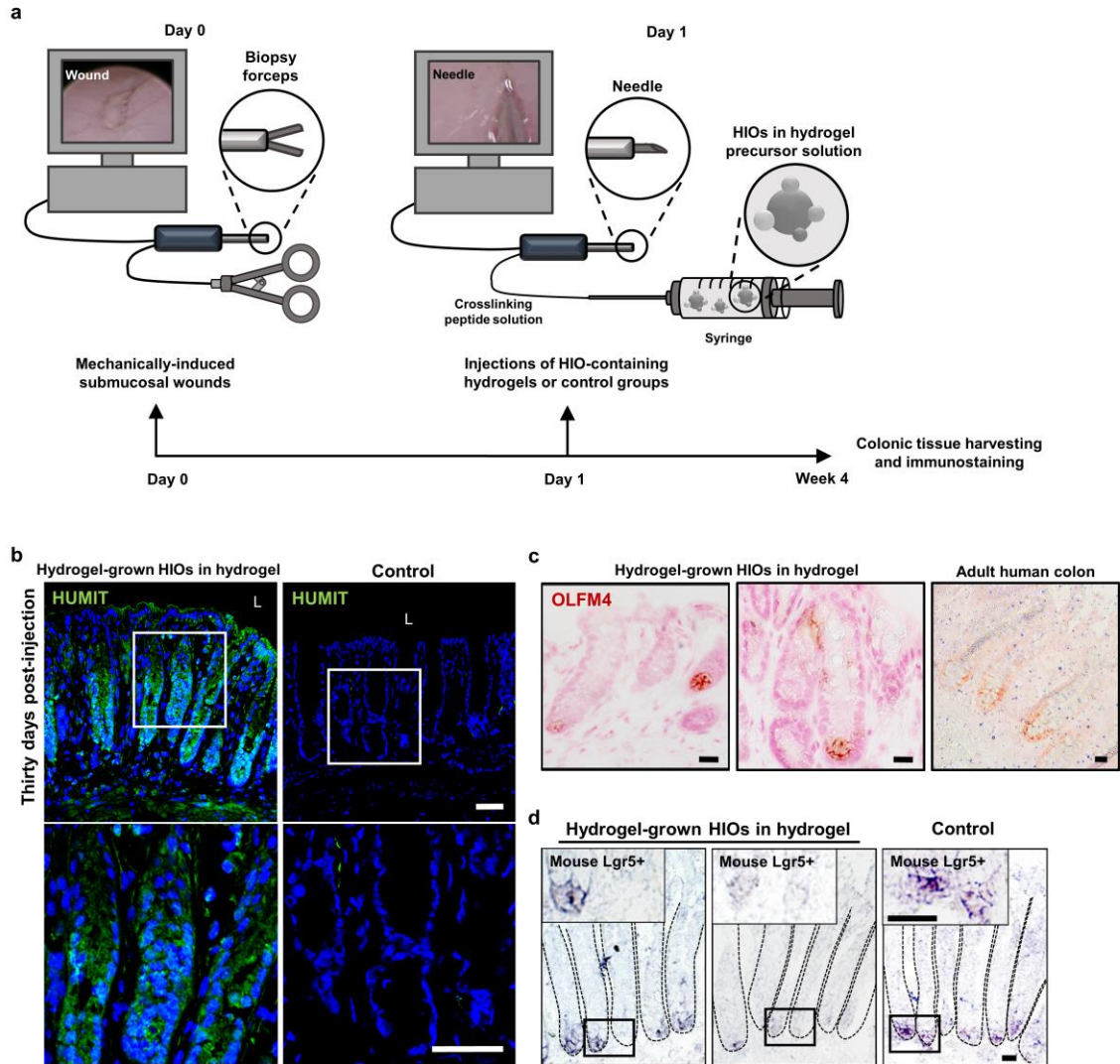
Figure 13: PEG-4MAL hydrogel serves as an injectable delivery vehicle in colonic mucosal wound model and promotes HIO engraftment. (a) Mechanically-induced submucosal wounds were performed in the distal colon of mice using a mechanical probe through a mouse colonoscope. One day post-wounding HIOs generated in engineered 4% PEG-4MAL-RGD hydrogels or Matrigel^{TM} were recovered from the matrix, mixed with the engineered hydrogel precursor solutions, and injected underneath the submucosal wounds. A group with no injections, HIOs injected in saline, or injection of HIO-free hydrogel precursor solutions were used as control groups. Distal colon tissue harvest, immunostaining and imaging was performed 4 weeks post-wounding. (b) Fluorescent microscopy images labeled for human mitochondria (HUMIT) of murine colonic tissue at the wound site at 4 weeks post-injection or control tissue. DAPI, counterstain. "L" indicates HIO lumen. Bars, 100 μm. (c) *In situ* hybridization images of (c) control adult human colon or sections taken at the mouse colonic wound site stained for human OLFM4+ cells. (d) *In situ* hybridization images of tissue sections from mice colon that did not undergo colonic injuries or received HIO injections (control) and sections taken at the mouse colonic wound

45

site stained for mouse Lgr5+ intestinal stem cells. Bars, 50 μm. Two independent experiments were performed and data is presented for one of the experiments. Experiments performed with 4 mice per experimental group (five colonic wounds/injections per mouse; b-d).

3.4   Discussion

In this study, we engineered a completely synthetic hydrogel that supports *in vitro* generation of intestinal organoids from hPSC-derived spheroids without the need of Matrigel[TM] encapsulation. Both mechanical and biochemical properties of the synthetic ECM were important to intestinal organoid formation, and we identified an optimal formulation that supports intestinal spheroid survival, expansion and epithelial differentiation into HIOs and differentiation into mature intestinal tissue *in vivo* to similar levels as Matrigel[TM]. Additionally, we showed that this synthetic matrix supports the development of other human organoids such as HLOs. The requirement for specific mechanical and cell adhesive properties in the synthetic matrix is consistent with previous work showing that epithelial cell cyst growth, polarization, and lumen formation are restricted to a narrow range of ECM elasticity and that adhesive peptide type regulates apicobasal polarity and lumenogenesis during epithelial morphogenesis in 3D cultures[9]. Interestingly, the mechanical properties and protease degradation characteristics that supported hPSC-derived organoids in this study are different from those recently identified for murine *Lrg5+* intestinal stem cell growth and organoid formation[100], which involved more complex, mechanically dynamic properties, and suggest differences between these two organoid sources. This fully synthetic matrix addresses major limitations of Matrigel[TM] associated with lot-to-lot compositional and structural variability and its tumor-derived nature that severely restrict scale-up applications and clinical translation.

We also established the use of the engineered hydrogel as a delivery vehicle for HIOs to murine intestinal mucosal wounds using a murine colonoscope. Although other studies have focused on the delivery of murine intestinal organoids into the colonic lumen as a suspension[24], we showed that absence of a delivery vehicle reduces HIO engraftment at the implantation site. Injection of hydrogel liquid precursors and HIOs to mucosal wounds resulted in an *in situ* polymerized hydrogel that supported localized organoid engraftment and enhanced wound repair. Therefore, this delivery strategy forms a basis for the development of HIO-based therapies to treat gastrointestinal diseases in humans involving intestinal epithelial wounds (e.g., IBD). Furthermore, the modular nature of this hydrogel platform allows for the adaptation to *in vitro* generation and *in vivo* delivery of other human PSC-derived organoids (e.g., lung) for regenerative medicine.

3.5   Methods

Immunofluorescence analysis

For immunofluorescence labeling of frozen sections from colon, HIOs, kidney capsule implanted-HIOs or HLOs, these were fixed with 3.7% (w/v) paraformaldehyde at room temperature for 15 min, followed by 0.5 % (w/v) Triton X-100 for 5 min. Primary antibody incubation was performed overnight at a 1:100 dilution, unless stated otherwise. Secondary antibody incubation was performed for 1 h at a 1:2000 dilution. Detailed information on the antibodies used including their resources (company names, catalogue numbers) and dilutions are provided in the Reporting Summary.

Differentiation of hPSCs into intestinal spheroids or HLOs

All work using human pluripotent stem cells was approved by the University of Michigan Human Pluripotent Stem Cell Oversight Committee (HPSCRO). Stem cell lines are routinely monitored for chromosomal karyotype, pluripotency (using a panel of antibody and RT-qPCR markers), and for the ability to undergo multi-lineage differentiation. For intestinal spheroid generation, mycoplasma-free human ES cells (H9, NIH registry #0062) and iPS cells (line 20.1, source as previously described[98]) were cultured on Matrigel™-coated plates and differentiated into intestinal tissue as previously described[98]. Floating spheroids present in the cultures on day 4 and day 5 of mid/hindgut induction were harvested for use in subsequent experiments. In some experiments, hESCs expressing a constitutively active H2BmCherry fluorescent reporter were used. This line was generated by infecting hESCs with a lentivirus containing PGK-H2BmCherry, which was a gift from Mark Mercola (Addgene plasmid # 21217)[117]. For HLO generation, human ES cells (UM63-1, NIH registry #0277) were maintained, differentiated and expanded into HLOs as previously described[109].

Hydrogel formation and *in vitro* intestinal spheroid/HIO

To prepare PEG hydrogels, PEG-4MAL macromer (MW 22,000 or 44,000; Laysan Bio) was dissolved in 4-(2-hydroxyethyl)piperazine-1-ethanesulfonic acid (HEPES) buffer (20 mM in DPBS, pH 7.4). Adhesive and GPQ-W crosslinking peptides were custom synthesized by AAPPTec. Adhesive peptides RGD (GRGDSPC), AG73 (CGGRKRLQVQLSIRT), GFOGER (GYGGGP(GPP)$_5$GFOGER (GPP)$_5$GPC), IKVAV (CGGAASIKVAVSADR) and RDG (GRDGSPC) were dissolved in HEPES at 10.0 mM (5X final ligand density) and mixed with PEG-4MAL at a 2:1 PEG-4MAL/ligand ratio to generate functionalized PEG-4MAL precursor. Bis-cysteine crosslinking peptide GPQ-W

(GCRDGPQG↓IWGQDRCG; ↓ denotes enzymatic cleavage site) or non-degradable crosslinking agent DTT (1,4-dithiothreitol; 3483-12-3, Sigma) was dissolved in HEPES at a density corresponding to 1:1 maleimide/cysteine ratio after accounting for maleimide groups reacted with adhesive peptide. For HIOs encapsulation, spheroids were embedded and expanded in Matrigel[TM] for up to 30 d. Resulting HIOs were dislodged from the Matrigel[TM] and resuspended at 5X final density (final density: 2-4 HIOs/hydrogel) in intestine growth medium[118] and kept on ice. For human intestinal spheroid encapsulation, spheroids were harvested immediately after differentiation and were resuspended at 5X final density (final density: 20-30 spheroids/hydrogel) in intestine growth medium and kept on ice. For HLOs encapsulation, these were dislodged from the Matrigel[TM] and resuspended at 5X final density (final density: 2-4 HLOs/hydrogel) in foregut growth medium[107,108] and kept on ice. To form hydrogels, adhesive peptide-functionalized PEG-4MAL macromer, cells, and crosslinking peptide were polymerized for 20 min before addition of intestine growth medium. Matrigel[TM]-generated hPSC-derived HIOs were generated and cultured as described previously[98,118]. Passaging of HIOs cultured in PEG-4MAL hydrogels was performed similarly to tissue embedded in Matrigel[TM], as previously described[107,118]. Briefly, HIOs were dislodged from the PEG-4MAL hydrogel, transferred to a sterile Petri dish, and manually cut into halves using a scalpel. HIO halves were resuspended at 5X final density (final density: 2-4 HIOs/hydrogel) in intestine growth medium[118] and mixed with hydrogel precursor solutions to form PEG-4MAL hydrogels. HIOs were passaged up to 3 times over the course of 3 weeks. Matrigel[TM]-generated HIOs were passaged as described previously[98,118]. Sample size was established as at least 4 hydrogels per condition with the premise that an outcome present in 4 different hydrogels

under a specific condition will reveal the population behavior submitted to this given condition.

Hydrogel characterization

The storage and loss moduli of hydrogels were assessed by dynamic oscillatory strain and frequency sweeps performed on a MCR 302 stress-controlled rheometer (Anton Paar) with a 9-mm diameter, 2° cone, and plate geometry. Oscillatory frequency sweeps were used to examine the storage and loss moduli ($\omega = 0.5$–100 rad s^{-1}) at a strain of 2.31%.

Viability assay and quantification

PEG-4MAL gels were incubated in 2 µM calcein-AM (live; Life Technologies), and 1 µM TOTO-3 iodide (dead; Life Technologies) in growth medium for 1 hr. Samples were imaged using an Axiovert 35, Zeiss microscope. Quantification of viability was performed by calculating the percentage of the total projected area of a spheroid/organoid that stained positive for the live or dead stain using ImageJ (National Institute of Health, USA). The results are representative of three different experiments performed with 6 PEG-4MAL/Matrigel^{TM} per condition

Inhibition of mediators of mechanotransduction

Inhibition of YAP, myosin II or Rho-associated kinase was performed using verteporfin (SML0534, Sigma), blebbistatin (203389, Calbiochem) and Y-27632 (688002, Calbiochem), respectively, by adding 10 or 30 µM to the intestine growth medium 20 min after spheroid encapsulation in hydrogel. Cell apoptosis/death was assessed 1 d after encapsulation using Annexin V/Dead Cell Apoptosis Kit (A13201, ThermoFisher).

Samples were imaged using an Axiovert 35, Zeiss microscope. The results are representative of two different experiments performed with 6 PEG-4MAL/Matrigel^{TM} per condition.

RT-qPCR

Total RNA from hESC day 0 spheroids or HIOs grown in PEG-4MAL hydrogels or Matrigel^{TM} was extracted using the MagMax RNA isolation system and MagMax-96 total RNA isolation Kit (AM1830, ThermoFisher Scientific). cDNA was synthesized using the SuperScript VILO cDNA Synthesis Kit (11754-250, ThermoFisher Scientific). RT-qPCR was carried out using the QuantiTect SYBR Green PCR Kit (204145, Qiagen). Relative gene expression was plotted as Arbitrary Units using the formula: [2^(housekeeping gene Ct – gene of interest Ct)] x 10,000. Primer sequences for RT-qPCR are provided in Supplementary Table 2.

Animal models

All animal studies were conducted following approved protocols established by University of Michigan's Institutional Animal Care and Use Committee (IACUC) in accordance with the U.S. Department of Agriculture (USDA) Animal and Plant Health Inspection Service (APHIS) regulations and the National Institutes of Health (NIH) Office of Laboratory Animal Welfare (OLAW) regulations governing the use of vertebrate animals. Male (8 weeks old) NOD-scid IL2Rg-null (NSG) mice (Jackson Laboratory) were used for all our experiments. Sample size was established as 3 with the premise that an outcome present in 3 different animals under a specific condition will reveal the population behavior submitted to this given condition. No statistical method was used to predetermine sample size.

Kidney capsule implantation

Organoids were implanted under the kidney capsule of male NOD-scid IL2Rg-null (NSG) mice (Jackson Laboratory) as previously described (Watson et al., 2014 and Finkbeiner et al., 2015)[104]. Briefly, mice were anesthetized using 2% isofluorane. The left flank was shaved and sterilized using chlorhexidine and isopropyl alcohol. A left flank incision was used to expose the kidney. HIOs were manually placed in a subcapsular pocket of the kidney using forceps. An intraperitoneal flush of Zosyn (100 mg/kg; Pfizer) was administered prior to closure in two layers. The mice were sacrificed and transplant retrieved after 12 weeks. The results are representative of one experiment performed with 3 mice per condition (one organoid implanted per kidney capsule).

Colonic mucosal wound and HIO injections

NSG mice were anesthetized by intraperitoneal injection of a ketamine (100 mg/kg)/xylazine (10 mg/kg) solution. A high-resolution miniaturized colonoscope system equipped with biopsy forceps (Coloview Veterinary Endoscope, Karl Stortz) was used to biopsy-injure the colonic mucosa at 3–5 sites along the dorsal artery. Wound size averaged approximately 1 mm^2. HIO injection was performed on day 1 after wounding with the aid of a custom-made device comprising a 27-gauge needle (OD: 0.41 mm) connected to a small tube (Fig. 13a). Endoscopic procedures were viewed with high-resolution (1,024 × 768 pixels) live video on a flat-panel color monitor. The results are representative of two independent experiments performed with 4 mice per condition (five colonic wounds/injections per mouse).

Wound closure quantification

Mice were anesthetized by intraperitoneal injection of a ketamine (10 g/l) xylazine (8 g/l) solution (10 μl/g body weight). To create mucosal injuries in the mouse colon and to monitor their regeneration, a high-resolution colonoscopy system was used. Each wound region was digitally photographed at day 1 and day 5, and wound areas were calculated using ImageJ (National Institute of Health, USA). In each experiment, 3 - 4 lesions per mouse were examined.

In situ **hybridization (ISH)**

ISH for mouse *Lgr5* expression was performed on frozen sections fixed with 4% paraformaldehyde (PFA). Slides were permeabilized with proteinase K (3115887001, Sigma-Aldrich) for 30 min at 37°C, washed with Saline-Sodium Citrate buffer and then acetylated at room temperature for 10 min. Pre-hybridization step was performed for 1 h at 37°C in a humidified chamber. A DIG-labeled riboprobe diluted in hybridization buffer was incubated overnight at 68°C. The slides were then washed and blocked for 1 h at room temperature followed by incubation with DIG antibody (11093274910, Sigma-Aldrich) overnight at 4°C. The developer solution (11681451001, Roche) was incubated for 72 h until the *Lgr5* cells became evident. ISH for *OLFM4* was performed using the RNAscope 2.5 HD manual assay with brown chromogenic detection (Advanced Cell Diagnostics, Inc.) per manufacturer's instructions. The human 20 base pair *OLFM4* probe was generated by Advanced Cell Diagnostics targeting 20 base pairs within 1111-2222 of *OLFM4* (gene accession NM_006418.4) and is commercially available. The results are representative of two independent experiments performed with 4 mice per condition (five colonic wounds/injections per mouse).

Statistics

All statistical analyses were performed using GraphPad Prism 6.0. Statistical significance was calculated by one-way analysis of variance (ANOVA) with Tukey's multiple comparisons test, two-way repeated measures ANOVA, or unpaired t-test with Welch's correction, as described in the figure legends. P-values of statistical significance are represented as $****P < 0.0001$, $***P < 0.001$, $**P < 0.01$, $*P < 0.05$.

CHAPTER 4.   SYNTHETIC HYDROGELS RECAPITULATE EPITHELIAL TUBULAR MORPHOGENETIC PROGRAM

4.1   Abstract

Recapitulating cell-extracellular matrix (ECM) interactions that regulate epithelial morphogenesis in a 3D *in vitro* environment is important to understand the formation of rudimentary epithelial organs. Therefore, naturally-derived materials have been used in organotypic cultures to recreate different kidney-associated tubular morphogenetic developmental programs. However, the lot-to-lot variability and inability of these materials to uncouple biophysical and biochemical matrix properties limit their reliability and use for the understanding of the independent contributions of physicochemical matrix properties to epithelial morphogenesis. Therefore, we engineered a fully defined, synthetic PEG-4MAL hydrogel with independent control over proteolytic degradation, mechanical properties, and adhesive ligand type and density to study the impact of ECM properties on the epithelial tubulogenesis program. We showed that sensitivity of the synthetic material to membrane-type matrix metalloproteinase-1 (MT1-MMP) was required for epithelial tubulogenesis. Additionally, a narrow range of matrix elasticity, presentation of specific adhesive ligand type, and a threshold level of adhesive ligand density of the MT1-MMP-sensitive hydrogel were important to direct epithelial tubulogenesis. Finally, we demonstrated that the engineered PEG-4MAL hydrogel supported organization of epithelial tubules that displayed lumen formation, polarization and secreted ECM components. The PEG-4MAL hydrogel serves as a platform to recapitulate epithelial tubular morphogenetic programs and to characterize the independent contributions of the

matrix properties to distinctive normal or abnormal epithelial phenotypes, while overcoming the limitations of natural materials.

4.2   Introduction

The extracellular matrix (ECM) provides mechanical and biochemical signals that convey important signals in modulating renal epithelium morphogenesis[9,119]. For instance, the ECM provides physical support for the three-dimensional (3D) spatial organization of renal epithelial cells into tubular structures. Additionally, interactions between ECM components and integrins receptors regulate mechanotransduction pathways and modulate the activity of signaling molecules (e.g. Wnt family) that mediate the formation of a polarized and differentiated epithelium[119,120]. In order to better understand these ECM contributions to epithelial tubulogenesis, 3D collagen gels and Matrigel[TM] have been used in organotypic *in vitro* cultures that recreate the epithelial morphogenetic developmental program[121,122]. In these naturally-derived matrices, murine inner medullary collecting duct (IMCD) cells proliferate from single cells to form multicellular tubular structures, recapitulating the morphogenetic program of a rudimentary epithelial organ[123,124] (Fig. 14a). Nevertheless, these natural matrices are inherently limited by lot-to-lot compositional and structural variability, and the inability to decouple biochemical and biomechanical properties[8,18]. Additionally, in the case of Matrigel[TM], its tumor-derived nature limits its translational potential[4,8]. Recently, a synthetic material containing animal-derived components that support epithelial tubulogenesis programs have been reported as an alternative to natural matrices[125].

Here, we describe a synthetic hydrogel that supports the epithelial morphogenesis program of IMCD cells without the use of naturally-derived materials or naturally-based

hydrogels. IMCD cells within PEG-4MAL hydrogels exhibit different multicellular structure phenotypes that can be classified as either "smooth clusters", "spiked clusters"' which were clusters with extensions, or "tubules", in accordance with previous reports[125,126] (Fig. 14b-d). Protease sensitivity, matrix elasticity, and adhesive ligand type and density of the synthetic hydrogel were important parameters to be considered for the engineering of a fully-synthetic matrix that supported the IMCD cell tubulogenesis program. The modular, well-defined design of this synthetic matrix overcomes limitations associated with the use of naturally-derived materials.

We selected a hydrogel platform based on a four-armed, maleimide-terminated poly(ethylene glycol) (PEG-4MAL) macromer that presents elements inspired by the ECM such as cell adhesion peptides and matrix metalloproteinase (MMP)-sensitive crosslinking peptides. Although other synthetic hydrogel systems have been developed to mimic properties of natural ECM, the PEG-4MAL hydrogel platform exhibits significant advantages including well-defined structure, stoichiometric incorporation of bioactive motifs, increased cytocompatibility, and improved crosslinking efficiency[9,10,127]. Additionally, the tunable properties of PEG-4MAL hydrogels allow the study of the independent contributions of the biophysical and biochemical matrix properties on both single and collective epithelial cell programs[9,127]. For instance, we showed using this platform that normal epithelial cyst growth, polarization, and lumen formation of Madin-Darby Canine Kidney (MDCK) cells were restricted to a narrow range of matrix elasticity, required a threshold level of cell-directed matrix degradability, and were dramatically regulated by adhesive peptide density[9]. Therefore, the modular design of this synthetic

matrix allows the study of the independent contributions of physicochemical matrix properties to IMCD cell tubulogenesis.
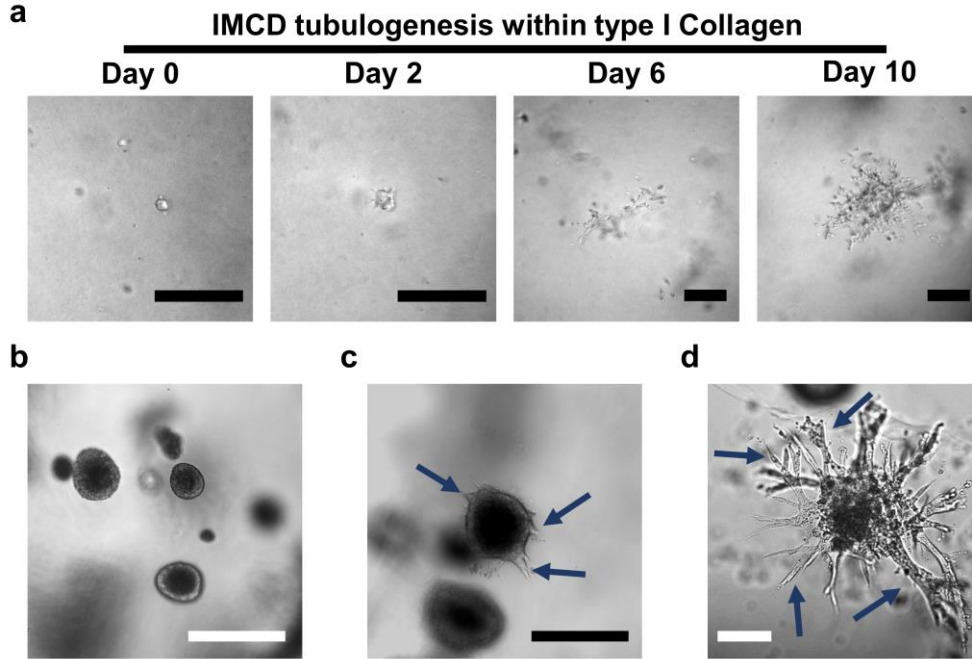
Figure 14: Epithelial IMCD cells proliferate to form multicellular tubular structures. (a) IMCD cells within type I collagen gels proliferate to form multicellular tubular structures over time. (b-d) IMCD cells within PEG-4MAL hydrogels exhibit different multicellular structure phenotypes. Transmitted light microscopy images of IMCD multicellular structures within PEG-4MAL hydrogels forming (b) smooth cluster, (c) spiked clusters, or (d) tubules after 21 d post-encapsulation. Blue arrows indicate (c) spikes or (d) tubules in multicellular IMCD structures. Bars, 100 μm.

4.3 Results

4.3.1 *PEG-4MAL hydrogel supports MT1-MMP-directed tubule formation in a polymer density-dependent manner*

PEG-4MAL hydrogels were functionalized with adhesive peptides and crosslinked in the presence of IMCD cells to generate PEG-4MAL hydrogels (Fig. 15a,b). The mechanical properties of the hydrogel were tuned by varying polymer density (Fig. 15c).

Because ECM mechanical properties influence epithelial cell behaviors[9,127], we investigated the influence of hydrogel polymer density (5-7% wt/vol; 10 kDa PEG-4MAL macromer size) on IMCD cell viability, proliferation and tubule formation (Fig. 16). This combination of macromer size and polymer densities can produce hydrogels with mechanical properties (storage modulus, G': 500 Pa) that has been demonstrated to support epithelial tubulogenesis[125]. Moreover, these synthetic hydrogels were engineered to present a constant 2.0 mM RGD adhesive peptide (GRGDSPC) density and crosslinked with the collagen-derived, protease-degradable peptide GPQ-W (GCRDGPQGIWGQDRCG). These adhesive peptide type and density and crosslinking peptide have been shown to support epithelial cell viability and cyst morphogenesis in PEG-4MAL hydrogels[9,127]. After 14 d in culture, IMCD cells showed high viability in all hydrogel conditions (Fig. 16a) and a polymer density-dependent effect on projected area and longest distance between two points along the projected area (Feret diameter; Fig. 16b,c). At 21 d post-encapsulation, no tubule formation or cell spreading was shown (Fig. 16d), and size analysis demonstrated a polymer density-dependent effect on projected area Feret diameter of the IMCD cell structures (Fig. 16e,f). Nevertheless, no significant differences in projected area or Feret diameter of encapsulated cellular clusters were observed between day 14 and 21 (Fig. 16g,h), demonstrating that the examined PEG-4MAL hydrogel properties do not support IMCD cell structure growth and tubulogenesis.
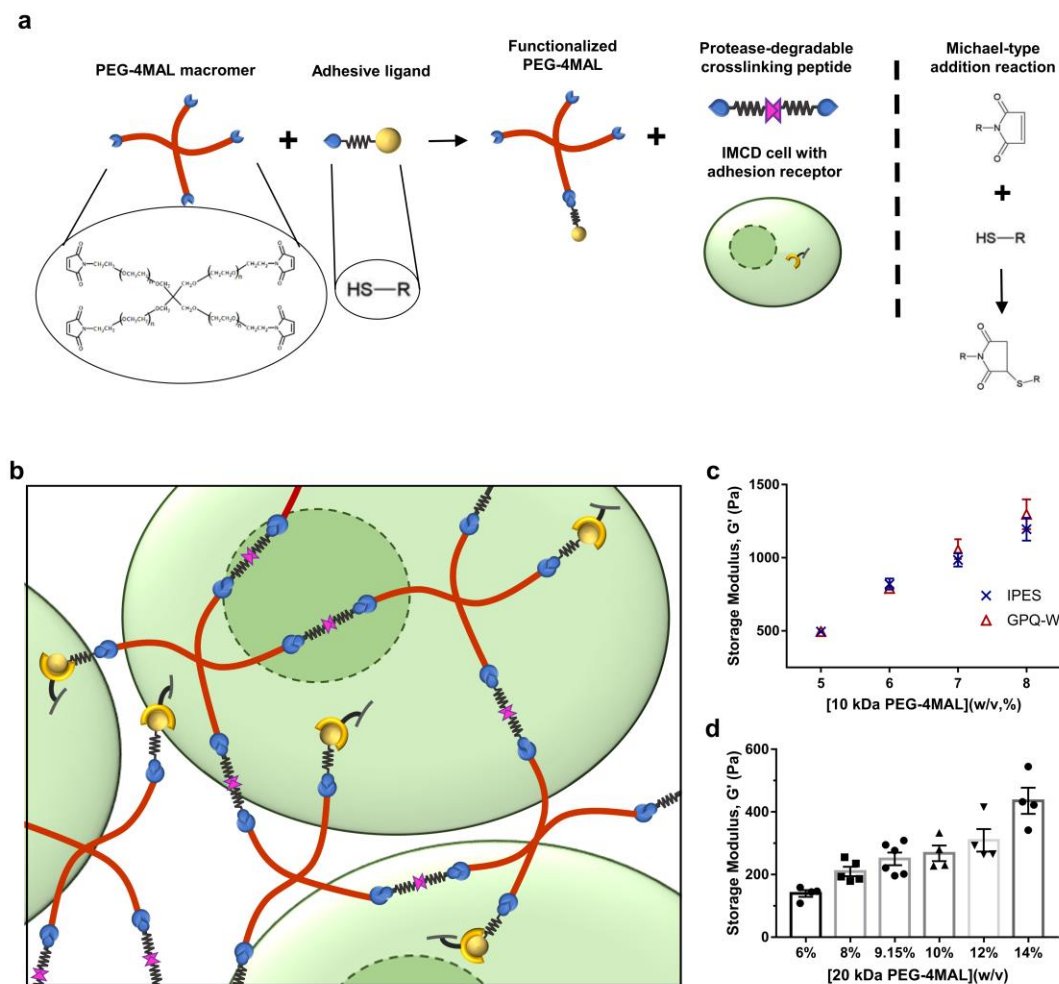
Figure 15: PEG-4MAL hydrogel preparation and mechanical properties. (a) PEG-4MAL macromers are conjugated with thiol-containing adhesive peptide to produce a functionalized PEG-4MAL macromer, which is then crosslinked in the presence of cells using protease-cleavable peptides containing terminal cysteines to form (b) a hydrogel network. (c) Relationship between polymer density (wt%) and storage modulus (mean ± SEM) of 10 kDa PEG-4MAL hydrogels functionalized with 2 mM RGD and crosslinked with GPQ-W or IPES. (d) Relationship between polymer density (wt%) and storage modulus (mean ± SEM) of 20 kDa PEG-4MAL hydrogels functionalized with 2 mM (for 6, 8, 10, 12 and 14%) or 4 mM RGD (for 9.15%) and crosslinked with IPES. Each data point represents an independently prepared hydrogel. Analysis performed to at least 4 PEG-4MAL hydrogels per experimental group.
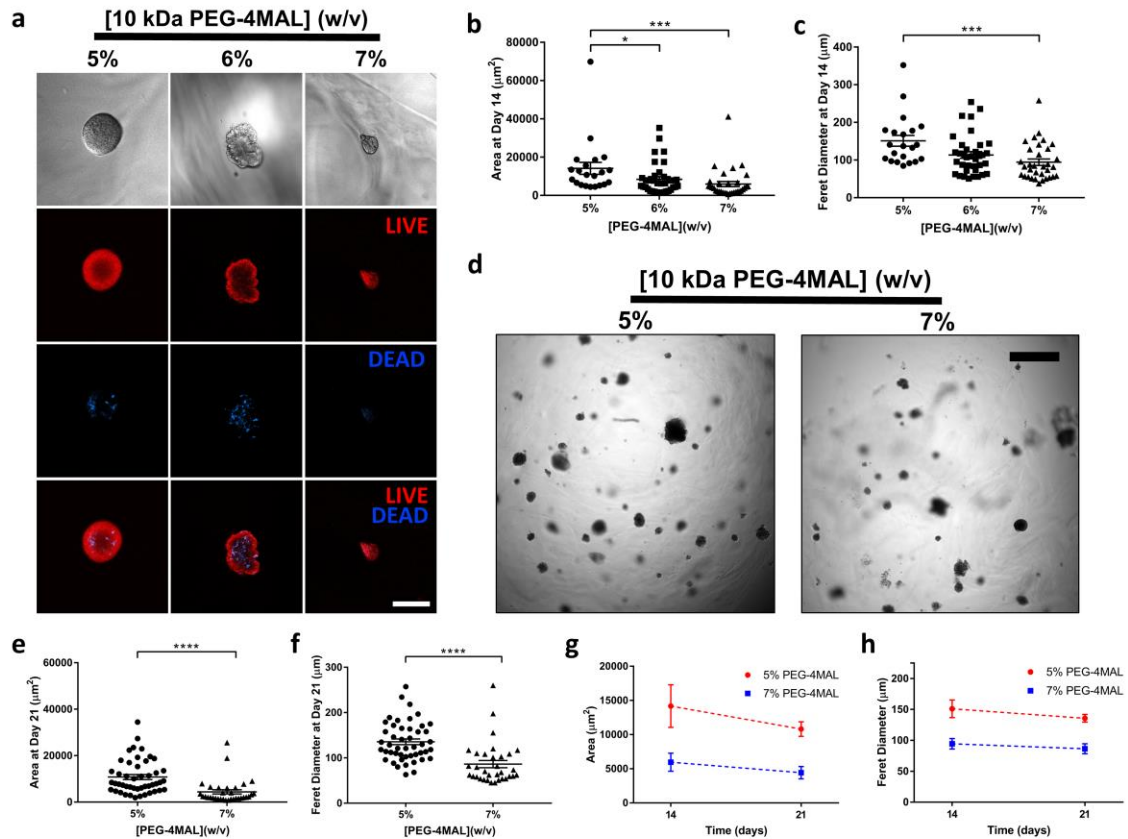
Figure 16: PEG-4MAL hydrogel crosslinked with GPQ-W peptide does not support tubule formation. (a) Transmitted light and fluorescence microscopy images of IMCD cells cultured in PEG-4MAL hydrogels of different polymer density and crosslinked with GPQ-W peptide. IMCD cell viability was assessed at 14 d after encapsulation. Bar, 100 μm. IMCD multicellular structure (b) projected area and (c) Feret diameter at 14 d after encapsulation in PEG-4MAL hydrogel. (d) Transmitted light images of IMCD cells at 21 d after encapsulation in PEG-4MAL hydrogel. Bar, 500 μm. IMCD multicellular structure (e) projected area and (f) Feret diameter at 21 d after encapsulation in PEG-4MAL hydrogels. Comparison of IMCD multicellular structure (g) projected area and (h) Feret diameter at 14 d and 21 d after encapsulation in PEG-4MAL hydrogels. Graph lines represents the mean of the individual data points. Each data point represents one multicellular structure. Krustal-Wallis with Dunn's multiple comparisons test or unpaired t-test with Welch's correction was used. P-values of statistical significance are represented as ****$P < 0.0001$, ***$P < 0.0002$, **$P < 0.0021$, *$P < 0.0332$. A p-value < 0.0332 was considered significant. Experiments performed with 6 PEG-4MAL hydrogels per experimental group.

Considering that proteolytic cleavage of ECM components by MT1-MMPs is essential for renal cell proliferation and tubulogenesis[119,128], we then examined whether

crosslinking of PEG-4MAL hydrogels with an MT1-MMP-sensitive crosslinking peptide is necessary to support IMCD cell tubulogenesis. These type of membrane-bound MMPs have been demonstrated to have an important role in directing renal development by cell-directed matrix remodeling and supporting IMCD cell proliferation and migration[128]. For this purpose, IMCD cells were encapsulated in RGD-functionalized hydrogels of different polymer densities (5 – 8%, 10kDa PEG-4MAL) and crosslinked with the MT1-MMP-sensitive crosslinking peptide IPES (GCRDIPESLRAGDRCG)[129,130]. These IPES-crosslinked hydrogels exhibited mechanical properties comparable to hydrogels of equal polymer densities but crosslinked with GPQ-W peptide (Fig. 15c). IMCD cells embedded in PEG-4MAL hydrogels maintained high viability 1 d post-encapsulation in all conditions (Fig. 17a,b). After 5 d in culture, IMCD cells had generated cellular clusters that showed a significant polymer density-dependent effect on cell proliferation, projected area and Feret diameter (Fig. 17c-f). When IMCD cell culture continued for at least 21 d, some of the cell clusters within the 5% and 6% hydrogels developed tubules, as opposed to cells within 7% and 8% hydrogels which remained as cellular clusters (Fig. 17g). These results suggest that GPQ-W crosslinking peptide does not support IMCD tubulogenesis due to its relatively low enzymatic specificity to MT1-MMPs[129,130], and that polymer density has a direct effect on IMCD cell proliferation, multi-cellular growth and tubule formation. Although 5% PEG-4MAL hydrogels supported tubule formation, this formulation was less mechanically stable compared with 6% PEG-4MAL hydrogels by 21 d in culture. We therefore selected 6.0% (10kDa) PEG-MAL hydrogels crosslinked with the MT1-MMP-sensitive IPES crosslinker for subsequent studies.
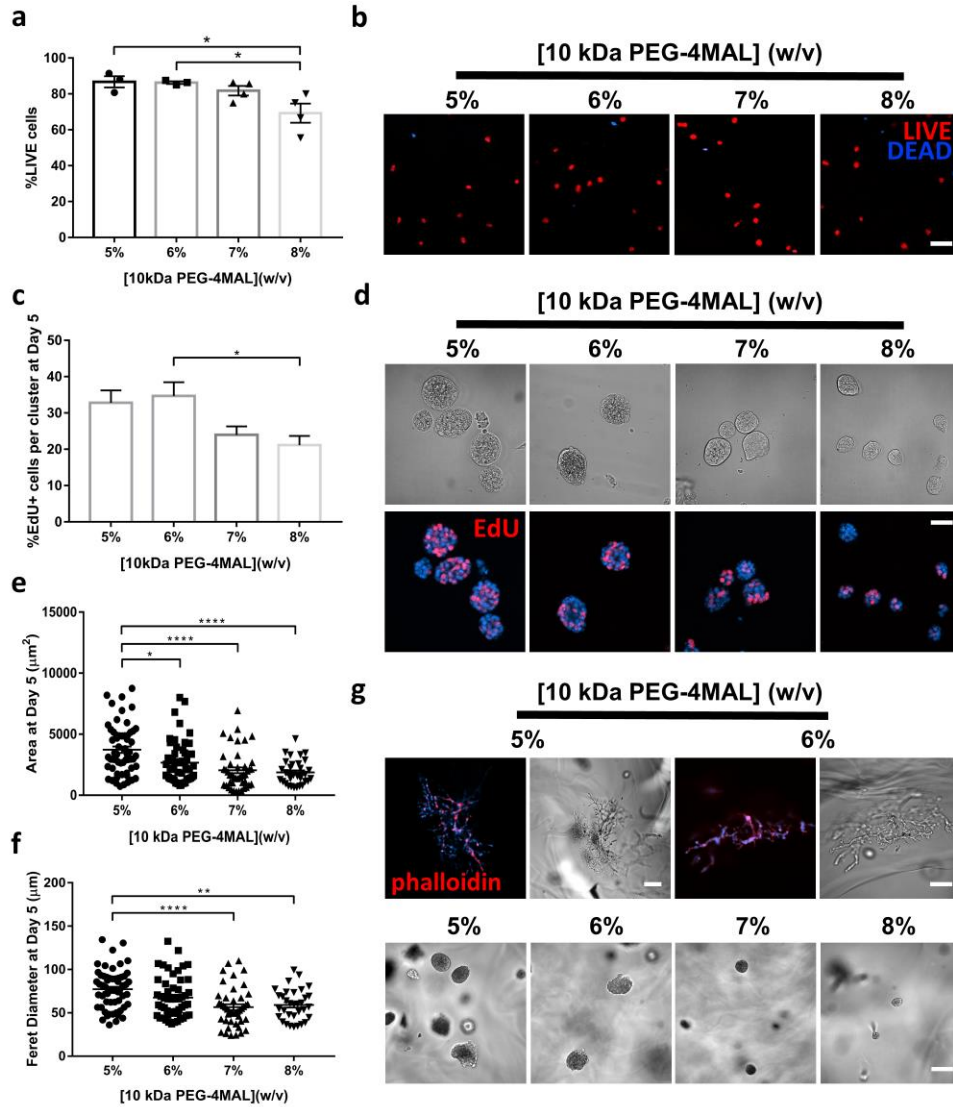
Figure 17: Polymer density of 10 kDa PEG-4MAL directs tubule formation. (a) Percentage of IMCD cells that stained for live (mean ± SEM) after 1 d of encapsulation in 10 kDa PEG-4MAL hydrogels of different polymer density. Each data point represents one independent hydrogel. At least 100 cells were assessed per condition. (b) Fluorescence microscopy images of IMCD cells cultured in PEG-4MAL hydrogels of different polymer density. IMCD cell viability was assessed at 1 d after encapsulation. Bar, 100 μm. (c) Percentage of IMCD cells per cluster that were labeled by EdU incorporation (mean ± SEM) after 5 d of encapsulation. At least 30 clusters were analyzed per condition. (d) Transmitted light and fluorescence microscopy images of proliferating (EdU) IMCD cells cultured in PEG-4MAL hydrogels of different polymer density. IMCD cell proliferation was assessed at 5 d after encapsulation. Bar, 50 μm. IMCD multicellular structure (e) projected area and (f) Feret diameter at 5 d after encapsulation in PEG-4MAL hydrogel. Graph line represents the mean of the individual data points. Each data point represents one multicellular structure. (g) Transmitted light and fluorescence microscopy images of

IMCD cells at 21 d after encapsulation in PEG-4MAL hydrogel and labeled for actin (phalloidin). DAPI, counterstain. Bars, 100 μm. Krustal-Wallis with Dunn's multiple comparisons test was used. P-values of statistical significance are represented as ****P < 0.0001, ***P < 0.0002, **P < 0.0021, *P < 0.0332. A p-value < 0. 0332 was considered significant. All experiments performed with at least 6 PEG-4MAL hydrogels per experimental group. Experiments performed with 6 PEG-4MAL hydrogels per experimental group.

4.3.2   Adhesive peptide type directs tubule formation

Interactions between adhesion receptors and ECM components provide signals critical for cell survival, proliferation and differentiation[4,101]. Therefore, we examined whether the adhesive ligand type in the synthetic hydrogel impacts tubule formation. IMCD cells were embedded within 6% PEG-4MAL (10kDa) hydrogel formulations crosslinked with a constant IPES density but functionalized with different cysteine-terminated adhesive peptides (all at 2.0 mM; Fig. 18): RGD, inactive scrambled peptide RDG (GRDGSPC), type I collagen-mimetic triple helical GFOGER (GYGGGP(GPP)$_5$GFOGER(GPP)$_5$GPC)[103], and laminin β1 chain-derived YIGSR (CGGEGYGEGYIGSR)[30]. IMCD cells encapsulated in RGD-functionalized hydrogels maintained the highest level of proliferation (Fig. 18a,b) and showed significant increase in projected area and Feret diameter as compared to GFOGER- or YIGSR-functionalized hydrogels at 5 d post-encapsulation (Fig. 18c,d). Additionally, IMCD cells encapsulated in PEG-4MAL hydrogels functionalized with inactive RDG peptide showed significant reduction in cell proliferation when compared to RGD (Fig. 18a,b) and reduced growth over all hydrogel conditions (Fig. 18c,d). Furthermore, at 21 d post-encapsulation cell structures were classified as either "smooth clusters", "spiked clusters"' which were clusters with extensions, or "tubules", in accordance with previous reports[125,126] (Fig. 18e; Fig. 14). IMCD cell tubule formation was observed in the RGD and GFOGER conditions,

whereas cells encapsulated in RDG or YIGSR-functionalized hydrogels did not generated tubules (Fig. 18e,f). These results suggest an adhesive peptide type-dependent effect on tubule morphogenesis of IMCD cells after 21 d in culture. As RGD-functionalized hydrogels supported the highest level of cell proliferation, and significant growth than GFOGER, we used RGD-functionalized hydrogels for subsequent studies.
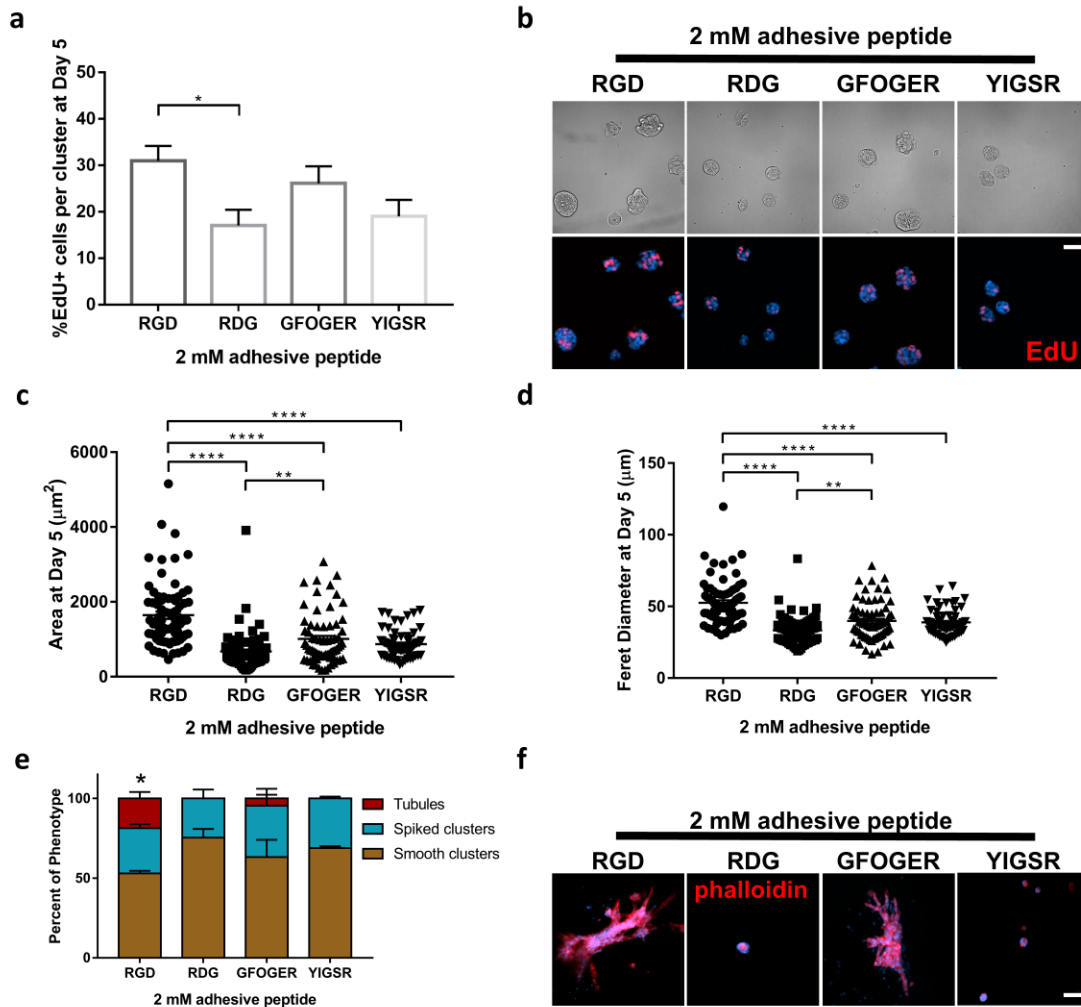
Figure 18: Adhesive peptide type in PEG-4MAL hydrogels directs tubule formation. (a) Percentage of IMCD cells per cluster that were labeled by EdU incorporation (mean ± SEM) after 5 d of encapsulation in PEG-4MAL hydrogels functionalized with different adhesive peptides. At least 30 clusters were analyzed per condition. (b) Transmitted light and fluorescence microscopy images of proliferating (EdU) IMCD cells cultured in PEG-

4MAL hydrogels functionalized with different adhesive peptides. IMCD cell proliferation was assessed at 5 d after encapsulation. Bar, 50 μm. IMCD multicellular structure (c) projected area and (d) Feret diameter at 5 d after encapsulation in PEG-4MAL hydrogel. Graph line represents the mean of the individual data points. Each data point represents one multicellular structure. (e) Percentage of IMCD multicellular structures (mean ± SEM) that classified as either "smooth clusters", "spiked clusters", or "tubules" after 21 d of encapsulation. At least 10 multicellular structures were analyzed per condition. (f) Fluorescence microscopy images of IMCD cells at 21 d after encapsulation in PEG-4MAL hydrogel and labeled for actin (phalloidin). DAPI, counterstain. Bars, 50 μm. (a,c,d) Krustal-Wallis with Dunn's multiple comparisons test was used. (e) χ^2 test with Bonferroni's correction was used; *, $P < 0.0002$ for RGD vs RDG and $P < 0.0021$ for RGD vs YIGSR. P-values of statistical significance are represented as ****$P < 0.0001$, ***$P < 0.0002$, **$P < 0.0021$, *$P < 0.0332$. A p-value < 0.0332 was considered significant. Experiments performed with 6 PEG-4MAL hydrogels per experimental group.

4.3.3   PEG-4MAL macromer size promotes early tubulogenesis

As previous studies have demonstrated that matrix elasticity influence epithelial cell behaviors[9,127], we investigated the influence of PEG-4MAL macromer size (10 and 20 kDa), which controls hydrogel mechanical properties[9,127], on IMCD cell viability, proliferation and tubule formation. As changes in PEG-4MAL macromer size and polymer density modulates synthetic matrix elasticity, IMCD cells were encapsulated in PEG-4MAL hydrogels of 20 kDa macromer size and a range of polymer densities (8-14% wt/vol) that exhibit a different range of matrix elasticity (Fig. 15d) as compared to 10 kDa PEG-4MAL hydrogels (Fig. 15c). We chose 20 kDa PEG-4MAL hydrogel as this macromer size have been previously used to recapitulate epithelial morphogenetic programs[9,127]. The synthetic hydrogels were functionalized with the adhesive ligand RGD and crosslinked using the MT1-MMP-sensitive IPES sequence. No differences in cell viability were observed in any of the hydrogel conditions at 1 d post-encapsulation (Fig. 19a,b), whereas IMCD cell proliferation, projected area and Feret diameter varied in a polymer density-dependent manner at 5 d post-encapsulation (Fig. 19c-f). Moreover, as

early as 7 d after encapsulation cell spreading was observed in the 8% condition whereas cell clusters continued to develop in all other conditions (Fig. 19g). By 14 d of culture in the synthetic matrix, tubule formation was observed in a polymer density-dependent manner, where the 8% PEG-4MAL condition had a higher number of cell structures presenting tubules whilst significantly less tubule formation was observed in the higher (12% and 14%) polymer density conditions (Fig. 20a,b). Further analysis of the Feret diameter of tubule-presenting cell structures demonstrated a significantly higher length of tubules in the 8% 20 kDa PEG-4MAL hydrogels, as compared to tubules formed in 6%, 10 kDa hydrogels (Fig. 20c). Therefore, these results demonstrate that IMCD cell encapsulation in PEG-4MAL hydrogels of 20 kDa macromer size resulted in cell spreading and tubule formation at an earlier time point and with an increased length of tubules, when compared to IMCD tubules formed in synthetic hydrogels of 10 kDa macromer size (Figs. 16, 19 and 20). Finally, additional observations demonstrated that, by 7 d post-encapsulation, cell viability was compromised in softer (6%, 20 kDa; Fig. 14d and Fig. 21a) or in GPQ-W-crosslinked (8%, 20 kDa; Fig. 21b) PEG-4MAL hydrogels, as compared to 8%, 20 kDa PEG-4MAL hydrogels (Fig. 21c). Therefore, we designated 8%, 20 kDa as the optimized polymer density and macromer size that provides the physical support and biomechanical signals necessary for optimal IMCD cell growth and tubule formation within PEG-4MAL hydrogels.

Figure 19: Polymer density of 20 kDa PEG-4MAL directs tubule formation. (a) Percentage of IMCD cells that stained for live (mean ± SEM) after 1 d of encapsulation in 20 kDa PEG-4MAL hydrogels of different polymer density. Each data point represents one independent hydrogel. At least 100 cells were assessed per condition. (b) Fluorescence microscopy images of IMCD cells cultured in PEG-4MAL hydrogels of different polymer density. IMCD cell viability was assessed at 1 d after encapsulation. Bar, 50 μm. (c) Percentage of IMCD cells per cluster that were labeled by EdU incorporation (mean ± SEM) after 5 d of encapsulation. At least 30 clusters were analyzed per condition. (d) Fluorescence microsco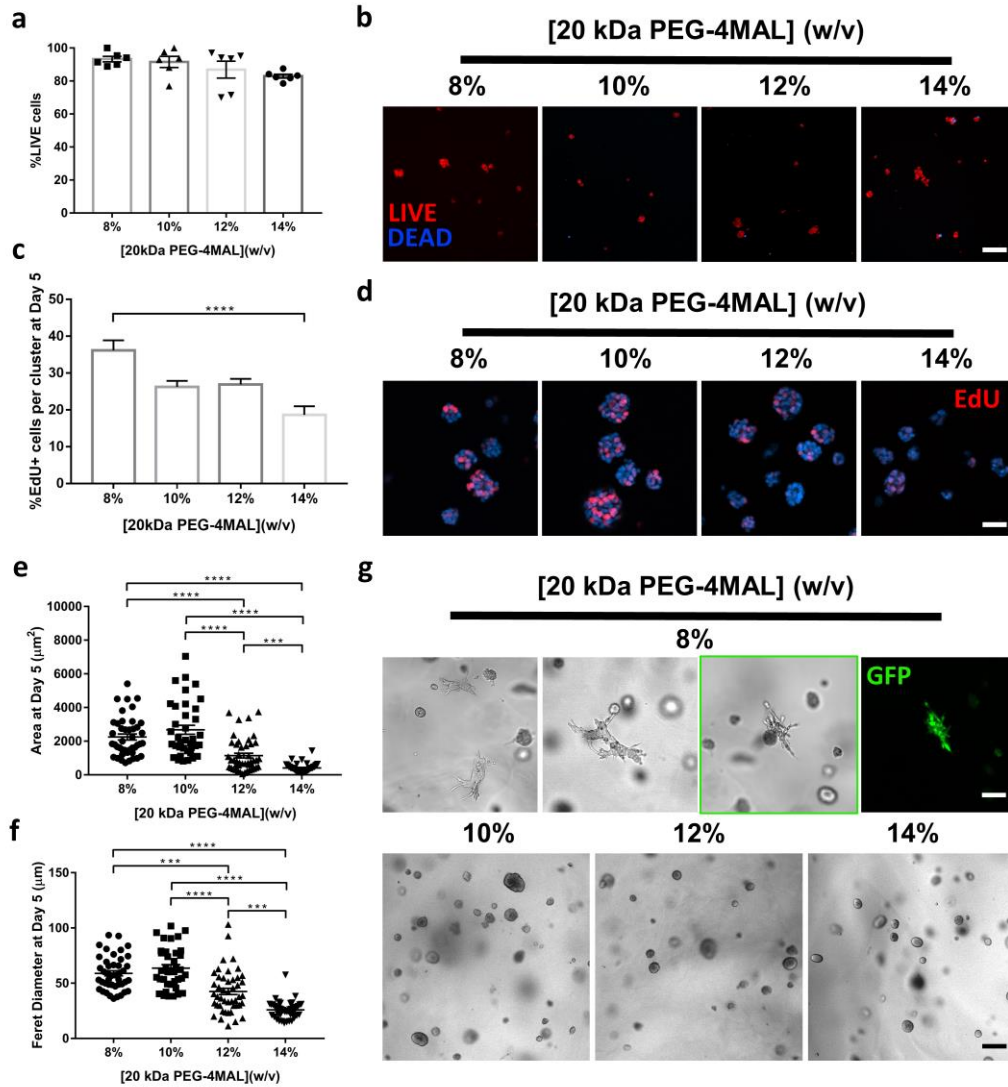py images of proliferating (EdU) IMCD cells cultured in PEG-4MAL hydrogels of different polymer density. IMCD cell proliferation was assessed at 5 d after encapsulation. Bar, 50 μm. IMCD multicellular structure (e) projected area and (f) Feret diameter at 5 d after encapsulation in PEG-4MAL hydrogel. Graph line represents the mean of the individual data points. Each data point represents one multicellular structure. (g) Transmitted light and fluorescence microscopy images of IMCD cells at 7 d

after encapsulation in PEG-4MAL hydrogel. Bars, 100 μm for 8% and 200 μm for other conditions. Krustal-Wallis with Dunn's multiple comparisons test was used. P-values of statistical significance are represented as ****$P < 0.0001$, ***$P < 0.0002$, **$P < 0.0021$, *$P < 0.0332$. A p-value < 0.0332 was considered significant. Experiments performed with 6 PEG-4MAL hydrogels per experimental group.
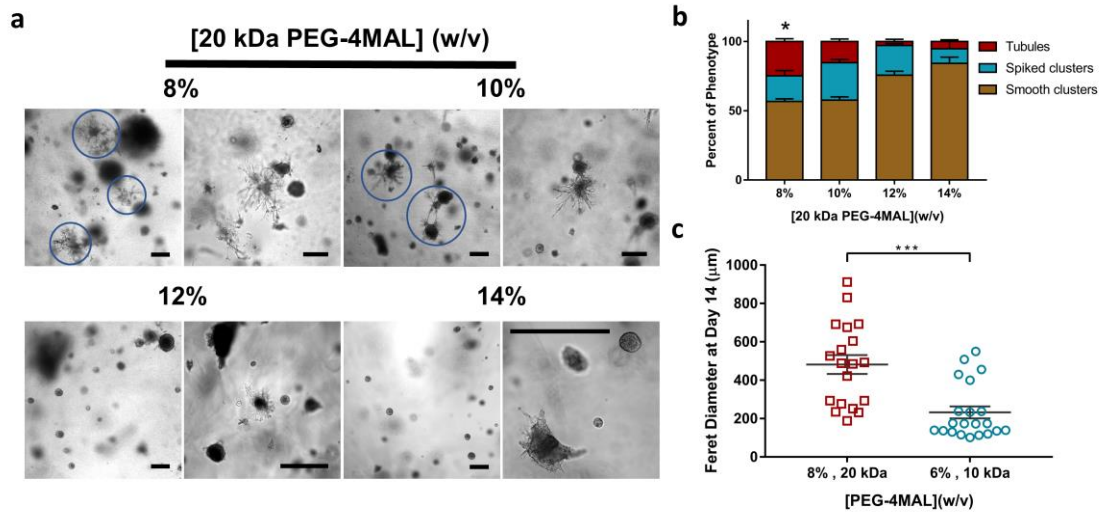
Figure 20: Polymer density and macromer size controls tubule formation. (a) Transmitted light images of IMCD cells cultured in 20 kDa PEG-4MAL hydrogels of different polymer density at 14 d after encapsulation. Bar, 200 μm. (b) Percentage of IMCD multicellular structures (mean ± SEM) that classified as either "smooth clusters", "spiked clusters", or "tubules" after 21 d of encapsulation. At least 10 multicellular structures were analyzed per condition. χ^2 test with Bonferroni's correction was used; *, $P < 0.0001$ for 8% vs 12% and $P < 0.0002$ for 8% vs 14%. (c) IMCD multicellular structure Feret diameter at 14 d after encapsulation in PEG-4MAL hydrogels of different macromere size. Graph line represents the mean of the individual data points. Each data point represents one multicellular structure. Unpaired t-test with Welch's correction was used. P-values of statistical significance are represented as ****$P < 0.0001$, ***$P < 0.0002$, **$P < 0.0021$, *$P < 0.0332$. A p-value < 0.0332 was considered significant. Experiments performed with 6 PEG-4MAL hydrogels per experimental group.
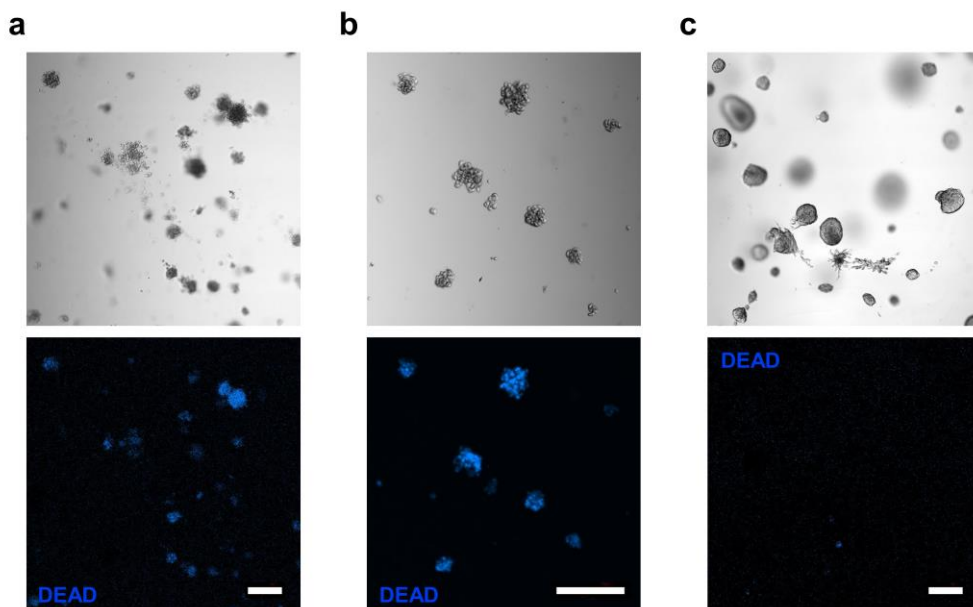
Figure 21: Threshold level of PEG-4MAL mechanical properties and matrix degradability dictates IMCD cell viability. Transmitted light and fluorescence microscopy images of IMCD cells cultured in PEG-4MAL hydrogels of different conditions stained for dead. IMCD cell viability was assessed at 7 d after encapsulation on (a) 6%, 20 kDa PEG-4MAL-RGD hydrogels crosslinked with IPES peptide, or (b) 8%, 20 kDa PEG-4MAL-RGD hydrogels crosslinked with GPQ-W peptide, or (c) 8%, 20 kDa PEG-4MAL-RGD hydrogels crosslinked with IPES peptide. Bar, 200 μm. Experiments performed with 6 PEG-4MAL hydrogels per experimental group.

4.3.4 Adhesive ligand density in PEG-4MAL hydrogels regulates tubule formation

We next examined the effects of RGD adhesive ligand density on tubulogenesis within PEG-4MAL hydrogels engineered to present optimized biophysical properties (8%, 20 kDa PEG-4MAL). A total density (2.0 mM) of a mixture of cell-adhesive RGD peptide and scrambled inactive RDG peptide was used to vary RGD density (0.4–2.0 mM) while maintaining identical structures among hydrogel formulations and constant IPES crosslinking peptide density (Fig. 22). Additionally, a hydrogel condition with a total RGD density of 4.0 mM (9.15%, 20 kDa) was used while preserving equal IPES crosslinking peptide density and mechanical properties (Fig. 14d, Fig. 22). Cell viability and

proliferation at 1 and 5 d post-encapsulation, respectively, was insensitive to RGD peptide density (Fig. 22a-d). However, cluster area and Feret diameter showed a significant dependence on RGD density after 5 d of encapsulation (Fig. 22e,f). Hydrogels presenting low (<2.0 mM) RGD densities supported the formation of relatively small multicellular structures with no significant differences among the groups (0.4, 1.0 and 1.6 mM RGD; Fig. 22e,f). In contrast, hydrogels presenting high (≥2.0 mM) RGD density formed relatively large structures with no statistical differences between these groups (2.0 and 4.0 mM RGD; Fig. 22e,f). Further analysis of cellular structures at 14 d post-encapsulation demonstrated an RGD density-dependent effect on the number of tubule-presenting cell structures and length of tubules (Fig. 22g-i). No significant differences were observed between the high-density (2 and 4 mM) RGD hydrogels. These results are consistent with previous studies that have shown that adhesive ligand density regulates epithelial morphogenesis independent of cell proliferation[9], and suggest that high RGD density promotes increased integrin-mediated cell migration that allows formation of longer tubules within the synthetic hydrogels. Moreover, combination of adhesive peptides RGD and GFOGER in PEG-4MAL hydrogels did not improved IMCD cell viability (Fig. 23a,b), proliferation (Fig. 23c,d), growth (Fig. 23e,f), or tubule formation (Fig. 23g) compared to hydrogels functionalized with 2.0 mM RGD, suggesting that tubule development is dominated by integrin interactions with RGD peptide. Additionally, these results show that although high RGD peptide density is not required for initial viability, proliferation and generation of cell aggregates, robust formation and growth of tubules requires a high density of RGD in the matrix. Taken together, these results identify an engineered hydrogel formulation (Storage modulus, G': 200 Pa; 8% polymer density; 20 kDa

71

macromer size; 2.0 mM RGD adhesive peptide; IPES crosslinking peptide) that supports

IMCD viability and optimized cell proliferation, growth and formation of tubules, and

which was used for subsequent experiments.

Figure 22: Adhesive ligand density in PEG-4MAL hydrogels regulates tubule formation. (a) Percentage of IMCD cells that stained for live (mean ± SEM) after 1 d of encapsulation in 8%, 20 kDa PEG-4MAL hydrogels functionalized with varying RGD density and crosslinked with IPES peptide. Each data point represents one independent hydrogel. At least 100 cells were assessed per condition. (b) Fluorescence microscopy images of IMCD cells cultured in PEG-4MAL hydrogel. IMCD cell viability was assessed at 1 d after encapsulation. Bar, 50 μm. (c) Percentage of IMCD cells per cluster that were labeled by EdU incorporation (mean ± SEM) after 5 d of encapsulation. At least 30 clusters were analyzed per condition. (d) Fluorescence microscopy images of proliferating (EdU) IMCD cells cultured in PEG-4MAL hydrogels of different polymer density. IMCD cell

proliferation was assessed at 5 d after encapsulation. Bar, 50 μm. IMCD multicellular structure (e) projected area and (f) Feret diameter at 5 d after encapsulation in PEG-4MAL hydrogel. Graph line represents the mean of the individual data points. Each data point represents one multicellular structure. (g) Transmitted light and fluorescence microscopy images of IMCD cells at 14 d after encapsulation in PEG-4MAL hydrogel. Bars, 100 μm. (h) Percentage of IMCD multicellular structures (mean ± SEM) that classified as "smooth clusters", "spiked clusters", or "tubules" after 14 d of encapsulation. At least 10 multicellular structures were analyzed per condition. χ^2 test with Bonferroni's correction was used; *, P < 0.0021 for 2.0 vs 0.4 mM RGD. (i) IMCD multicellular structure Feret diameter at 14 d after encapsulation in PEG-4MAL hydrogel. Graph line represents the mean of the individual data points. Each data point represents one multicellular structure. Krustal-Wallis with Dunn's multiple comparisons test was used. P-values of statistical significance are represented as ****P < 0.0001, ***P < 0.0002, **P < 0.0021, *P < 0.0332. A p-value < 0. 0332 was considered significant. Experiments performed with 6 PEG-4MAL hydrogels per experimental group.
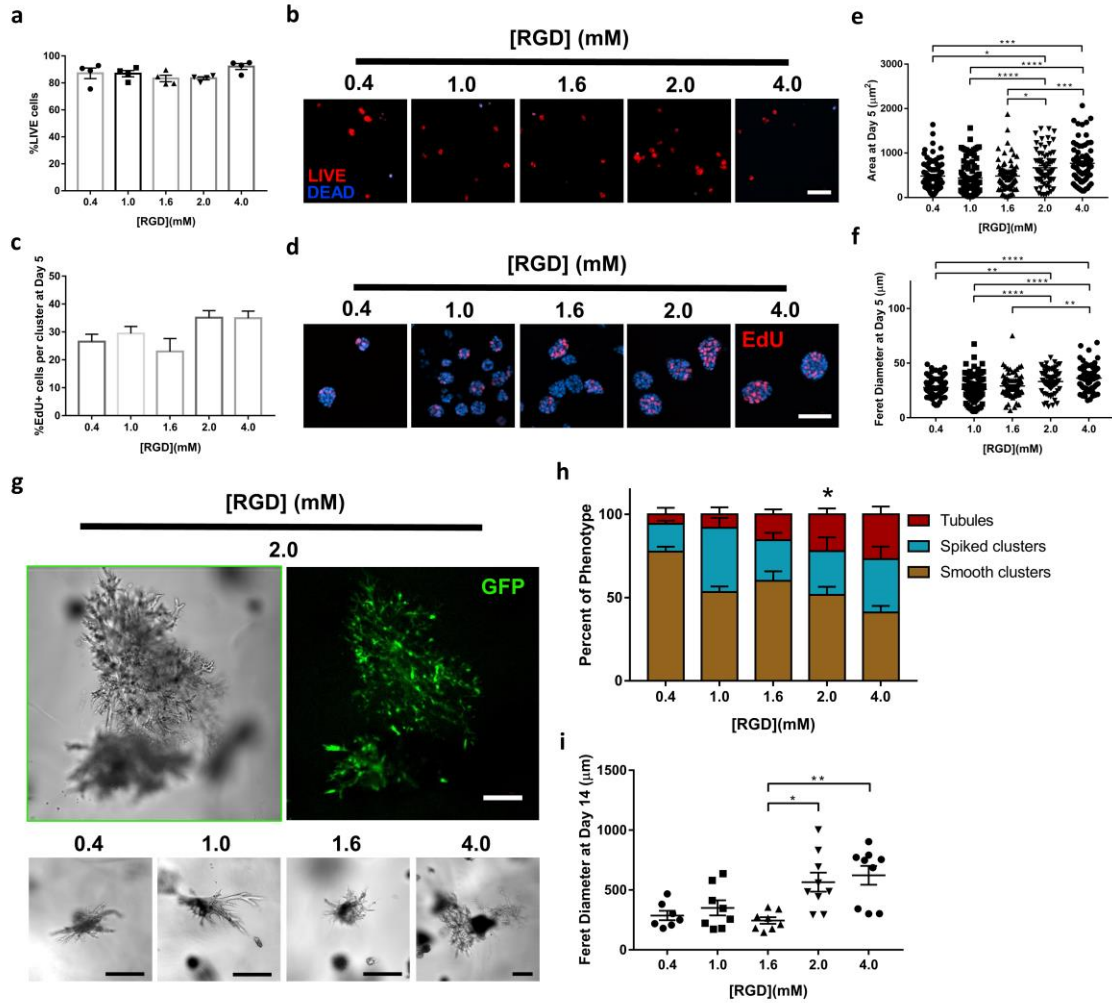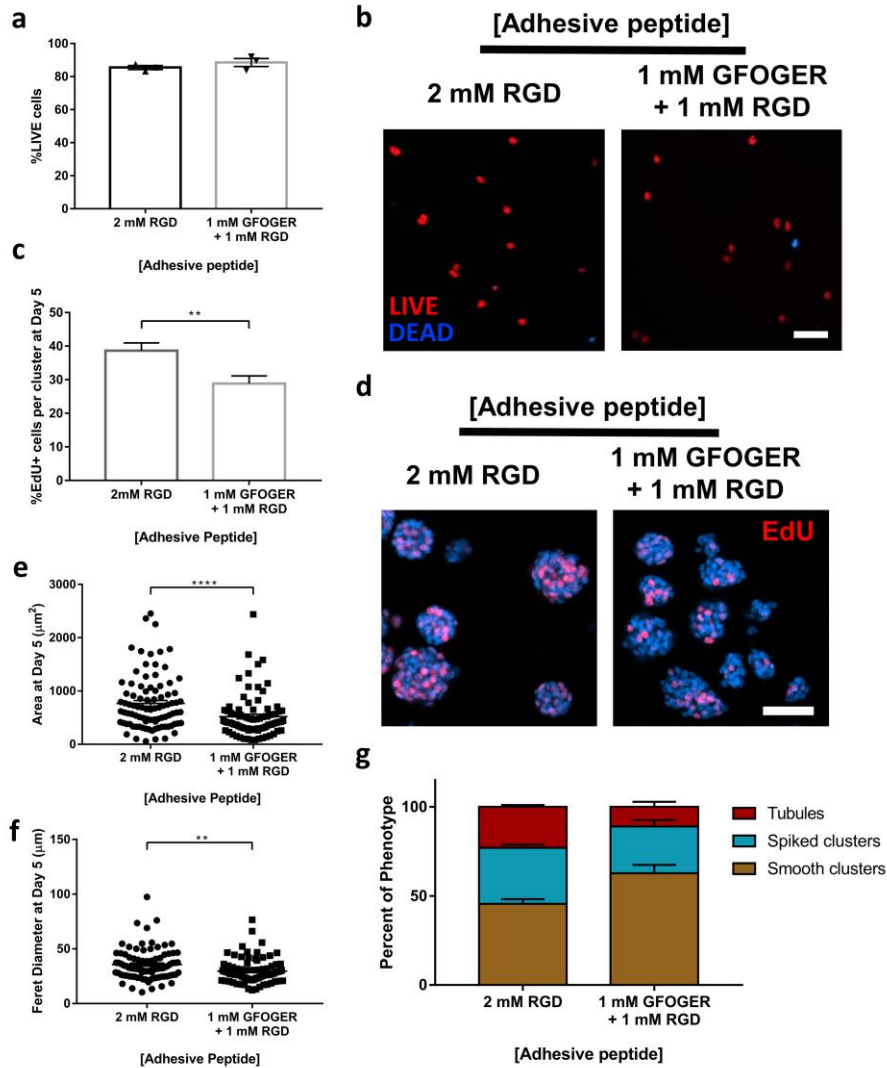
Figure 23: PEG-4MAL hydrogels regulates tubule formation via cell receptor interactions with RGD peptide. (a) Percentage of IMCD cells that stained for live (mean ± SEM) after 1 d of encapsulation in 8%, 20 kDa PEG-4MAL hydrogels functionalized with RGD or GFOGER and RGD, and crosslinked with IPES peptide. Each data point represents one independent hydrogel. At least 100 cells were assessed per condition. (b) Fluorescence microscopy images of IMCD cells cultured in PEG-4MAL hydrogel. IMCD cell viability was assessed at 1 d after encapsulation. Bar, 50 μm. (c) Percentage of IMCD cells per cluster that were labeled by EdU incorporation (mean ± SEM) after 5 d of encapsulation. At least 30 clusters were analyzed per condition. (d) Fluorescence microscopy images of proliferating (EdU) IMCD cells cultured in PEG-4MAL hydrogels functionalized with different adhesive type and density. IMCD cell proliferation was assessed at 5 d after encapsulation. Bar, 50 μm. IMCD multicellular structure (e) projected area and (f) Feret diameter at 5 d after encapsulation in PEG-4MAL hydrogel. Graph line represents the mean of the individual data points. Each data point represents one multicellular structure. (g) Percentage of IMCD multicellular structures (mean ± SEM) that classified as "smooth

clusters", "spiked clusters", or "tubules" after 21 d of encapsulation. At least 10 multicellular structures were analyzed per condition. (c,e,f) Unpaired t-test with Welch's correction was used. P-values of statistical significance are represented as ****P < 0.0001, ***P < 0.0002, **P < 0.0021, *P < 0.0332. A p-value < 0. 0332 was considered significant. Experiments performed with 6 PEG-4MAL hydrogels per experimental group.

4.3.5   Engineered hydrogel support IMCD cell tubulogenesis program

IMCD cell tubulogenesis program is characterized by the 3D assembly of epithelial cell into tubules and formation of a polarized and differentiated epithelium[119]. Interactions between laminin and integrin receptors are required for renal epithelial differentiation[119,120,124,131,132]. Therefore, to further characterize IMCD tubule differentiation we examined epithelial polarity and laminin secretion of IMCD cell tubules generated within the engineered synthetic matrix. For at least 21 d, the engineered synthetic hydrogel allowed a significant increase in the number of multicellular structures forming tubules over time (Fig. 24a). The hydrogel-generated IMCD tubules demonstrated an organized tubular assembly, appropriate apical polarization of the luminal protein, cystic fibrosis transmembrane conductance regulator (CFTR)[133], and secretion of laminin into the basal side of the tubular structures[119,128] (Fig. 24b,c).
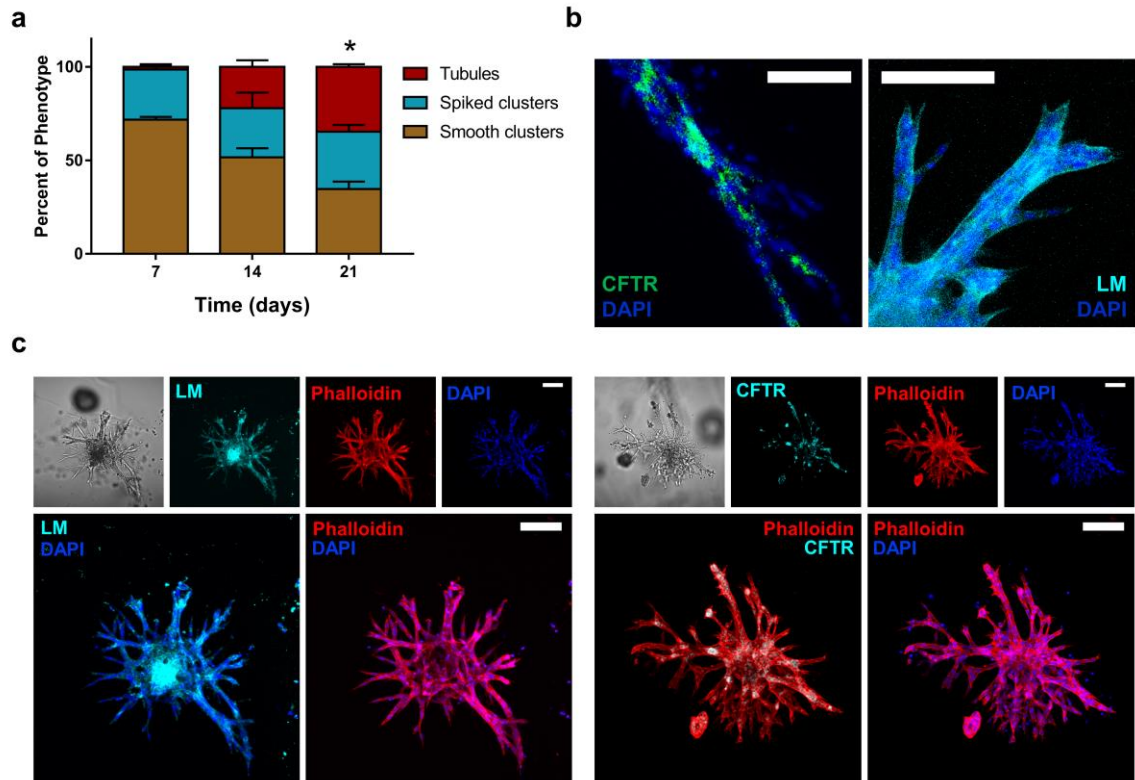
Figure 24: Engineered PEG-4MAL hydrogel promotes epithelial polarity and laminin secretion. (a) Percentage of IMCD multicellular structures (mean ± SEM) that classified as either "smooth clusters", "spiked clusters", or "tubules" after 7, 14 and 21 d of encapsulation in the engineered hydrogel. χ^2 test with Bonferroni's correction was used; *, $P < 0.0001$ for day 7 vs day 21. At least 10 multicellular structures were analyzed per condition. (b) Fluorescence microscopy images of IMCD tubules within engineered hydrogel stained for apical polarity marker (CFTR) and secreted laminin (LM). (d) Transmitted light and fluorescence microscopy images of IMCD tubules within engineered hydrogel stained for CFTR, LM, actin (phalloidin) and nuclei (DAPI). Bars, 100 μm. Experiments performed with 6 PEG-4MAL hydrogels per experimental group.

Moreover, we evaluated the role of integrin receptors and mediators of mechanotransduction pathways on IMCD cell tubulogenesis program within the engineered hydrogel. Previous studies have demonstrated that IMCD cells morphogenesis program requires sequential cell adhesion to ECM, via laminin (e.g. $\alpha_3\beta_1$) and collagen ($\alpha_1\beta_1$ and $\alpha_2\beta_1$) receptors, that promotes cell spreading, proliferation and migration to ultimately form multicellular tubular structures[119,124,132]. Addition of blocking antibodies

76

against α_1, α_2, and β_1 integrin subunits resulted in a significant reduction of tubule formation at 21 d post-encapsulation as compared to control group (DMSO; Fig. 25). Additionally, treatment with blebbistatin or Y-27632, which inhibit myosin II and Rho-associated kinase[105,106], respectively, resulted in significant reduction of tubule formation as observed 21 d post-encapsulation (Fig. 25), suggesting that cellular contractility are important in the initial stages of IMCD tubulogenesis program. Finally, we also incubated IMCD cells embedded in the engineered hydrogel in an anti-MT1-MMP inhibitor or the broad-range MMP inhibitor GM6001, and demonstrated that IMCD cell viability was compromised after MT1-MMP inhibition within 7 d of culture (Fig. 26a), and no tubule formation was observed at day 21 after MMP inhibition by GM6001 (Fig. 26b,c), compared with the vehicle-only (DMSO) control. Previous *in vitro* studies have demonstrated that MT1-MMP expression is essential for renal epithelial branching tubulogenesis as early as 3 d post-encapsulation[134], and expression of MMP-2 and MMP-9 mediate embryonic branching morphogenesis[119], suggesting that the engineered hydrogel supports MMP-mediated epithelial tubulogenesis. Taken together, these results demonstrate that the engineered PEG-4MAL hydrogel robustly supports tubular differentiation of IMCD cells. Additionally, these results provide preliminary indication that IMCD tubulogenesis in the synthetic matrix is also directed by cell receptor interactions with secreted laminin, and cellular contractility and MMP expression at initial stages of tubule development.
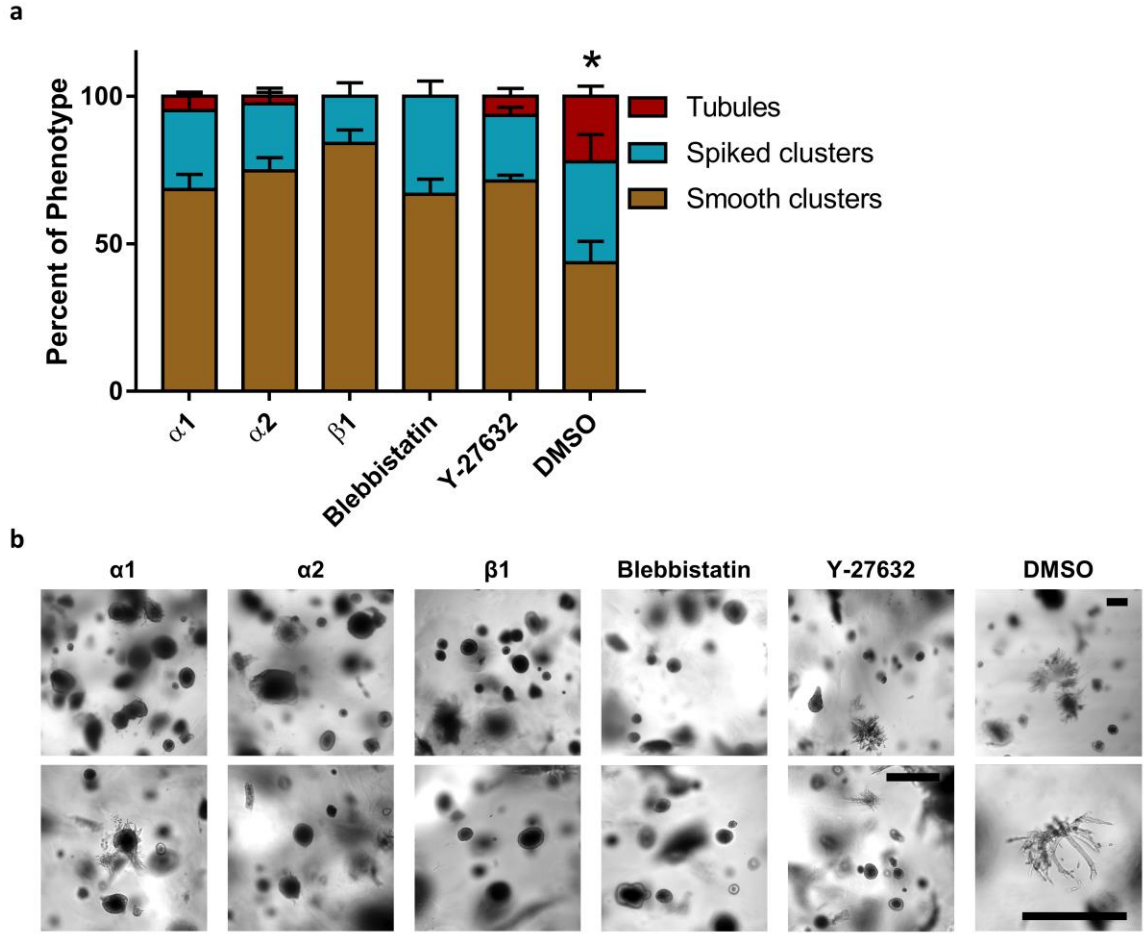
Figure 25: Engineered PEG-4MAL hydrogel promotes epithelial tubule differentiation via integrin receptors and cellular contractility. (a) Percentage of IMCD multicellular structures (mean ± SEM) that classified as either "smooth clusters", "spiked clusters", or "tubules" after 21 d of encapsulation in the engineered hydrogel and in the presence of inhibitors of integrin subunits and cellular contractility. χ^2 test with Bonferroni's correction was used; *, $P < 0.0002$ for DMSO vs α_1, $P < 0.0002$ for DMSO vs α_2, $P < 0.0001$ for DMSO vs β_1, $P < 0.0002$ for DMSO vs blebbistatin, and $P < 0.0012$ for DMSO vs Y-27632. At least 10 multicellular structures were analyzed per condition. (b) Transmitted light images of IMCD multicellular structures at 21 d post encapsulation in the engineered hydrogel in the presence of inhibitors of integrin subunits and cellular contractility. Bars, 200 μm. Experiments performed with 6 PEG-4MAL hydrogels per experimental group. A p-value < 0. 0332 was considered significant.
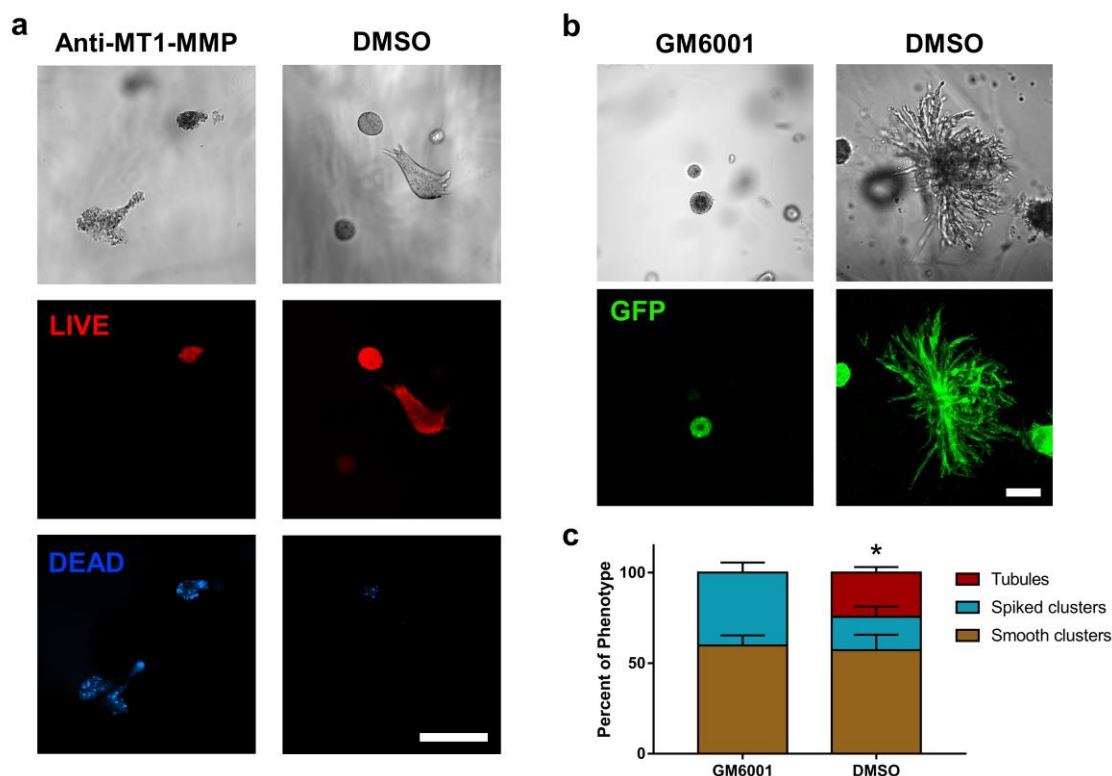
Figure 26: PEG-4MAL hydrogels supports MMP-mediated tubulogenesis. (a) Transmitted light and fluorescence microscopy images of IMCD cells cultured within engineered PEG-4MAL hydrogel and in the presence of an MT1-MMP inhibitor or vehicle control (DMSO). IMCD cell viability was assessed at 7 d after encapsulation. Bar, 100 µm. (b) Transmitted light and fluorescence microscopy images of IMCD cells cultured in engineered PEG-4MAL hydrogel and in the presence of a broad-range MMP inhibitor (GM6001) or vehicle control (DMSO). Bar, 100 µm. (c) Percentage of IMCD multicellular structures (mean ± SEM) that classified as "smooth clusters", "spiked clusters", or "tubules" after 21 d of encapsulation. At least 10 multicellular structures were analyzed per condition. χ^2 test with Bonferroni's correction was used; *, P < 0.0002 for DMSO vs GM6001. P-values of statistical significance are represented as ****P < 0.0001, ***P < 0.0002, **P < 0.0021, *P < 0.0332. A p-value < 0. 0332 was considered significant. Experiments performed with 6 PEG-4MAL hydrogels per experimental group

4.4   Discussion

This study establishes a modular, fully synthetic hydrogel platform with controlled presentation of cell-adhesive ligands, tunable mechanical properties, and protease-dependent degradation that can be precisely engineered to study the contributions of the

biophysical and biochemical matrix properties on the epithelial tubular morphogenetic program of murine IMCD cells. Systematic changes in hydrogel formulation to independently tune hydrogel macromer size and polymer density, adhesive ligand type and density, and MMP-dependent degradation revealed that each of these properties has profound effects on specific stages of this coordinated multicellular morphogenetic process, including cell viability, proliferation and tubular structure development. Additionally, we identified an engineered synthetic hydrogel formulation that promotes tubule polarization and lumen formation, integrin- and MT1-MMP-mediated growth of tubules, and supports continuous increase in number of tubules over time. Because of their inherent complexity, these new insights into the contributions of matrix biochemical and mechanical properties to the regulation of epithelial morphogenesis are simply not tractable using naturally-derived ECMs. The differences in mechanical properties that support IMCD tubulogenesis between naturally-derived matrices (e.g. type I collagen gels) and PEG-4MAL hydrogels may be elucidated by the structural and compositional differences of these materials. Moreover, the mechanical properties and protease degradation characteristics that supported murine IMCD tubulogenesis in this study are different from those recently identified for human renal epithelial cells[125], which involved more complex, naturally-based hydrogels, and suggest differences between these two epithelial cell sources. This fully synthetic matrix addresses major limitations of naturally-derived materials or naturally-based hydrogels associated with lot-to-lot compositional and structural variability and tumor-derived nature that severely restrict scale-up applications and clinical translation. Furthermore, the modular nature of this hydrogel platform allows

80

the characterization of the elementary matrix property contributions to renal organ development.

4.5 Methods

Immunofluorescence analysis

Primary antibodies used were mouse anti-CFTR (A3, University of North Carolina, Chapel Hill) and rabbit anti-laminin (L9393, Sigma). The following secondary antibodies were used: goat anti-mouse IgG Alexa Fluor 647 (Thermo Fisher Scientific), and donkey anti-rabbit IgG Dylight 649 (Thermo Fisher Scientific). Nuclei were stained with DAPI and filamentous actin was stained with rhodamine phalloidin (Thermo Fisher Scientific). Antibody dilutions were performed according to manufacturer's instructions.

Cell culture

Mouse inner medullary collecting duct (IMCD) cells (isolated from αv flox/flox mice) where maintained in Dulbecco's Modified Eagle's Medium (DMEM)/Nutrient Mixture F-12 Ham (DMEM/F-12 50/50; D8437, SIGMA) supplemented with 10% fetal bovine serum (Life Technologies) and 1% Antibiotic-Antimycotic solution (MT-30-004-CI, MediaTech).

Hydrogel formation and 3D cell encapsulation

To prepare PEG hydrogels, PEG-4MAL macromer (MW 22,000 or 11,000; Laysan Bio) was dissolved in 4-(2-hydroxyethyl)piperazine-1-ethanesulfonic acid (HEPES) buffer (20 mM in DPBS, pH 7.4). Adhesive and crosslinking peptides were custom synthesized by AAPPTec. Adhesive peptides RGD (GRGDSPC), GFOGER (GYGGGP(GPP)₅GFOGER

(GPP)$_5$GPC), YIGSR (CGGEGYGEGYIGSR) and RDG (GRDGSPC) were dissolved in HEPES at 10.0 mM (5X final ligand density) and mixed with PEG-4MAL at a 2:1 PEG-4MAL/ligand ratio to generate functionalized PEG-4MAL precursor. Bis-cysteine crosslinking peptides IPES (GCRDIPES ↓ LRAGDRCG; ↓ denotes enzymatic cleavage site) or GPQ-W (GCRDGPQG ↓ IWGQDRCG) was dissolved in HEPES at a density corresponding to 1:1 maleimide/cysteine ratio after accounting for maleimide groups reacted with adhesive peptide. IMCD cells were resuspended at 5X final density in ice-cold serum-free media and kept on ice. To form hydrogels, adhesive peptide-functionalized PEG-4MAL macromer, cells, and crosslinking peptide were polymerized for 20 min before addition of complete growth medium. A final density of 75,000 cells/mL were encapsulated in all hydrogels. Full growth medium change was performed every 2 – 3 d. Sample size was established as at least 4 hydrogels per condition with the premise that an outcome present in 4 different hydrogels under a specific condition will reveal the population behavior submitted to this given condition.

Hydrogel characterization

The storage and loss moduli of hydrogels were assessed by dynamic oscillatory strain and frequency sweeps performed on a MCR 302 stress-controlled rheometer (Anton Paar) with a 9-mm diameter, 2° cone, and plate geometry. Oscillatory frequency sweeps were used to examine the storage and loss moduli (ω = 0.5–100 rad s^{-1}) at a strain of 2.31%.

Viability and proliferation assays

For cell viability assessment, PEG-4MAL gels were incubated in 0.5% collagenase I (Worthington Biochemical), 0.5 μM C$_{12}$-Resazurin (live; L34951, Thermo Fisher

Scientific), and 1 μM TOTO-3 iodide (dead; T3604, Thermo Fisher Scientific) in serum-free media until hydrogel was completely dissolved and cells settled at bottom of well. Proliferation was assayed using the Click-iT EdU Imaging Kit (C10338, Thermo Fisher Scientific) following manufacturer's instructions. Samples were imaged with Nikon Plan Fluor 10× (NA 0.30) or Plan Fluor 20× (NA 0.45) objectives in a C2-Plus Confocal System (NIS Elements acquisition software). Cells were counted with ImageJ (NIH) macros.

Immunofluorescence labeling of cysts

Gels were washed extensively in DPBS and fixed in 4% formaldehyde in DPBS for 20 min. Gels were incubated for 30 min in blocking buffer (1% bovine serum albumin, 1% goat serum, 0.1% fish skin gelatin, 0.5% Triton X-100, 0.05% sodium azide in PBS). Samples were incubated in primary antibodies diluted in blocking buffer on an orbital shaker at 4ºC overnight. Secondary antibodies and nuclear stain were diluted in blocking buffer and incubated on an orbital shaker at 4ºC overnight. Fluorescent images for tubule assessment were captured with 20X or 40X objectives in a Nikon Eclipse Ti microscope connected to a C2+ confocal module. Area and Feret diameter of multicellular IMCD structures were measured from fluorescent images of specimen cross sections using ImageJ macros.

Inhibition of mediators of mechanotransduction, MMPs and integrin subunits

Inhibition of myosin II or Rho-associated kinase was performed using blebbistatin (203389, Calbiochem) or Y-27632 (688002, Calbiochem), respectively, by adding 25 μM to the growth medium 5 d after cell encapsulation in hydrogel. Broad inhibition of matrix metalloproteinases (MMPs) or MT1-MMPs was performed by adding 25 µM of GM6001

MMP Inhibitor (CC1010, Millipore) or 200 µM of Anti-MT1-MMP antibody (AB6005, Millipore), respectively, to the growth medium 3 d after cell encapsulation in hydrogel. Inhibition of integrin subunits α1, α2 or β1 was performed by adding 0.5 µg/mL of anti-rat/mouse CD49a (555001, BD Pharmingen), anti-rat/mouse CD49b (554998, BD Pharmingen) or AIIB2 (Developmental Studies Hybridoma Bank), respectively. Samples were imaged using a Nikon Eclipse Ti microscope connected to a C2+ confocal module.

Statistical analyses

Statistical analyses were performed using GraphPad Prism 6.0. For normally distributed data with equal variances, one-way ANOVA with Tukey's multiple comparison test was used, and unpaired t-test with Welch's correction. For non-normally distributed data, Krustal-Wallis with Dunn's multiple comparisons test was used. P-values of statistical significance are represented as ****$P < 0.0001$, ***$P < 0.0002$, **$P < 0.0021$, *$P < 0.0332$. A p-value < 0.0332 was considered significant.

CHAPTER 5.   PEG-4MAL HYDROGELS FOR HUMAN ORGANOID GENERATION, CULTURE, AND IN VIVO DELIVERY[3]

5.1   Abstract

In vitro differentiation of human organoids (HOs) generated from embryonic stem cells and induced pluripotent stem cells offers unparalleled means to produce multi-cellular 3D structures analogous to native human tissues. Most current methods for generating HOs rely on Matrigel[TM], a poorly defined, basement membrane derivative secreted by Engelbreth-Holm-Swarm (EHS) mouse sarcoma cells, limiting the potential use of HOs for regenerative medicine applications. Here, we describe a protocol for the synthesis of a fully defined, synthetic hydrogel that supports the generation and culture of HOs. Modular, cell-encapsulating hydrogels are formed from a four-armed poly(ethylene glycol) macromer having at each terminus maleimide groups (PEG-4MAL), which are conjugated to cysteine-containing adhesive peptides and crosslinked via protease-degradable peptides. The protocol also includes guidelines for the localized in vivo delivery of PEG-4MAL hydrogel-encapsulated HOs that support engraftment and accelerate colonic wound repair. This culture and delivery strategy forms a basis for the development of HO-based therapies to treat injury and disease. Hydrogel and tissue preparation and subsequent encapsulation

---

[3] In Revision: PEG-4MAL hydrogels for human organoid generation, culture, and in vivo delivery. Cruz-Acuña, R., Quirós, M., Huang, S., Siuda, D., Spence, J.R., Nusrat, A., and García, A.J. *Nature Protocols*

can be performed within 2.5 to 3.5 h. HOs cultured in synthetic hydrogels for at least 14 d can be delivered for wound repair applications in under 5 h.

5.2 Introduction

Human pluripotent stem cell (hPSC)-derived organoids (HOs) offer unparalleled strategies for generating multi-cellular 3D structures recapitulating important features of epithelial and mesenchymal tissue, making them valuable tools in the study of a range of cellular processes[25,135]. In this context, protocols have been developed for the *in vitro* generation of different HOs (e.g., intestine[98,107], lung[109,136], brain[137], retina[138], and kidney[139]) that provide powerful platforms to model human organ development and chronic diseases, for example, cancer and inflammatory bowel disease[97]. Furthermore, HOs can potentially serve as tissue sources for patient-specific regenerative therapies[135]. For example, efficient methods have been developed to direct differentiation of hPSCs into 3D structures (spheroids) followed by culture in specific *in vitro* culture conditions that enable the spheroids to differentiate further into human intestinal organoids (HIOs)[107]. As spheroids bud off from the pluripotent stem cell monolayer, they are initially composed of two multipotent cell populations, intestinal epithelial and mesenchymal populations. Spheroids are transferred to 3D culture where they further differentiate and expand into HIOs, giving rise to several different epithelial (enterocytes, goblet cells, Paneth cells, enteroendocrine cells, intestinal stem cells) and mesenchymal (subepithelial myofibroblasts, smooth muscle cells) populations. The development of HIOs has been shown to closely mimic the development of embryonic intestinal tissue[98,104,107,140]. Most currently available protocols for organoid generation require encapsulation of spheroids within biologically-derived materials, such as Matrigel™, which are not well characterized

and thus exhibit considerable lot-to-lot variability, poor experimental control, and the inability to decouple their biochemical and biophysical properties[8,141,142]. Additionally, in the case of Matrigel[TM], the fact that this material is derived from murine cancerous cells limits its translational potential[4,143]. Fully defined, synthetic hydrogels that present tunable physicochemical properties are promising alternatives to current organoid culture biologically-derived matrices, as they can mediate innate cellular responses via presentation of bioactive motifs that promote cell-matrix adhesive interactions and cell-directed matrix degradation[127,143].

5.2.1 Development and advantages of the protocol

Hydrogels are water-swollen, crosslinked polymer networks with attractive mechanical and biochemical properties for a variety of biomedical and biotechnological applications[4]. The fully defined synthetic hydrogel system described in this protocol is based on a four-armed, maleimide-terminated poly(ethylene glycol) (PEG-4MAL) macromer that is engineered to present elements and traits inspired by extracellular matrices, such as cell-adhesion peptides and matrix sensitivity to cell-secreted proteases. Although many synthetic hydrogel systems have been developed to mimic the properties of natural extracellular matrices, the PEG-4MAL hydrogel platform exhibits substantial advantages over the other synthetic hydrogels developed thus far, including a well-defined structure, the stoichiometric incorporation of cell adhesive peptides (and other biological signals), increased cytocompatibility, and improved crosslinking efficiency[9,10,127]. Additionally, the fact that the properties of PEG-4MAL hydrogels are tunable enables the study of the independent contributions of the biophysical and biochemical properties of the matrix on both single cell and multicellular programs. For instance, using this platform, we

87

showed that normal cyst growth, polarization, and lumen formation of renal epithelial Madin–Darby canine kidney (MDCK) cells could only take place within a narrow range of values for the elasticity of the matrix, required a threshold level of cell-directed matrix degradability, and were subject to a tight regulation imposed by the adhesive peptide density[9]. Furthermore, we have recently reported that both the *in vitro* generation and culture of HIOs from hPSC-derived spheroids, and the culture of human lung organoids (HLOs), were dependent on the mechanical and biochemical properties of the PEG-4MAL hydrogel[127]. Finally, for comparison purposes, the total cost of hydrogel components necessary to produce a total of 10 mL of fully crosslinked synthetic hydrogel is approximately \$140, whereas 10 mL of Matrigel[TM] costs approximately \$305. Therefore, PEG-4MAL hydrogels serve as an *in vitro* synthetic platform that can be modulated to support different cellular developmental programs, like HO development, while overcoming the limitations of biologically-derived materials, such as Matrigel[TM].

Additionally, use of the PEG-4MAL hydrogel affords tunable reaction time scales for *in situ* gelation for *in vivo* applications. In fact, this synthetic hydrogel system has been successfully used as a delivery vehicle featuring rapid gelation and integration at the transplantation site. This hydrogel system has also been demonstrated to support the viability of encapsulated cells and to readily undergo the cell-mediated degradation that promotes engraftment of delivered cells into the host tissue[11,144]. We demonstrated that injection of HIOs and the liquid precursors of the hydrogel into mucosal wounds in the murine intestine resulted in *in situ*–formation of a polymerized hydrogel that supported localized organoid engraftment and accelerated wound repair[127]. Furthermore, the base macromer exhibits minimal toxicity and inflammation *in vivo*; additionally, it is rapidly

excreted via the urine. These are important advantageous traits to have when evaluating the safety and translational potential of hydrogels[11]. Consequently, PEG-4MAL hydrogels have shown to be a suitable cellular delivery tool with the potential to be used for cell-based therapies for regenerative medicine applications.

5.2.2   *Overview of the procedure*

We describe a protocol for the synthesis of a fully synthetic PEG-4MAL hydrogel that supports the robust and highly reproducible *in vitro* generation of HOs from human induced pluripotent stem cell (hiPSC)- and embryonic stem cell (hESC)-derived spheroids that does not involve Matrigel[TM] encapsulation. Additionally, we provide guidelines for the subsequent *in vitro* culture and passaging of fully-developed HOs within the PEG-4MAL hydrogel.

Briefly, to generate hydrogels, the PEG-4MAL macromer is conjugated to an adhesive peptide to form a functionalized PEG-4MAL macromer (Fig. 27). The functionalized PEG-4MAL macromers are mixed with hPSC-derived spheroids or HOs and then crosslinked with a protease-degradable peptide for 20 min, before adding growth medium to the polymerized hydrogel (Fig 28)[127]. As discussed previously[9,10,127], the macromer size (e.g., 10 kDa vs. 20 kDa) and polymer density can be modified to tune the density of crosslinks within the hydrogel which translates to changes in its biophysical properties. Moreover, the type and density of adhesive and crosslinking peptides can be modulated to confer specific biochemical properties onto this synthetic matrix. The ability to tune the biophysical and biochemical characteristics of the synthetic matrix is an important attribute of this platform because different cell types will respond differently to the biophysical and biochemical properties of their microenvironment. For example, we

have identified the elementary biophysical and biochemical matrix properties needed to support hPSC-derived organoid generation, which are different from the more mechanically-dynamic matrix properties needed to support the generation of organoids from single murine *Lrg5+* intestinal stem cells[143]. More information regarding changes to the biophysical and biochemical matrix properties is included in the Experimental Design section.
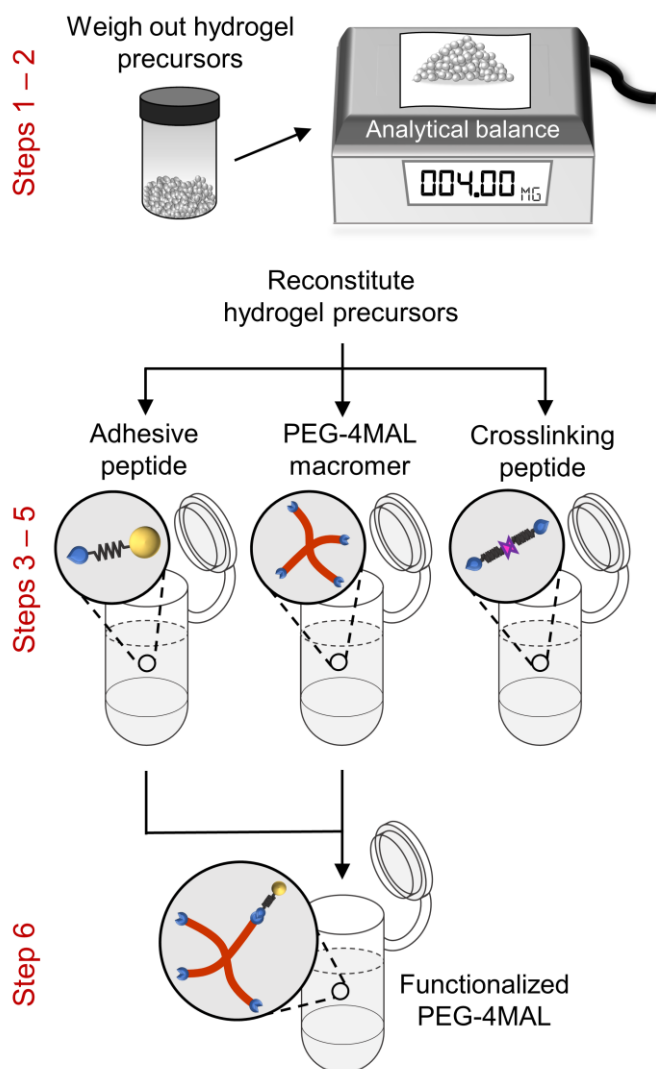
Figure 27: Preparation of the solutions of the precursor of the PEG-4MAL hydrogel.
Hydrogel precursor solutions are reconstituted in separate tubes, and functionalized PEG-4MAL macromer is produced by mixing the solution of the PEG-4MAL macromer with that of the adhesive ligand. The relevant steps of the protocol are highlighted in red. Adapted from Cruz-Acuña and Quirós et al. (2017).
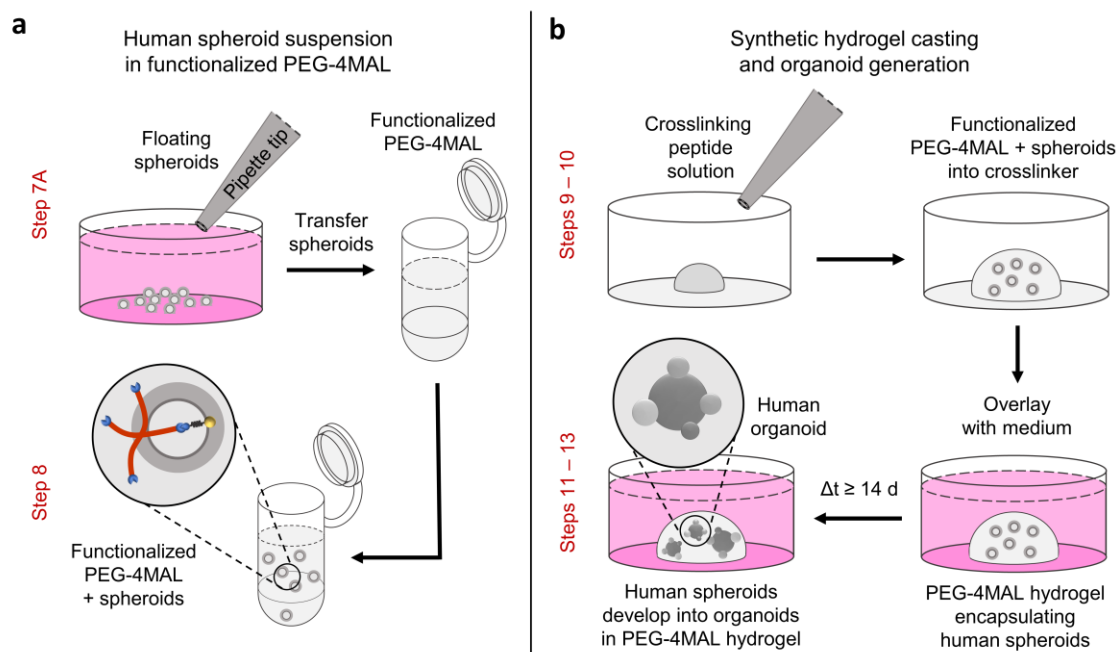
Figure 28: Synthesis of PEG-4MAL hydrogel and organoid generation. (a) Floating, hPSC-derived human spheroids (generated as previously described[98,107]) are collected and mixed with a solution of functionalized PEG-4MAL macromer. (b) PEG-4MAL hydrogel is casted by pipetting the mixture of functionalized PEG-4MAL and spheroids into the solution of the crosslinker. Encapsulated spheroids will expand and develop into human organoids. The relevant steps of the protocol are highlighted in red. Adapted from Cruz-Acuña and Quirós et al. (2017).

The present protocol also explains how to deliver hydrogel-containing HIOs generated in the PEG-4MAL hydrogel or a biologically-derived matrix to colonic mucosal wounds by injection via a colonoscope, which results in organoid survival, engraftment, and accelerated wound repair[127]. Briefly, a miniaturized colonoscope system equipped with biopsy forceps is used to biopsy-injure the colonic mucosa of mice (as previously described[112,145]), and to inject a HO-containing hydrogel 1 d after wounding with the aid of a custom-made injection device (Fig 29). The ability of this synthetic matrix to deliver HOs via endoscopic techniques and the minimal toxicity and inflammatory response associated with its use *in vivo*[10,11] are a proof of concept that hydrogel-encapsulated HOs

may be used therapeutically to treat intestinal injury, overcoming the limitations associated with the use of Matrigel[TM] for HO technologies[127]. Moreover, the ability to tune the polymerization kinetics (gelling rate) of this injectable system renders possible its application in other settings. For example, by controlling the polymerization rate, different physical forms of the hydrogel can be generated such as a patch that forms on the surface of the heart to localize cells in rats; as an injectable matrix to deliver vasculogenic proteins that promote the vascularization and engraftment of pancreatic islets in rodents; or as a liquid drug carrier delivered via a double-lumen catheter to produce a conformal drug depot in the pericardial space of pigs[144,146,147].

Organoid injection into mucosal wound bed

Dislodge organoids
from hydrogel

Transfer
organoids

**27G
needle**
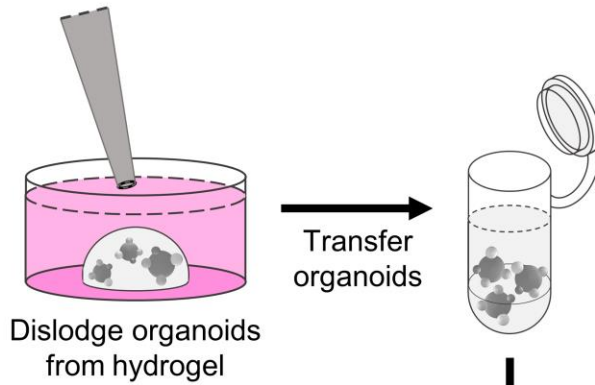
Load crosslinker
solutions into
custom-made
device

Transfer organoids
to functionalized PEG-4MAL
(prepared as steps 1 – 6)

Wound

Needle

Needle

Organoid in hydrogel
precursor solution

Crosslinking
peptide solution

Syringe
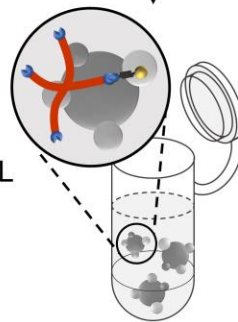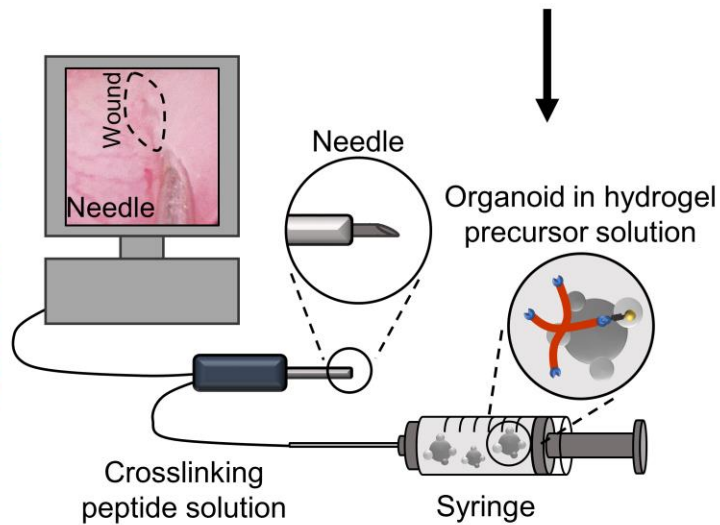
Figure 29: Preparation of PEG-4MAL hydrogel-generated organoids and set-up for mucosal injection. HIOs generated in PEG-4MAL hydrogels are recovered from the matrix, mixed with hydrogel precursor solutions, and injected underneath the submucosal wounds using a custom-made device (comprising a 10-cm piece of intramedic polyethylene tube with a 27G needle at each end) via a colonoscope. The relevant steps of the protocol are highlighted in red. Adapted from Cruz-Acuña and Quirós et al. (2017).

5.2.3   Limitations of the protocol

An important aspect of this engineered hydrogel platform is its rapid reaction kinetics that may result, if mixing is not conducted properly, in the formation of an inhomogeneous gel that presents variabilities in its physicochemical properties. Therefore, to avoid inhomogeneities in the hydrogel properties due to premature crosslinking, the functionalized macromer and crosslinker solutions may need to be delivered separately and mixed at the in vivo delivery site, or mixed prior to rapid delivery into the in vivo site. Furthermore, for adhesive ligands and crosslinking peptides to be incorporated into PEG-4MAL hydrogels, these molecules must have free thiol groups that can react with the maleimide moieties of the hydrogel backbone. Therefore, these signaling sequences might need to be custom-synthesized to contain a free thiol group (e.g., a cysteine residue) that enables the chemical coupling into PEG-4MAL hydrogels to take place.

5.2.4   Application and extension of the method for human organoid generation and delivery

The PEG-4MAL hydrogel system serves as a robust platform for the *in vitro* generation and culture of different types of HOs that facilitates the study of the contributions of the extracellular matrix to human organ development, differentiation, and function. For this purpose, we reported an engineered hydrogel (storage modulus (G'): 100 Pa; 4.0%, 20 kDa PEG-4MAL; 2.0 mM RGD; GPQ-W crosslinker) that supports the *in*

vitro generation of HIOs from hPSC-derived spheroids and culture of HLOs[109], establishing its potential to generate and maintain different types of HOs[127]. The modular design of the PEG-4MAL hydrogel system provides the means to independently optimize the physicochemical properties of the synthetic matrix to identify the engineered formulation that supports HO generation. For instance, we demonstrated[9,10,127] that the mechanical properties of the synthetic matrix can be controlled by varying the polymer density, independently from the matrix's biochemical properties (adhesive peptide type or density). Conversely, the biochemical characteristics of the material can be modified by changes in the adhesive peptide type (e.g. laminin- or collagen-derived peptides) or density, independently from the material's mechanical properties. These modifications of the matrix properties were proven to have a direct effect on the epithelial morphogenesis of different cell systems and on spheroid development into HIOs[9,127]. Therefore, in addition to the inherent potential of the engineered hydrogel, its modular design supports the adaptability of this synthetic material to assist with the generation and culture of different types of HOs.

Furthermore, we have established that the engineered hydrogel can be used as a HIO delivery vehicle to mucosal wounds that supports localized organoid engraftment and accelerated wound repair[127]. We also demonstrated that the presence of the delivery hydrogel is required for HIO engraftment at the implantation site[127]. Therefore, this delivery strategy may be the starting point for the development of HO-based tissue replacement therapies that are based on the direct engraftment into injured or diseased organs, for example as an approach to treat human gastrointestinal diseases associated with intestinal epithelial wounds (e.g. inflammatory bowel disease).

5.3   Experimental Design

PEG-4MAL hydrogels have previously demonstrated to be a reproducible platform for the *in vitro* generation and *in vivo* delivery of HOs[127]. The reproducibility of the synthetic hydrogel has been established with a sample size of at least 4 hydrogels per condition (20-30 spheroids/hydrogel or 2-4 HOs/hydrogel) for *in vitro* experimentation, and 4 mice per condition (4–5 injections per mouse) for *in vivo* experimentation, with the premise that an outcome present in all hydrogels or animals under a specific condition will reveal the population behavior submitted to this given condition[127]. Additionally, for a particular hydrogel formulation, consistent biophysical and biochemical properties, as well as the resulting spheroid/HO responses, have been observed across independent experimental runs performed on different days, demonstrating high reproducibility. For all *in vitro* experiments, if making more than one functionalized PEG-4MAL precursor solution, it is recommended to allocate all human spheroid or HO suspension in one tube (as indicated in the protocol) and ensure proper mixing prior to mixing with the hydrogel precursor solutions, to ensure a random distribution of the biological tissue. No specific randomization scheme is recommended for *in vivo* delivery of HOs, although randomization of samples is highly recommended. Finally, to avoid research bias, it is recommended that the researcher(s) performing the experiments is(are) different from the researcher(s) processing and analyzing the experimental results.

5.3.1   *Synthetic hydrogels for hPSC-derived spheroids and HOs*

Efficient methods have been developed to generate HOs from *in vitro* hPSC cultures through direct differentiation protocols that are specific to the developmental

program of the tissue origin of interest[135]. During the initial differentiation stages of hPSCs, human spheroids arise by budding from the hPSC monolayer and detaching. To generate the HOs, the detached, floating spheroids are collected and transferred to 3D culture, most commonly in Matrigel™, where they further differentiate and expand into HOs, giving rise to several differentiated tissue-specific cellular populations. The generated HOs can be further cultured and undergo passaging in the 3D culture environment for research purposes that encompass studying organ development and tissue-specific disease progression[135]. Nevertheless, biologically-derived, 3D culture environments exhibit considerable lot-to-lot variability, the inability to decouple its biochemical and biophysical properties[8,141,142], and in the case of Matrigel™, the fact that it is derived from murine cancerous cells limits its translational potential[4,143]. Consequently, fully defined, PEG-4MAL hydrogels that present tunable physicochemical properties have demonstrated to be a promising alternative to current organoid culture matrices for translational medicine applications[127].

This protocol provides guidelines to engineer a PEG-4MAL hydrogel for the *in vitro* generation of the desired HO by substituting the use of Matrigel™ on the encapsulation of floating 3D spheroids generated from hPSC cultures by directed differentiation (e.g. midgut and hindgut spheroids for generation of HIOs, as previously described[98,107,127]). Additionally, the synthetic matrix can be used for the continuous 3D culture and passaging of hPSC-derived human organoids that were generated using the synthetic material or using Matrigel™ (e.g., HIOs generated in Matrigel™ for at least 14 d, as previously described[98,107,127]). Moreover, because this protocol is intended for the generation and culture of hPSC-derived HOs, the passaging steps provided here differ from

trypsin-based passage protocols used for primary tissue-derived organoids[142,148]. For instance, due to the mesenchymal layer and the large size of HIOs, these cannot be passaged in a manner similar to organoids derived from primary tissue and required manual cutting[107], as described in this protocol. We emphasize that manual cutting has been previously reported for HIO cultures in Matrigel[TM,(107)] and thus the procedure and time required to manually cut organoids into halves is independent of the matrix used and does not represent a limitation of the synthetic hydrogel. For hPSC-derived human organoids that do not require manual cutting, such as HLOs[109], this specific step can be skipped.

5.3.2   *Synthetic hydrogels can be adapted for different HO systems*

An attractive feature of the PEG-4MAL hydrogel system is the ability to independently tune its biophysical and biochemical properties, which allows for its adaptation to the culture of different types of HOs. The macromer size (e.g., 10 kDa vs. 20 kDa) and polymer density can be modified to tune the density of crosslinks within the hydrogel, which translates to changes in its biophysical properties; moreover, the type and density of adhesive and crosslinking peptides can be modulated to confer specific biochemical properties onto this synthetic matrix. For instance, variations to the PEG-4MAL polymer density directly controls its stiffness[9,10,127] (storage modulus, G'; biophysical property), independently from its adhesive peptide type and density (2.0 mM RGD, biochemical property) (Fig. 30). Given a constant adhesive peptide concentration, when the PEG-4MAL polymer density is increased (decreased), the number of additional (fewer) maleimide moieties must be compensated by a higher (lower) concentration of crosslinks (e.g. GPQ-W crosslinking peptide) which in turn increases (decreases) the matrix stiffness. Therefore, in this hydrogel system, the mechanical properties (e.g., elastic

modulus, or the related storage modulus determined by rheometry) are determined by the density of crosslinks in the hydrogel network. Matrix stiffness is an important biophysical property to consider when designing a synthetic cellular matrix for the type of HO of interest, as we have previously shown that different biophysical cues (4% and 6% PEG-4MAL polymer density, Fig. 30) support the morphogenesis program of different epithelial cell lines (MDCK and Caco-2, respectively)[9]. Therefore, PEG-4MAL polymer density can be modified to tune the density of crosslinks and identify a matrix stiffness that provides the physical support and promotes the essential mechanosignals for the generation and culture of the HO of interest. For reference, we have previously shown that PEG-4MAL polymer density controls HIO generation from hPSC-derived intestinal spheroids and influences the prolonged viability of HIOs generated in Matrigel[TM,127].
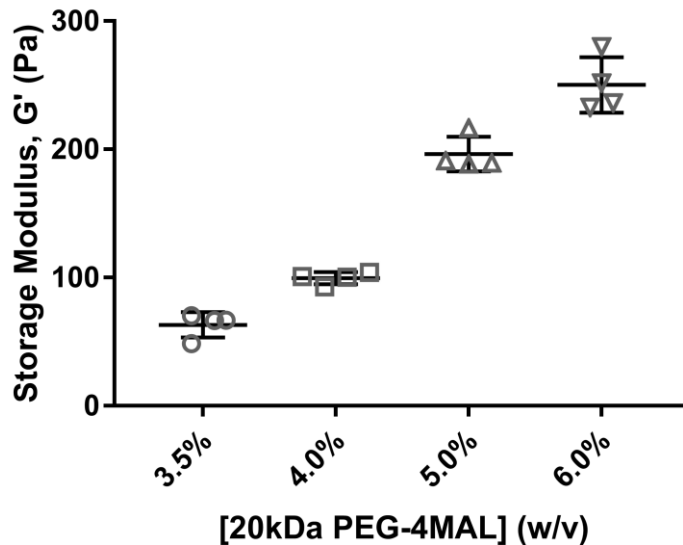
Figure 30: Typical results of rheometric characterization of PEG-4MAL hydrogels. Relationship between polymer density (wt%) and storage modulus of 20 kDa PEG-4MAL hydrogels with constant biochemical properties (2.0 mM RGD, using GPQ-W crosslinker). Data is presented as mean ± SEM; n = 4 independently prepared hydrogels per condition.

The functionalization of the PEG-4MAL macromer using adhesive peptides is an important biochemical property to consider when designing a synthetic cellular matrix that best resembles the biochemical environment of the native tissue of interest[4]. In this context, given a constant density of PEG-4MAL, the hydrogel macromer can be functionalized with different types and densities of cysteine-terminated adhesive peptides (e.g. RGD, laminin-, or collagen-derived peptides) to modify the biochemical characteristics of the material, considering that all unreacted maleimide groups remaining are crosslinked. For reference, we have previously shown that the adhesive peptide type has a significant effect on HIO viability[127], and that adhesive peptide (RGD) density dramatically regulates cyst polarity and lumen phenotypes of epithelial cells[9]. Finally, the capacity of cells to modify their microenvironment via matrix degradation is essential for tissue remodeling and homeostasis[4,149]. In this context, given a constant density of PEG-4MAL and a fixed type and density of adhesive peptide, the level of hydrogel degradability by proteases can be modulated by varying the ratio between a relatively fast-degrading (e.g. GPQ-W) and a slow- or non-degrading (e.g. GPQ-A[9] or DTT[127], respectively) crosslinking agent. Therefore, when designing a PEG-4MAL hydrogel matrix for the HO of interest, it is important to consider the use of a crosslinking peptide that is sensitive to the proteases expressed by the HO. We have previously demonstrated that prolonged survival of HIOs requires a degradable matrix crosslinked with the collagen-derived GPQ-W peptide[127], and that normal epithelial cyst polarity and lumen formation required a threshold level (80% fast-degrading GPQ-W) of protease-directed matrix degradability[9]. Finally, as in a previous report, users can evaluate the suitability of the synthetic hydrogel for the

generation of HIOs by assessing human intestinal spheroid/HIO viability at different time points, proliferation, growth and morphological changes of the HIO structure[127].

This protocol describes a synthetic hydrogel platform that can be established to support the *in vitro* generation and culture of different types of HOs via modulation of its biophysical and biochemical matrix properties, as described. Furthermore, this protocol provides guidelines (Box 1) to generate an engineered hydrogel formulation (storage modulus (G'): 100 Pa; 4.0%, 20 kDa PEG-4MAL; 2.0 mM RGD; GPQ-W crosslinker) that supports the *in vitro* generation of HIOs from hPSC-derived spheroids and culture of HLOs[127]. Therefore, this engineered formulation should be used as a starting point for designing a PEG-4MAL hydrogel for the *in vitro* generation and culture of the HO of interest. Further variations to the biophysical and biochemical matrix properties described above can be explored if the initial hydrogel formulation (Box 1) does not support the viability and growth of the human spheroid/HO of interest. Further discussion regarding variations to the biophysical and biochemical matrix properties is presented in Box 1.

5.3.3   *Murine model for HIO transplant into colonic wounds*

Another attractive feature of the PEG-4MAL hydrogel platform is that it affords tunable reaction time scales for *in situ* gelation for *in vivo* applications. For example, adjusting the pH of the hydrogel precursor solutions to slightly below physiological pH (6.5–7.4) will reduce the reaction kinetics. Reducing the speed of reaction can help prevent premature crosslinking that may occur during hydrogel delivery via custom-made devices, such as the injection device described later (Fig. 29).

We provide a procedure to develop a custom-made device for the injection of HIOs and the liquid precursors of the hydrogel through a colonoscope into murine mucosal wounds resulting in *in situ*–formation of a polymerized hydrogel at the injection site. We recommend the use of NOD-scid IL2Rg-null (NSG) mice as recipients for transplantation of human organoids using synthetic hydrogels to minimize immune rejection by the host to transplanted human tissue. NSG mice have demonstrated to be consistently better for human stem cell engraftment as compared to several other immunocompromised mouse strains[150]. We recommend male animals around 12 weeks old as male mice have longer colons than females, providing more space for colonoscopy purposes. At 12 weeks old, mice are less susceptible to suffer intestinal perforations as a consequence of the biopsy injury and have optimal repair programming. Nevertheless, we have conducted studies with C57BL/B6 mice at different ages and found no differences in wound repair between 3 months old up to 1 year old. We have previously used 8-week old, male NSG mice as a proof of concept for the use of the synthetic hydrogel as a delivery vehicle for HIOs to murine colonic wounds using a colonoscope, promoting HIO engraftment and accelerated wound healing[127].

5.4 Materials

REAGENTS

- PEG-4MAL macromer (MW 22,000, >95% MAL functionalization; Laysan Bio, Cat. No. 4arm-PEG-MAL-20K)

- RGD: GRGDSPC (AAPPTec, custom synthesis, purity: > 95%, TFA removal)

- GPQ-W: GCRDGPQGIWGQDRCG (AAPPTec, custom synthesis, purity: > 95%, TFA removal)

- Human spheroid derived from hESCs (we have used H9 [NIH registry #0062] and derived these to human intestinal spheroids as described in ref[98,107]), human spheroid derived from hiPSCs (we have used line 20.1, generated by the Pluripotent Stem Cell Facility, Cincinnati Children's Hospital Medical Center[98], and derived these to human intestinal spheroids as described in ref[98,107]), HIOs derived from an hESC (we have used H9; NIH registry #0062; we derived these as described in ref[98,107]), HIOs derived from an hiPSC (we have used line 20.1; generated by the Pluripotent Stem Cell Facility, Cincinnati Children's Hospital Medical Center[98]; we derived these as described in ref[98,107]), or HLOs derived from hESC (UM63-1; NIH registry #0277; we derived these as described in ref [109])

CAUTION: We regularly monitor stem cell lines for chromosomal karyotype. For this purpose, the number of chromosomes are confirmed, chromosomal abnormalities are ruled out and sex chromosomes of each line are confirmed. Assessment of functional and molecular authentication for pluripotency and for the ability of the cells to undergo multi-lineage differentiation is performed using a panel of antibody and qRT-PCR markers.

- Advanced DMEM-F12 medium (Invitrogen, Cat. No. 12634-010)

- L-Glutamine (100×; Invitrogen, Cat. No. 25030-081)

- Penicillin–streptomycin (100×; Invitrogen, Cat. No. 15140-122)

- B27 supplement (50×; Invitrogen, Cat. No. 17504044)

- N-2 supplement (100×; Gibco; Cat. No. 17502048)

- Fetal bovine serum (FBS; Life Technologies, Cat. No. 16000-044)

- Noggin (R&D Systems, Cat. No. 6057-NG)

- R-spondin1 (R&D Systems, Cat. No. 4645-RS)

- Epidermal growth factor (EGF; R&D Systems, Cat. No. 236-EG)

- Fibroblast growth factor 10 (FGF-10; R&D Systems, Cat. No. 345-FG-025/CF)

- HEPES solution (Sigma, Cat. No. H0887)

- DPBS (Thermo Fisher Scientific, Cat. No. 14040133)

- Matrigel^{TM} (BD Biosciences, Cat. No. 354234)

- Recipient mice for transplant of organoids. We recommend the use of 12-week old, male NOD-scid IL2Rg-null (NSG) mice for the example application we describe in the procedure (Jackson Laboratory)

Caution: All animal studies must be reviewed and approved by the relevant animal care committees and must conform to all relevant institutional and national ethics regulations. The method we describe here was approved by University of Michigan's Institutional Animal Care and Use Committee (IACUC) in accordance with the U.S. Department of Agriculture (USDA) Animal and Plant Health Inspection Service (APHIS) regulations and the National Institutes of Health (NIH) Office of Laboratory Animal Welfare (OLAW) regulations governing the use of vertebrate animals.

- Ketamine-HCL (Hospira, Cat. No. RL-3760)

- Xylazine (Lloyd laboratories, Cat. No. 4811)

EQUIPMENT

- Stereomicroscope (Olympus SZ61)

- Horizontal clean bench (Labcono)

- Costar® multi-well ultra-low attachment plate (Corning, Cat. No. 3473; 24-well plate, recommended)

- Costar® Spin-X Centrifuge Tubes (Cole-Palmer, Cat. No. UX-01937-32)

- Microcentrifuge tubes (VWR, Cat. No. 10025-724)

- High-precision analytical balance (Mettler Toledo, Cat. No. XPE105, or equivalent)

- pH bench meter (Mettler Toledo, Cat. No. SC S220-B)

- MI-410 Combination pH microprobe (Microelectrodes, Inc.), or equivalent

- Microcentrifuge (Beckman Coulter, Cat. No. B30137)

- Large orifice pipette tips (USA Scientific, Cat. No. 1011-8410 and 1011-9410)

- Forceps and/or tungsten needle

- Disposable scalpel (size 15; Exelint, cat. no. 29556)

- Colonoscope (Mainz Coloview® Veterinary Endoscope, Karl Storz)

- Biopsy forceps (Mainz Coloview® Veterinary Endoscope, Karl Storz)

- 27G needles (BD, Cat. No. 305109)

- TB syringes (BD, Cat. No. 309659)

- Polyethylene tubing (Bector Dickinson, Cat. No. 427406)

- Plastic feeding (gavage) needles (Instech, Cat. No. GTP-20-30-50)

- 10 mL syringes (BD, Cat. No. 309604)

REAGENT SETUP

20 mM HEPES buffer, pH 7.4. To prepare 100 mL of 20 mM HEPES buffer, mix 2 mL of HEPES solution with 90 mL of DPBS. Adjust the pH to 7.4 using 6 M NaOH and adjust the volume of the resulting solution to 100 mL with DPBS. Sterile 20 mM HEPES buffer can be stored for 2 months at room temperature.

Intestine growth medium. For 500 mL of intestine growth medium, pool together 459.7 mL of advanced DMEM-F12 medium, 5 mL of L-glutamine (final concentration, 2 mM), 7.5 mL of HEPES solution (final concentration, 15 mM), 20 mL of B27 supplement (1X final dilution = 2 mL per 50 mL of medium), 5 mL of penicillin–streptomycin (final concentration, 100 U/mL penicillin, and 100 µg/mL streptomycin), 200 µL of Noggin (250µg/mL; final concentration, 100 ng/mL), 100 µL of EGF (500 µg/mL; final

concentration, 100 ng/mL), and 2.5 mL of R-Spondin1 (100μg/mL; final concentration, 500 ng/mL). The intestine growth medium is best if freshly made, but can be stored for 1 week at 4 °C.

Foregut basal medium. For 500 mL of foregut basal medium, pool together 470 mL of advanced DMEM-F12 medium, 5 mL of L-glutamine (final concentration, 2 mM), 5 mL of HEPES solution (final concentration, 10 mM), 5 mL of penicillin–streptomycin (final concentration, 100 U/mL penicillin, and 100 µg/mL streptomycin), 10 mL of B27 supplement (1X final dilution = 1 mL per 50 mL of medium), 5 mL of N-2 supplement (1X final dilution = 0.5 mL per 50 mL of medium). This Foregut basal medium can be stored at 4ºC for up to 1 month.

Human lung organoid growth medium. On the day of use, aliquot 49.5 mL of foregut basal medium into a 50 mL conical tube. Add 500 µL of FBS (final concentration, 1%) and 250 µL of FGF-10 (100µg/mL stock; final concentration, 500 ng/mL). The human lung organoid growth medium is best if freshly made, but can be stored for 1 week at 4 °C.

Anesthesia solution. Prepare anesthesia solution by diluting ketamine and xylazine in DPBS in a 1:1 ratio of ketamine 20 mg/mL and xylazine 2 mg/mL dilution. Prepare solution considering that 1 mL of anesthesia solution is needed per 0.1 kg of murine body weight. Prepare this solution fresh every time.

Hydrogel components. Aliquot each hydrogel component. We aliquote PEG-4MAL macromer, RGD, and GPQ-W peptides (powder) in 100 mg, 25 mg and 50 mg aliquots, respectively, to avoid humidity exposure caused by the components experiencing multiple temperature changes. We also recommend to dissolve the necessary amount of hydrogel

components on the same day of experimentation. We do not recommend dissolving and then storing the PEG-4MAL macromer, as the maleimide groups may hydrolyze.

CRITICAL: Upon receipt, immediately store PEG-4MAL macromer, RGD, and GPQ-W peptides (powder) at -20 ºC.

Custom-made device for injections. Remove the metalic needle of a 27G needle (OD: 0.41 mm) from the hub. Carefully attach the blunt end of the needle to one end of a 10 cm piece of intramedic polyethylene tube (OD: 1.09 mm), leaving the needle bevel exposed. Connect another complete neddle to the other end of the tube through the needle bevel (Fig. 29). Prepare one custom-made device for each injection to avoid clogging. We recommend to prepare the custom-made device before starting the experimental procedure described in Step 13B.

5.5 Procedure

5.5.1 Preparation of hydrogel precursor solutions

1. Allow an aliquot of PEG-4MAL macromer, adhesive peptide (RGD) and crosslinker (GPQ-W) to reach room temperature (~20 ºC).

2. Weigh out 100.0 mg of PEG-4MAL macromer, 4.06 mg of RGD and 13.27 mg of GPQ-W using a high-precision analytical balance and place each component into a separate microcentrifuge tube (see Box 1 for sample calculation).

Critical step: This amount of hydrogel precursors produces a total of 2.5 mL hydrogel volume of 4.0% (wt./vol.), 20 kDa PEG-4MAL hydrogels (G': 100 Pa) functionalized with

2.0 mM RGD and crosslinked with GPQ-W peptide. This specific hydrogel formulation was previously reported for HIO generation and HLO culture[127], and thus serves as a starting point to identify a hydrogel formulation for the generation and culture of the HO of interest.

Critical step: Variations to the biophysical and biochemical matrix properties can be explored if the hydrogel formulation described here does not support the viability and growth of the human spheroid/HO of interest. These changes may change the values used in this example but do not change the steps described in this protocol. Please refer to Box 1 for further information.

3. Dissolve the GPQ-W and RGD peptides using 0.5 mL of 20 mM HEPES buffer for each peptide to produce 15.57 mM and 11.76 mM peptide solutions, respectively, after considering the purity of the peptides (as demonstrated in Box 1).

Critical step: Adjust the pH of each peptide solution to 7.4 using 6 M NaOH, while measuring pH using a pH meter combined with a pH microprobe.

Critical step: These RGD and GPQ-W peptide concentrations correspond to 5 times the concentration of their final density (see Box 1 for example calculation). This concentration factor can be changed given that all maleimide groups of the PEG-4MAL are conjugated after all hydrogel components are mixed.

4. Filter RGD solution (prepared in step 3), GPQ-W solution (prepared in step 3) and 1 mL of 20 mM HEPES buffer by transferring each solution to a separate Costar Spin-X centrifuge tube and centrifuge each tube at 9,000 *g* for 1 min at room temperature.

5. Dissolve the PEG-4MAL macromer using 1 mL of 20 mM HEPES buffer filtered in step 4 to produce a 4.55 mM solution (Fig. 27).

Critical step: This PEG-4MAL macromer concentration corresponds to 2.5 times the concentration of its final density (see Box 1 for example calculation). This concentration factor can be changed given that all maleimide groups of the PEG-4MAL are conjugated after all hydrogel components are mixed. (see Box 1 for example calculation).

Critical step: Steps 5–13 must be performed in a sterile environment (e.g. using a horizontal clean bench and sterile tools).

6. Mix the solutions of PEG-4MAL macromer and adhesive peptide (RGD) in a 2:1 PEG-4MAL/adhesive peptide volume ratio (1.0 mL of PEG-4MAL macromer and 0.5 mL of RGD peptide for this example) to generate the solution of the functionalized PEG-4MAL precursor. Incubate then the solution thus obtained for at least 15 min at 37 $^{\circ}$C (Fig. 27).

Critical step: This step produces the conjugation between the maleimide groups of the PEG-4MAL and the thiol groups of the peptides.

Critical step: The solution can be then stored at room temperature for no more than 3 h to avoid hydrolyzation of the maleimide groups, and to allow time to complete the next step.

7. Prepare a hPSC-derived 3D spheroid (option A), or hPSC-derived HO (option B) suspension in a separate microcentrifuge tube.

Critical step: This step applies to (option A) any type of hPSC-derived 3D spheroids generated *in vitro* by directed differentiation protocols (e.g. midgut and hindgut spheroids for generation of HIOs, as previously described[98,107]) with the purpose of generating HOs, or (option B) any type of hPSC-derived HO that was generated in Matrigel[TM] for a period of time established by its differentiation protocol (e.g. HIOs and HLOs generated in Matrigel[TM] for at least 14 d, as previously described[98,107,109,127]) or similar matrix.

A. Preparation of a human spheroid suspension (Timing: 30 min)

   i.   Harvest floating hiPSC- or hESC-derived spheroids that have reached the desired differentiation stage (e.g. midgut and hindgut spheroids present in the cultures on day 4 and day 5 of mid/hindgut induction as previously described[98,107]) by pipetting with large orifice pipette tips, and transfer them to a microcentrifuge tube containing growth medium (Fig. 28a).

  ii.   Adjust the volume of the spheroid suspension using growth medium (to a total volume of at least 0.5 mL for this example) to obtain a spheroid density that corresponds to 5 times the concentration of their final density in the hydrogels, and keep on ice (Fig. 28a). We recommend a final density of 20–30 spheroids per 40 μL of hydrogel and to not store the spheroid solution in ice for longer than 1 h, as previously reported for intestinal spheroids[127].

B. Preparation of a human organoid suspension (Timing: 30 min)

i. Mechanically dislodge HOs generated in Matrigel[TM] (e.g. HIOs and HLOs, as previously described[98,107,109,127]) or a similar matrix by vigorously pipetting the matrix with large orifice pipette tips to free the organoids, and transfer them to a microcentrifuge tube containing growth medium.

We have used HIOs and HLOs that have been generated from Matrigel[TM]-encapsulated spheroids for at least 14 d (as previosuly reported[127]), although it is likely that other types of hPSC-derived HOs that were generated in Matrigel[TM] or similar matrix for a different time frame can be used.

ii. Adjust the volume of the HO suspension using growth medium (for this example, to a total volume of at least 0.5 mL) to obtain a HO density that corresponds to 5 times the concentration of their final density in the hydrogels, and keep on ice. We recommend a final density of 2–4 HOs per 40 µL of hydrogel and to not store the HO solution in ice for longer than 1 h, as previously reported for HIOs and HLOs[127].

5.5.2 *Synthetic hydrogel casting*

8. Mix the human spheroid suspension or the HO suspension with the functionalized PEG-4MAL precursor solution (prepared in step 6) at a 3:1 functionalized PEG-4MAL/cell suspension volume ratio (for this example, 1.5 mL of functionalized PEG-4MAL precursor and 0.5 mL of human spheroid suspension or HO suspension) using large orifice pipette tips, and keep on ice for no longer than 30 min (Fig. 28a).

9. Add crosslinking peptide solution (GPQ-W) prepared in Step 4 (20% of desired final hydrogel volume, as shown in Box 1 — we recommend adding 8 µL of GPQ-W to

each well, to produce 40 µL of hydrogel in each well) to the bottom (centered) of each well of a multi-well plate (Fig. 28b).

Critical step: Perform this step in the shortest time possible to avoid crosslinker evaporation.

10. Pipette the mixture comprising the functionalized PEG-4MAL precursor and the cell mixture prepared in Step 8 (80% of desired final hydrogel volume, as shown in Box 1 — as mentioned in the previous step, we recommend adding 32 µL of this solution, to produce 40 µL of hydrogel in each well) into the crosslinker solution in each well using large orifice pipette tips (Fig. 28b).

Critical step: Mix the solution by pipetting several times to obtain a homogenous solution. Critical step: Use a new pipette tip to cast each different hydrogel.

Critical step: Perform this step in the shortest time possible to avoid crosslinker evaporation.

11. Allow the hydrogel to form by incubating the plate at 37 °C for 20 min.

? Troubleshooting

Overlay each hydrogel with 500 µL of medium (e.g. intestine growth medium for intestinal spheroids or HIOs, or human lung organoid growth medium for HLOs), ensuring that the hydrogel is covered by medium. Replace the medium every 4 d, or when the phenol red (included in the Advanced DMEM-F12 medium) in the medium turns yellow (Fig. 28b).

5.5.3   Organoid generation/culture and delivery

12. Passage human spheroids or HOs encapsulated in PEG-4MAL hydrogels every 7–10 days (option A), and continue the culture for the desired time frame. If generating HIOs

or culturing HIOs generated in a different matrix, these can then be delivered with synthetic hydrogel precursor solutions via injection into a colonic wound (option B).

Critical point: The hydrogel degradation, and thus, the frequency of passages may vary according to the type and density of encapsulated spheroids/HOs within the hydrogel. Proceed to passage human spheroids/HOs when these starts to settle to the bottom of the well of the culture plate.

Critical point: The culture timeframe of human spheroids can vary according to its type and its timeline of expansion into HO. For reference, we allow at least 14 d of expansion of encapsulated intestinal spheroids into HIOs (Fig. 28b), and we have successfully passaged HIOs for up to 3 passages, spanning approximately 21 d, stopping only for an experimental endpoint, as previously reported[127]. It is likely that HIOs will continue to grow and expand for a much longer period than the mentioned 21 d.

? Troubleshooting

A. Organoid passaging (Timing: Variable)

Critical step: Organoid passaging as described here is intended for hPSC-derived HOs and differs from the trypsin-based passage protocols used for primary tissue-derived organoids.

    i.   Repeat Steps 1–6 ("Preparation of hydrogel precursor solutions") to prepare the hydrogel precursor solutions needed to make new hydrogels.

ii.   Mechanically dislodge organoids from the PEG-4MAL hydrogel by vigorously pipetting the hydrogel with large orifice pipette tips to free the organoids from the matrix.

iii.   Pool all the hydrogel + organoids + medium from each well into a sterile Petri dish containing 10 mL of warm advanced DMEM-F12 medium. By using a sterile tungsten needle or sterile fine forceps, dislodge any large pieces of hydrogel that still adhere to the organoids.

iv.   Under a stereomicroscope, manually cut the organoids into halves using a scalpel.

Critical step: This step is only required for HOs that have been previously reported to require manual cutting during passaging. For example, manual cutting is required for HIOs[107] due to the mesenchymal layer present and large size. For other types of HOs that do not require manual cutting, such as HLOs[109], this step can be skipped.

v.   Transfer organoid to a microcentrifuge tube, and adjust the volume of the suspension using growth medium (for this example, to a total volume of at least 0.5 mL) to obtain a HO density that corresponds to 5 times the concentration of their final density in the hydrogels, and keep on ice. We recommend a final density of 2–4 HOs per 40 µL of hydrogel and to not store the HO solution in ice for longer than 1 h, as previously reported for HIOs and HLOs[127].

vi.   Repeat Steps 8–13 ("Synthetic hydrogel casting") using the organoid suspension prepared in step 13A v, to form new HO-containing hydrogels.

B. Organoid encapsulation and injection into colonic mucosal wound bed (Timing: 5 h)

Critical step: Organoid encapsulation and injection into colonic mucosal wound beds as described here is recommended for hPSC-derived HIOs generated in the PEG-4MAL hydrogel or Matrigel[TM], as previously demonstrated[127].

i. One day before injection, mechanically induce mucosal wounds in recipient mice, as previously described[145]. We use NOD-scid IL2Rg-null (NSG) mice and use biopsy forceps to induce injury. Briefly, we introduce the biopsy forceps through the auxiliary pocket until the tip of the forceps is observed through the high-resolution colonoscope camera. We then carefully make 4–5 wounds of ~1 mm in diameter in the colonic mucosa of each mouse, as previously reported[127,145].

Caution: All animal studies must be reviewed and approved by the relevant animal care committees and must conform to all relevant institutional and national ethics regulations.

ii. Repeat Steps 1–6 ("Preparation of hydrogel precursor solutions") to prepare the hydrogel precursor solutions needed to make new 4% PEG-4MAL hydrogels functionalized with 2.0 mM RGD and crosslinked with GPQ-W peptide for the injections (Fig. 27; Box 1). We have previously reported that this hydrogel formulation promotes HIO engraftment into host tissue and accelerated wound repair[127].

iii.   Mechanically dislodge from the matrix HIOs generated within PEG-4MAL hydrogels (as described above) or Matrigel™ (as previously described[98,107,127]) by vigorously pipetting with large orifice pipette tips to free the organoids (Fig. 29).

iv.   Transfer HIOs to a microcentrifuge tube, and adjust the volume of the suspension using intestine growth medium (for this example, to a total volume of at least 0.5 mL) to obtain a HIO density that corresponds to 5 times the concentration of their final density in the hydrogels, and keep on ice. We recommend a final density of 10 HIOs per 50 µL of hydrogel and to not store the HIO solution in ice for longer than 1 h, as previously reported[127] (Fig. 29).

v.   Load 10 µL of the crosslinker solution onto the custom-made device, whose preparation is described in the Equipment setup.

    Critical step: One custom-made device is needed for each injection to avoid clogging.

vi.   Mix the HIO suspension prepared in step 13B iv with the PEG-4MAL-RGD precursor solution prepared in step 13B ii in a 3:1 PEG-4MAL-RGD/HIO suspension volume ratio (for this example, 1.5 mL of functionalized PEG-4MAL precursor and 0.5 mL of HIO suspension) using large orifice pipette tips and keep the resulting mixture on ice for the duration of the following steps (Fig. 29).

vii.   Load the PEG-4MAL-RGD precursor + HIO mixture solution prepared in the previous step in a 1-mL TB syringe. Please note that 40 µL of this solution will be used per injection (Fig. 29).

viii.   Connect the custom-made device containing the crosslinker solution (see step 13B v) to the TB syringe containing the PEG-4MAL-RGD + HIO suspension (Fig. 29). Insert the nedle bevel through the colonoscope forceps auxiliary pocket.

ix.   Anesthetize mice by intraperitoneal injection of the anesthesia solution (1 mL/kg). Ensure that the mouse is adequately anesthetized by testing its pedal reflex and monitoring its respiration.

x.   Use DPBS in a plastic gavage neddle to lubricate and insert the colonoscope probe into the rectum. Use a colonoscope equipped with a high-resolution camera to identify the mucosal wounds.

xi.   Once a wound has been found, position the colonoscope probe close to the distal end of the wound. Push the tubing through the auxiliary pocket until the needle bevel is observed through the camera and proceed to carefully penetrate the mucosa and locate the needle bevel right at the wound bed (as demonstrated previously[145]; Fig. 29, Fig. 31).

xii.   Inject 40 µL of the functionalized PEG-4MAL-RGD + HIO suspension, which will mix with the crosslinker solution in the tubing, leading to the *in situ* formation of the hydrogel at the injection site. Monitor the success of the procedure by checking to see that small, yet visible, protrusion appears at the injection site (as demonstrated previously[145]).

? Troubleshooting

xiii.   Pull the needle out and repeat injections at a different wound site if required.

Critical step: We recommend performing one injection per wound to avoid risk of perforation.

Critical step: A new custom-made device containing the crossliker will be needed for each injection.

TIMING:

Steps 1–6, Preparation of hydrogel precursor solutions: 1–2 h

Step 7A, Preparation of human spheroid suspension: 30 min

Step 7B, Preparation of human organoid suspension: 30 min

Steps 8–12, Synthetic hydrogel casting: 1 h

Step 13, Organoid culture and delivery: Variable

Step 13A, Organoid passaging: Variable

Step 13B, Organoid encapsulation and injection into colonic mucosal wound bed: 5 hr
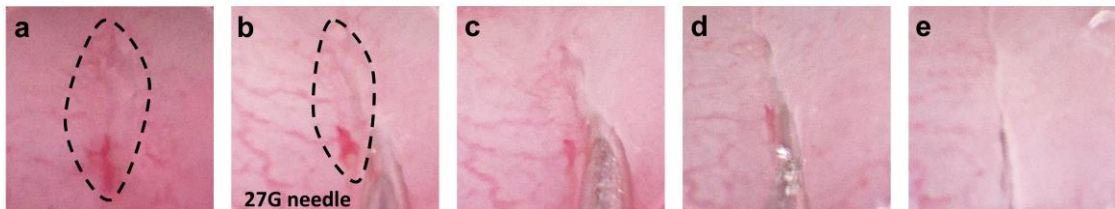
Figure 31: PEG-4MAL hydrogel serves as an injectable delivery vehicle in colonic mucosal wound model. (a) A wound is observed through the camera. (b) The needle is

inserted at the distal end of the wound by carefully penetrating the mucosa. (c-d) The contents of the custom-made device are injected into the site. (e) The needle is removed. The dotted line highlights the wound. Images show a 27-gauge needle (OD: 0.41 mm). All experiments with mice were performed while following institutional and national guidelines.

5.6   Example Calculation

This is an example of calculations needed to prepare hydrogel precursor solutions starting with 100 mg of PEG-4MAL macromer, which is used to produce a total of 2.5 mL hydrogel volume of 4.0% (wt./vol.), 20 kDa PEG-4MAL hydrogels (G': 100 Pa) functionalized with 2.0 mM RGD and crosslinked with GPQ-W peptide. This volume of PEG-4MAL hydrogel is enough for approximately sixty 40 µL-hydrogels for *in vitro* HO encapsulation or approximately fifty 50 µL-hydrogels for *in vivo* injections of HO-containing hydrogels, as previously reported for HIO generation and HLO culture[127]. The total volume of hydrogel can be varied based on the total volume and number of hydrogels needed for experimentation. As discussed in the Experimental Design section, PEG-4MAL macromer size and density, and the type and density of adhesive and crosslinking peptides can be varied, providing that all maleimide groups are conjugated, to reach the desired biophysical and biochemical matrix properties, respectively. Variations to the biophysical and biochemical matrix properties can be explored if the hydrogel formulation described here does not support the viability and growth of the human spheroid/HO of interest. In this case, this example would serve as a guide of the calculations required to form the desired hydrogel. It is important to highlight that changes to the biophysical and biochemical matrix properties may change the values used in this example calculation but do not change the steps described in this protocol. As shown here, it is essential to consider the purity of the peptides and the maleimide substitution efficiency of the PEG-4MAL,

provided by the vendors, to achieve complete crosslinking of the hydrogel. The volume fractions provided in the example (0.4 for PEG-4MAL and 0.2 for adhesive and crosslinking peptides) correspond to the volume ratios described in the protocol (2:1:1, PEG-4MAL/adhesive peptide/crosslinking peptide) and are recommended based on previous reports[9,127]. It is recommended to translate this example of calculations into a spreadsheet for convenience.

The specific hydrogel formulation provided in this example was previously reported for HIO generation and HLO culture[127], and thus serves as a starting point to identify a hydrogel formulation for the generation and culture of the HO of interest.

Table 2: Example calculation.

$MW_{PEG-4MAL}$	22000 Da (molecular weight of PEG-4MAL provided by vendor)
MW_{RGD}	690.6 Da (molecular weight of RGD provided by vendor)
MW_{GPQ-W}	1704.9 Da (molecular weight of GPQ-W provided by vendor)
4	maleimide groups per PEG-4MAL macromer
$P_{PEG-4MAL}$	0.96 (maleimide substitution efficiency provided by the vendor)
P_{RGD}	0.85 (RGD fraction concentration provided by vendor)
P_{GPQ-W}	0.8 (GPQ-W fraction concentration provided by vendor)
$C_{PEG-4MAL}$	4.0 %wt./vol. (desired final PEG-4MAL density)

C_{RGD} 2.0 mM (desired final adhesive ligand density)

$X_{PEG\text{-}4MAL}$ 0.4 (volume fraction of PEG-4MAL in hydrogel)

X_{RGD} 0.2 (volume fraction of RGD in hydrogel)

$X_{GPQ\text{-}W}$ 0.2 (volume fraction of GPQ-W in hydrogel)

1. Determine ($V_{PEG\text{-}4MAL}$) the volume needed to reconstitute $m_{PEG\text{-}4MAL} = 100$ mg of PEG-4MAL:

   $V_{PEG\text{-}4MAL} = m_{PEG\text{-}4MAL} * \dfrac{X_{PEG\text{-}4MAL}}{C_{PEG\text{-}4MAL}} = 1.0$ mL

2. Determine final molarity of maleimide groups (M_{MAL}) based on $m_{PEG\text{-}4MAL}$ and $V_{PEG\text{-}4MAL}$:

   $$M_{MAL} = m_{PEG\text{-}4MAL} * \dfrac{4 * X_{PEG\text{-}4MAL} * P_{PEG\text{-}4MAL}}{MW_{PEG\text{-}4MAL} * V_{PEG\text{-}4MAL}} = 6.98 \text{ mM}$$

3. Determine the volume needed to reconstitute the (V_{RGD}) RGD and ($V_{GPQ\text{-}W}$) GPQ-W:

   $V_{RGD} = V_{PEG\text{-}4MAL} * \dfrac{X_{RGD} \, (\text{or } X_{GPQ\text{-}W})}{X_{PEG\text{-}4MAl}} = V_{GPQ\text{-}W} = 0.5$ mL

4. Determine the mass of RGD (m_{RGD}) needed to obtain C_{RGD}:

   $m_{RGD} = C_{RGD} * \dfrac{MW_{RGD} * V_{RGD}}{P_{RGD} * X_{RGD}} = 4.06$ mg

5. Determine the final molarity of free maleimide groups ($M_{MAL\text{-}GPQ\text{-}W}$) after accounting for maleimide groups reacted with RGD:

   $M_{MAL\text{-}GPQ\text{-}W} = M_{MAL} - C_{RGD} = 4.98$ mM

6. Determine the mass of GPQ-W ($m_{GPQ\text{-}W}$) needed to react with $M_{MAL\text{-}GPQ\text{-}W}$:

   $m_{GPQ\text{-}W} = M_{MAL\text{-}GPQ\text{-}W} * \dfrac{MW_{GPQ\text{-}W} * V_{GPQ\text{-}W}}{2 * P_{GPQ\text{-}W} * X_{GPQ\text{-}W}} = 13.27$ mg

TROUBLESHOOTING:

Troubleshooting advice can be found in Table 1.

Step	Problem	Possible reason(s)	Solution (s)
11, 13B xi	Hydrogels do not form	Inadequate pH adjustment of the peptide solutions	Adjust pH to 7.4
		Purity level of peptides was not considered when calculating mass	Consider the peptide purity provided by vendor as shown in Box 1. Determine peptide purity by UV absorption spectroscopy, as previously described[151].
		Incomplete tissue penetration of the needle bevel at wound site (only for step 13B xi)	Penetrate the tissue slightly past the needle bevel to ensure full delivery of hydrogel solution
13	Spheroids do not develop into HOs	Insufficient number of medium changes	Change medium every 3 – 4 d
		Absence of growth factors/low growth factor activity	Ensure that the growth factors are freshly added
13	Spheroids sink to the bottom of the dish and fail to develop into HOs	The hydrogel is degrading too fast or is not properly polymerized	Reduce spheroid density per hydrogel Increase frequency of passages to every 5–7 d
		Spheroids were too close to the bottom of the dish during hydrogel crosslinking	During hydrogel crosslinking, flip the plate upside-down to ensure spheroids are not too close to the bottom of the dish
13B xii	Low or no HO engraftment into host tissue	Gravity settling of HOs to one end of the syringe	Shake the syringe gently before each injection

Clogging in the tubing due to hydrogel crosslinking	Untimely mixing of the hydrogel precursor solutions in the tube prior to injection	Verify that there is no leakage from the syringe into the tube prior to injections
	pH is too high	Reduce the pH of the crosslinker solution to delay reaction during injection

Table 3: Troubleshooting table.

5.7   Anticipated Results

This protocol outlines the synthesis of PEG-4MAL hydrogels that can generate and maintain hPSC-derived HOs starting from hPSC-derived 3D spheroids for multiple passages without the need for Matrigel™ encapsulation. Additionally, this synthetic matrix can be used as a delivery vehicle to promote HIO engraftment and accelerated wound healing of injured colonic tissue[127]. Intestinal spheroids embedded in the engineered hydrogel (Storage modulus (G'): 100 Pa; 4.0%, 20 kDa PEG-4MAL; 2.0 mM RGD; GPQ-W crosslinker) develop into HIOs with lumens after 4–5 d in culture (Fig. 32a,b). During expansion, spheroids change shape and display epithelial budding at the interface with the hydrogel (Fig. 32b). Furthermore, hydrogel-generated HIOs can be passaged into fresh hydrogels every 7–10 days to support further differentiation of HIOs, demonstrating that PEG-4MAL hydrogels can generate and maintain fully-developed HIOs to similar levels as Matrigel™ (Fig. 32c,d). We have successfully passaged HIOs for up to 3 passages, spanning approximately 21 d, stopping only for an experimental endpoint. It is likely that HIOs will continue to grow and expand for a much longer period than the mentioned 21 d. Established HIOs grow in size, change shape, maintain a central lumen, and display cell outgrowths migrating into the hydrogel (Fig. 32b,c). In Figure 33 we show that cells

expressing markers of human cells have engrafted in the host tissue 4 weeks following *in vivo* injection of HIO-containing PEG-4MAL precursor solutions to the colonic mucosal wound bed, consistent with our previous study[18].
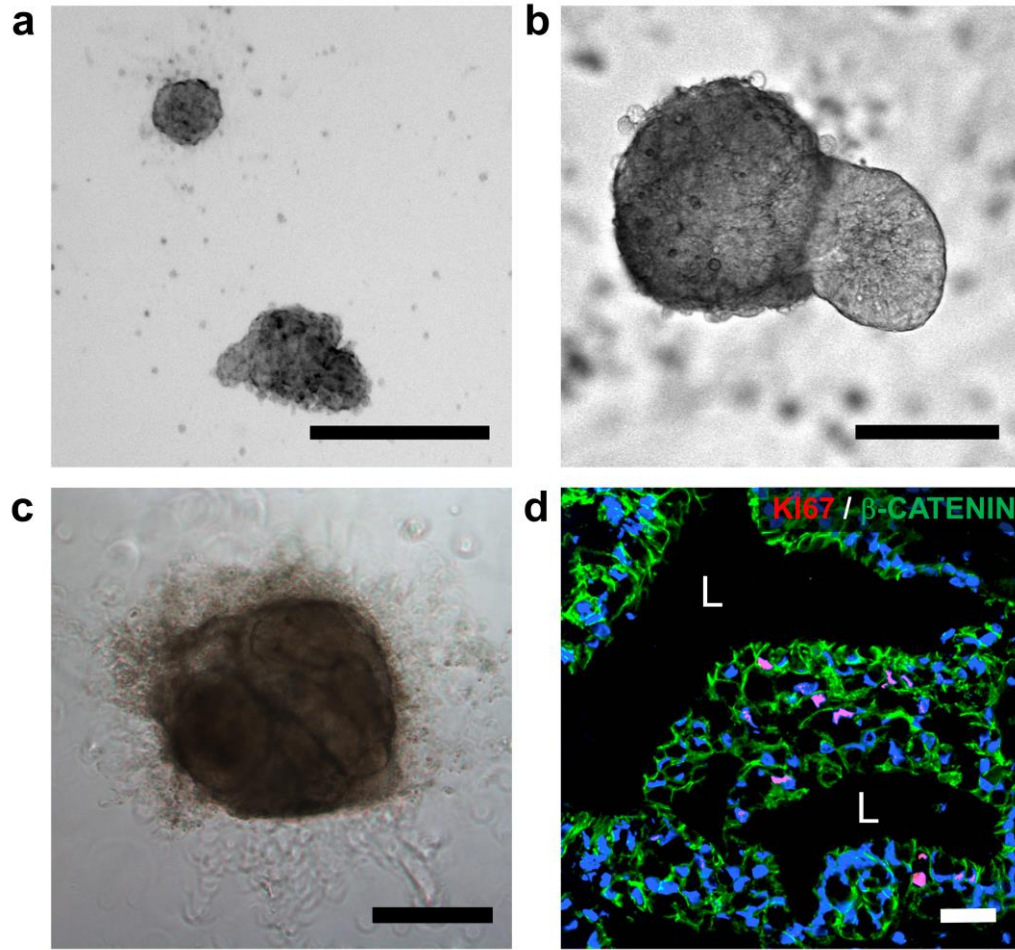
Figure 32: PEG-4MAL hydrogel supports hPSC-derived intestinal spheroid development into HIOs. Transmitted light microscopy images of hiPSC-derived HIO generated within 4.0% PEG-4MAL-RGD hydrogels after (a) 1 d, (b) 5 d, and (c) 21 d since encapsulation. HIO in (c) has undergone two passages before this time-point. Scale bars: 100 μm (a, b) and 500 μm (c). (d) Fluorescence microscopy image of a HIO taken 21 d after encapsulation in 4.0% PEG-4MAL-RGD hydrogel. HIO was labeled for cell-cell junctions (β-CATENIN; 1:100; BD biosciences, cat. no. 610153) and proliferative cells (KI67; 1:100; Abcam, cat. no. ab15580). DAPI (1:1000), counterstain. "L" indicates HIO lumen. Bar, 100 μm. Samples were imaged using an Axiovert 35, Zeiss microscope and analyzed with LAS X software (Leica Microsystems, Inc.).
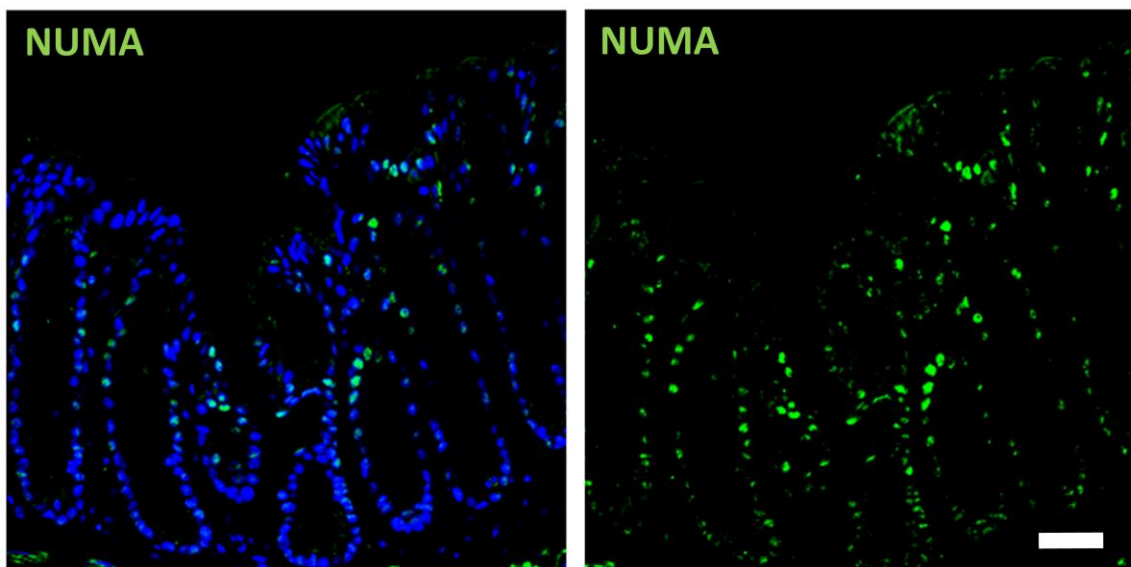
Figure 33: PEG-4MAL hydrogel promotes HIO engraftment into mucosal wounds.
Fluorescence microscopy images of murine colonic tissue at the wound site labeled for human cell nuclei (NUMA; 1:100; EMD Millipore, cat. no. MAB1281) taken 4 weeks post-delivery. DAPI (1:1000), counterstain. Bar, 100 µm. All experiments with mice were performed while following institutional and national guidelines. This data is representative of the results we saw following injection of hydrogels containing HIO in two independent studies (n = 4 mice per condition, 5 injections per mouse). Further results from this study are published[127]. Samples were imaged using an Axiovert 35, Zeiss microscope and analyzed with LAS X software (Leica Microsystems, Inc.).

CHAPTER 6.   CONCLUSIONS AND FUTURE

CONSIDERATIONS

This overarching objective of this thesis was to develop an engineered synthetic hydrogel matrix that presents independently-tunable basement membrane-like bioactivity and mechanical properties that supports different epithelial morphogenetic programs. Although naturally-derived materials have been extensively used to recapitulate epithelial morphogenesis, they are inherently limited by lot-to-lot compositional and structural variability, and the inability to decouple biochemical and biomechanical properties. Additionally, in the case of Matrigel^{TM}, its tumor-derived nature limits its translational potential. We have demonstrated that the fully defined, synthetic PEG-4MAL hydrogel platform allows the study of the independent contributions of ECM properties to different epithelial morphogenetic programs, and supports epithelial cell survival, proliferation, polarization, and assembly into 3D multicellular structures, recapitulating different epithelial morphogenesis program. Additionally, this synthetic material has the capacity to present adhesive peptides and protease-degradable crosslinks that support cell functions and promote cell engraftment *in vivo*.

In Aim 1, we developed a PEG-4MAL hydrogel that supports robust and highly reproducible *in vitro* growth and expansion of hPSC-derived human intestinal organoids such that 3D structures are never embedded in tumor-derived ECM. Both mechanical and biochemical properties of the synthetic ECM were important to intestinal organoid formation, and we identified an optimal formulation that supports intestinal spheroid survival, expansion and epithelial differentiation into HIOs and differentiation into mature

128

intestinal tissue *in vivo* to similar levels as Matrigel^{TM}. Additionally, we showed that this synthetic matrix supports the development of other human organoids such as HLOs. We also demonstrated that the hydrogel serves as an injectable HIO vehicle that can be delivered into injured intestinal mucosa resulting in HIO engraftment and improved colonic wound repair.

In Aim 2, we engineered a PEG-4MAL hydrogel with independent control over proteolytic degradation, mechanical properties, and adhesive ligand type and density to study the impact of ECM properties on epithelial tubulogenesis program. We showed that sensitivity of the synthetic material to membrane-type matrix metalloproteinase-1 (MT1-MMP) was required for epithelial tubulogenesis. Additionally, a narrow range of matrix elasticity, presentation of specific adhesive ligand type, and a threshold level of adhesive ligand density of the MT1-MMP-sensitive hydrogel were important to direct epithelial tubulogenesis. Finally, we demonstrated that the engineered PEG-4MAL hydrogel supported organization of epithelial tubules that displayed lumen formation, polarization and secreted ECM components. The PEG-4MAL hydrogel serves as a platform to recapitulate epithelial tubular morphogenetic programs and to characterize the independent contributions of the matrix properties to distinctive normal or abnormal epithelial phenotypes.

Together, these studies establish PEG-4MAL hydrogel as a platform to study the independent contributions of the matrix properties to different epithelial morphogenetic programs. Additionally, we demonstrated that PEG-4MAL hydrogels can be used as a cell delivery vehicle that may be used therapeutically to treat intestinal injury, overcoming the limitations of natural materials. Nevertheless, translation of this technology to the human

scale will require significantly more validation. This will include evaluation of the cell delivery efficacy in larger animal models of epithelial injury. The synthetic, well defined composition of the material may increase the probability of successful scaling. Each component can be synthesized in scalable amounts at very high purity, which allows for consistent and repeatable material synthesis. However, an important consideration of this engineered hydrogel platform is its rapid reaction kinetics that may result, if mixing is not conducted properly, in the formation of an inhomogeneous gel that presents variabilities in its physicochemical properties. Therefore, to avoid inhomogeneities in the hydrogel properties due to premature crosslinking, the functionalized macromer and crosslinker solutions may need to be delivered separately and mixed at the in vivo delivery site, or mixed prior to rapid delivery into the in vivo site.

Although the studies discussed in this thesis have developed novel artificial hydrogel matrices that present BM-like properties, several challenges need to be addressed to continue engineering synthetic matrices that recapitulate and direct complex cellular processes. For instance, there is a need for hydrogels that can recapitulate the in vivo microenvironment by presentation of multiple adhesive ligand types at specific densities that can orchestrate complex cellular responses. Such artificial matrix designs are important for the support of complex cellular systems (e.g. primary and stem cells) that still represent a challenge due to their increased sensitivity, and to further direct innate cellular functions. Furthermore, as different studies have demonstrated successful recapitulation of complex epithelial morphogenetic programs using Matrigel™, future developments of BM-like synthetic hydrogels should move towards designing hydrogels that recapitulate mechanical and structural (e.g., fibrillar structure) properties of Matrigel™

and collagen gels. Therefore, as new ways of integrating bioactivity into hydrogel matrices are designed, novel engineered synthetic materials will continue to offer new developments in regenerative medicine and tissue engineering fields, and promise innovative therapeutic options that naturally derived materials cannot provide.

Overall, the engineered PEG-4MAL hydrogel systems developed here begin to address the need for modular synthetic organotypic *in vitro* culture materials that recreate the epithelial morphogenetic developmental programs, and can be used to study the independent contributions of the matrix properties to epithelial morphogenesis. Finally, these data show our simple, injectable, biomaterial based delivery carrier outperforms tumor-derived materials, establishing its its translational potential for regenerative medicine applications.

APPENDIX A.

6.1 Publication List

1. Cruz-Acuña, R.*, Quirós, M.*, Farkas, A. E., Dedhia, P. H., Huang, S., Siuda, D., García-Hernández, V., Spence, J. R., Nusrat, A. and García, A. J. Synthetic Hydrogels for Human Intestinal Organoid Generation and Colonic Wound Repair. Nature Cell Biology, (2017) Nov;19(11):1326-1335.
   *Co-first authors.

2. Cruz-Acuña, R. & García, A. J. Synthetic hydrogels mimicking basement membrane matrices to promote cell-matrix interactions. Matrix Biology, (2016) Jan;57-58:324-333.

3. Enemchukwu, N. O., Cruz-Acuña, R., Bongiorno T., Johnson, C. T., García, J. R., Sulchek, T., & García, A.J. (2016). Synthetic matrices reveal contributions of ECM biophysical and biochemical properties to epithelial morphogenesis. Journal of Cell Biology, 212(1), 113-24.

4. Cruz-Acuña, M., Bailón-Ruiz, S., Marti-Figueroa, C. R., Cruz-Acuña, R., & Perales-Pérez, O. J. (2015). Synthesis, Characterization and Evaluation of the Cytotoxicity of Ni-Doped Zn(Se,S) Quantum Dots. Journal of Nanomaterials, 20151-8.

5. Alamo-Nole, L., Bailon-Ruiz, S., Cruz-Acuña, R., Perales-Perez, O., & Roman, F. (2014). Quantum Dots of ZnSe(S) Doped with Copper as Nanophotocatalyst in the Degradation of Organic Dyes. Journal of Nanoscience and Nanotechnology, 14(9), 7333-7339.

6. Peña-Luengas, S. L., Marin, G. H., Aviles, K., Cruz-Acuña, R., Roque, G., Rodríguez-Nieto, F., & Mansilla, E. (2014). Enhanced singlet oxygen production by photodynamic therapy and a novel method for its intracellular measurement. Cancer Biotherapy & Radiopharmaceuticals, 29(10), 435-443.

REFERENCES

1   Lukashev, M. E. & Werb, Z. ECM signalling: orchestrating cell behaviour and misbehaviour. *Trends in Cell Biology* **8**, 437-441, doi:http://dx.doi.org/10.1016/S0962-8924(98)01362-2 (1998).

2   Midwood, K. S., Williams, L. V. & Schwarzbauer, J. E. Tissue repair and the dynamics of the extracellular matrix. *The International Journal of Biochemistry & Cell Biology* **36**, 1031-1037, doi:http://dx.doi.org/10.1016/j.biocel.2003.12.003 (2004).

3   Streuli, C. Extracellular matrix remodelling and cellular differentiation. *Current Opinion in Cell Biology* **11**, 634-640, doi:http://dx.doi.org/10.1016/S0955-0674(99)00026-5 (1999).

4   Cruz-Acuña, R. & García, A. J. Synthetic hydrogels mimicking basement membrane matrices to promote cell-matrix interactions. *Matrix Biology*, doi:http://dx.doi.org/10.1016/j.matbio.2016.06.002 (2016).

5   O'Brien, L. E. *et al.* Rac1 orientates epithelial apical polarity through effects on basolateral laminin assembly. *Nature cell biology* **3**, 831-838 (2001).

6   Montesano, R., Schaller, G. & Orci, L. Induction of epithelial tubular morphogenesis in vitro by fibroblast-derived soluble factors. *Cell* **66**, 697-711 (1991).

7   Barcellos-Hoff, M. H., Aggeler, J., Ram, T. G. & Bissell, M. J. Functional differentiation and alveolar morphogenesis of primary mammary cultures on reconstituted basement membrane. *Development* **105**, 223-235 (1989).

8   Hughes, C. S., Postovit, L. M. & Lajoie, G. A. Matrigel: a complex protein mixture required for optimal growth of cell culture. *Proteomics* **10**, 1886-1890, doi:10.1002/pmic.200900758 (2010).

9   Enemchukwu, N. O. *et al.* Synthetic matrices reveal contributions of ECM biophysical and biochemical properties to epithelial morphogenesis. *The Journal of cell biology* **212**, 113-124, doi:10.1083/jcb.201506055 (2016).

10   Phelps, E. A. *et al.* Maleimide cross-linked bioactive PEG hydrogel exhibits improved reaction kinetics and cross-linking for cell encapsulation and in situ delivery. *Advanced materials* **24**, 64-70, 62, doi:10.1002/adma.201103574 (2012).

11   Phelps, E. A., Headen, D. M., Taylor, W. R., Thule, P. M. & Garcia, A. J. Vasculogenic bio-synthetic hydrogel for enhancement of pancreatic islet engraftment and function in type 1 diabetes. *Biomaterials* **34**, 4602-4611, doi:10.1016/j.biomaterials.2013.03.012 (2013).

12   Phelps, E. A., Landazuri, N., Thule, P. M., Taylor, W. R. & Garcia, A. J. Bioartificial matrices for therapeutic vascularization. *Proc Natl Acad Sci U S A* **107**, 3323-3328, doi:0905447107 [pii]

        10.1073/pnas.0905447107 (2010).

13   Salimath, A. S. *et al.* Dual delivery of hepatocyte and vascular endothelial growth factors via a protease-degradable hydrogel improves cardiac function in rats. *PLoS One* **7**, e50980, doi:10.1371/journal.pone.0050980 (2012).

14   Chung, I. M. *et al.* Bioadhesive hydrogel microenvironments to modulate epithelial morphogenesis. *Biomaterials* **29**, 2637-2645, doi:S0142-9612(08)00181-6 [pii]

        10.1016/j.biomaterials.2008.03.008 [doi] (2008).

15   Wolf, K. *et al.* Collagen-based cell migration models in vitro and in vivo. *Seminars in cell & developmental biology* **20**, 931-941, doi:10.1016/j.semcdb.2009.08.005 (2009).

16   Gaggioli, C. *et al.* Fibroblast-led collective invasion of carcinoma cells with differing roles for RhoGTPases in leading and following cells. *Nature cell biology* **9**, 1392-1400, doi:10.1038/ncb1658 (2007).

17   Nguyen-Ngoc, K. V. *et al.* ECM microenvironment regulates collective migration and local dissemination in normal and malignant mammary epithelium. *Proc Natl Acad Sci U S A* **109**, E2595-2604, doi:10.1073/pnas.1212834109 (2012).

18   Yu, W. *et al.* β1-Integrin Orients Epithelial Polarity via Rac1 and Laminin. *Molecular Biology of the Cell* **16**, 433-445, doi:10.1091/mbc.E04-05-0435 (2005).

19   Shamir, E. R. & Ewald, A. J. Three-dimensional organotypic culture: experimental models of mammalian biology and disease. *Nat Rev Mol Cell Biol* **15**, 647-664, doi:10.1038/nrm3873 (2014).

20   Yurchenco, P. D. Basement membranes: cell scaffoldings and signaling platforms. *Cold Spring Harbor perspectives in biology* **3**, doi:10.1101/cshperspect.a004911 (2011).

21   Peng, J. *et al.* Phosphoinositide 3-kinase p110delta promotes lumen formation through the enhancement of apico-basal polarity and basal membrane organization. *Nature communications* **6**, 5937, doi:10.1038/ncomms6937 (2015).

22   Debnath, J., Muthuswamy, S. K. & Brugge, J. S. Morphogenesis and oncogenesis of MCF-10A mammary epithelial acini grown in three-dimensional basement membrane cultures. *Methods* **30**, 256-268, doi:10.1016/s1046-2023(03)00032-x (2003).

23   Sato, T. & Clevers, H. Growing self-organizing mini-guts from a single intestinal stem cell: mechanism and applications. *Science* **340**, 1190-1194, doi:10.1126/science.1234852 (2013).

24   Yui, S. *et al.* Functional engraftment of colon epithelium expanded in vitro from a single adult Lgr5(+) stem cell. *Nat Med* **18**, 618-623, doi:10.1038/nm.2695 (2012).

25   Fatehullah, A., Tan, S. H. & Barker, N. Organoids as an in vitro model of human development and disease. *Nature cell biology* **18**, 246-254, doi:10.1038/ncb3312 (2016).

26   Sato, T. *et al.* Single Lgr5 stem cells build crypt-villus structures in vitro without a mesenchymal niche. *Nature* **459**, 262-265, doi:10.1038/nature07935 (2009).

27   Siler, U. *et al.* Characterization and functional analysis of laminin isoforms in human bone marrow. *Blood* **96**, 4194-4203 (2000).

28   Engbring, J. A. & Kleinman, H. K. The basement membrane matrix in malignancy. *The Journal of pathology* **200**, 465-470, doi:10.1002/path.1396 (2003).

29   Colognato, H. & Yurchenco, P. D. Form and function: The laminin family of heterotrimers. *Developmental Dynamics* **218**, 213-234, doi:10.1002/(SICI)1097-0177(200006)218:2<213::AID-DVDY1>3.0.CO;2-R (2000).

30   Kikkawa, Y. *et al.* Laminin-111-derived peptides and cancer. *Cell adhesion & migration* **7**, 150-256, doi:10.4161/cam.22827 (2013).

31   Turpeenniemi-Hujanen, T., Thorgeirsson, U. P., Rao, C. N. & Liotta, L. A. Laminin increases the release of type IV collagenase from malignant cells. *Journal of Biological Chemistry* **261**, 1883-1889 (1986).

32   Ekblom, M., Falk, M., Salmivirta, K., Durbeej, M. & Ekblom, P. Laminin Isoforms and Epithelial Development. *Annals of the New York Academy of Sciences* **857**, 194-211, doi:10.1111/j.1749-6632.1998.tb10117.x (1998).

33   Li, J., Sun, H., Feltri, M. L. & Mercurio, A. M. Integrin beta4 regulation of PTHrP underlies its contribution to mammary gland development. *Developmental biology* **407**, 313-320, doi:10.1016/j.ydbio.2015.09.015 (2015).

34   Durbeej, M. *et al.* Expression of laminin α1, α5 and β2 chains during embryogenesis of the kidney and vasculature. *Matrix Biology* **15**, 397-413, doi:http://dx.doi.org/10.1016/S0945-053X(96)90159-6 (1996).

35   Janmey, P. A., Winer, J. P. & Weisel, J. W. Fibrin gels and their clinical and bioengineering applications. *Journal of the Royal Society, Interface / the Royal Society* **6**, 1-10, doi:10.1098/rsif.2008.0327 (2009).

36   Riopel, M., Trinder, M. & Wang, R. Fibrin, a scaffold material for islet transplantation and pancreatic endocrine tissue engineering. *Tissue engineering. Part B, Reviews* **21**, 34-44, doi:10.1089/ten.TEB.2014.0188 (2015).

37   Matricardi, P., Di Meo, C., Coviello, T., Hennink, W. E. & Alhaique, F. Interpenetrating Polymer Networks polysaccharide hydrogels for drug delivery and tissue engineering. *Adv Drug Deliv Rev* **65**, 1172-1187, doi:10.1016/j.addr.2013.04.002 (2013).

38   Lee, K. Y. & Mooney, D. J. Alginate: properties and biomedical applications. *Progress in polymer science* **37**, 106-126, doi:10.1016/j.progpolymsci.2011.06.003 (2012).

39   Kim, I. L., Mauck, R. L. & Burdick, J. A. Hydrogel design for cartilage tissue engineering: a case study with hyaluronic acid. *Biomaterials* **32**, 8771-8782, doi:10.1016/j.biomaterials.2011.08.073 (2011).

40   Lam, J., Truong, N. F. & Segura, T. Design of cell-matrix interactions in hyaluronic acid hydrogel scaffolds. *Acta biomaterialia* **10**, 1571-1580, doi:10.1016/j.actbio.2013.07.025 (2014).

41   Beck, J. N., Singh, A., Rothenberg, A. R., Elisseeff, J. H. & Ewald, A. J. The independent roles of mechanical, structural and adhesion characteristics of 3D hydrogels on the regulation of cancer invasion and dissemination. *Biomaterials* **34**, 9486-9495, doi:10.1016/j.biomaterials.2013.08.077 (2013).

42   Hutson, C. B. *et al.* Synthesis and characterization of tunable poly(ethylene glycol): gelatin methacrylate composite hydrogels. *Tissue engineering. Part A* **17**, 1713-1723, doi:10.1089/ten.TEA.2010.0666 (2011).

43   Zhu, J. Bioactive modification of poly(ethylene glycol) hydrogels for tissue engineering. *Biomaterials* **31**, 4639-4656, doi:10.1016/j.biomaterials.2010.02.044 (2010).

44   Peppas, N. A., Huang, Y., Torres-Lugo, M., Ward, J. H. & Zhang, J. Physicochemical Foundations and Structural Design of Hydrogels in Medicine and Biology. *Annual Review of Biomedical Engineering* **2**, 9-29, doi:10.1146/annurev.bioeng.2.1.9 (2000).

45   Flory, P. J. & Rehner, J. Statistical Mechanics of Cross-Linked Polymer Networks II. Swelling. *The Journal of Chemical Physics* **11**, 521, doi:10.1063/1.1723792 (1943).

46   Drury, J. L. & Mooney, D. J. Hydrogels for tissue engineering: scaffold design variables and applications. *Biomaterials* **24**, 4337-4351, doi:10.1016/s0142-9612(03)00340-5 (2003).

47   Lutolf, M. P. *et al.* Synthetic matrix metalloproteinase-sensitive hydrogels for the conduction of tissue regeneration: engineering cell-invasion characteristics. *Proceedings of the National Academy of Sciences of the United States of America* **100**, 5413-5418, doi:10.1073/pnas.0737381100 (2003).

48   Das, R. K., Gocheva, V., Hammink, R., Zouani, O. F. & Rowan, A. E. Stress-stiffening-mediated stem-cell commitment switch in soft responsive hydrogels. *Nature materials* **15**, 318-325, doi:10.1038/nmat4483 (2016).

49   Hoffman, A. S. Hydrogel for biomedical applications. *Advanced Drug Delivery Reviews* **54**, 3-12, doi:10.1016/S0169-409X(01)00239-3 (2002).

50   Kloxin, A. M., Tibbitt, M. W. & Anseth, K. S. Synthesis of photodegradable hydrogels as dynamically tunable cell culture platforms. *Nature protocols* **5**, 1867-1887, doi:10.1038/nprot.2010.139 (2010).

51   Nguyen, K. T. & West, J. L. Photopolymerizable hydrogels for tissue engineering applications. *Biomaterials* **23**, 4307-4314, doi:http://dx.doi.org/10.1016/S0142-9612(02)00175-8 (2002).

52   Lee, T. T. *et al.* Light-triggered in vivo activation of adhesive peptides regulates cell adhesion, inflammation and vascularization of biomaterials. *Nat Mater* **14**, 352-360, doi:10.1038/nmat4157 (2015).

53   Hu, B., Su, J. & Messersmith, P. B. Hydrogels cross-linked by native chemical ligation. *Biomacromolecules* **10**, 2194-2200, doi:10.1021/bm900366e (2009).

54   Polizzotti, B. D., Fairbanks, B. D. & Anseth, K. S. Three-Dimensional Biochemical Patterning of Click-Based Composite Hydrogels via Thiolene Photopolymerization. *Biomacromolecules* **9**, 1084-1087, doi:10.1021/bm7012636 (2008).

55   Lu, P., Takai, K., Weaver, V. M. & Werb, Z. Extracellular matrix degradation and remodeling in development and disease. *Cold Spring Harb Perspect Biol* **3**, doi:10.1101/cshperspect.a005058 (2011).

56   Hynes, R. O. Integrins: bidirectional, allosteric signaling machines. *Cell* **110**, 673-687 (2002).

57   Giancotti, F. G. & Ruoslahti, E. Integrin signaling. *Science* **285**, 1028-1033 (1999).

58   Danen, E. H. & Sonnenberg, A. Integrins in regulation of tissue development and function. *The Journal of pathology* **201**, 632-641, doi:10.1002/path.1472 (2003).

59   Danen, E. H. J. Integrins: Regulators of Tissue Function and Cancer Progression. *Current Pharmaceutical Design* **11**, 881-891, doi:http://dx.doi.org/10.2174/1381612053381756 (2005).

60   Ruoslahti, E. The RGD story: a personal account. *Matrix Biology* **22**, 459-465, doi:10.1016/s0945-053x(03)00083-0 (2003).

61   Schmedlen, R. H., Masters, K. S. & West, J. L. Photocrosslinkable polyvinyl alcohol hydrogels that can be modified with cell adhesion peptides for use in tissue engineering. *Biomaterials* **23**, 4325-4332 (2002).

62   Puperi, D. S., Balaoing, L. R., O'Connell, R. W., West, J. L. & Grande-Allen, K. J. 3-Dimensional spatially organized PEG-based hydrogels for an aortic valve co-culture model. *Biomaterials* **67**, 354-364, doi:10.1016/j.biomaterials.2015.07.039 (2015).

63   Halstenberg, S., Panitch, A., Rizzi, S., Hall, H. & Hubbell, J. A. Biologically Engineered Protein-graft-Poly(ethylene glycol) Hydrogels: A Cell Adhesive and Plasmin-Degradable Biosynthetic Material for Tissue Repair. *Biomacromolecules* **3**, 710-723, doi:10.1021/bm015629o (2002).

64   Nuttelman, C. R., Tripodi, M. C. & Anseth, K. S. Synthetic hydrogel niches that promote hMSC viability. *Matrix biology : journal of the International Society for Matrix Biology* **24**, 208-218, doi:10.1016/j.matbio.2005.03.004 (2005).

65   Saha, K., Irwin, E. F., Kozhukh, J., Schaffer, D. V. & Healy, K. E. Biomimetic interfacial interpenetrating polymer networks control neural stem cell behavior. *J Biomed Mater Res A* **81**, 240-249 (2007).

66   Fittkau, M. H. *et al.* The selective modulation of endothelial cell mobility on RGD peptide containing surfaces by YIGSR peptides. *Biomaterials* **26**, 167-174 (2005).

67   Sternlicht, M. D. & Werb, Z. How matrix metalloproteinases regulate cell behavior. *Annual review of cell and developmental biology* **17**, 463 (2001).

68   Mann, B. K., Gobin, A. S., Tsai, A. T., Schmedlen, R. H. & West, J. L. Smooth muscle cell growth in photopolymerized hydrogels with cell adhesive and proteolytically degradable domains: synthetic ECM analogs for tissue engineering. *Biomaterials* **22**, 3045-3051 (2001).

69   Rape, A. D., Zibinsky, M., Murthy, N. & Kumar, S. A synthetic hydrogel for the high-throughput study of cell-ECM interactions. *Nature communications* **6**, 8129, doi:10.1038/ncomms9129 (2015).

70   Guvendiren, M. & Burdick, J. A. Engineering synthetic hydrogel microenvironments to instruct stem cells. *Current opinion in biotechnology* **24**, 841-846, doi:10.1016/j.copbio.2013.03.009 (2013).

71   Halfter, W., Dong, S., Schurer, B. & Cole, G. J. Collagen XVIII Is a Basement Membrane Heparan Sulfate Proteoglycan. *Journal of Biological Chemistry* **273**, 25404-25412, doi:10.1074/jbc.273.39.25404 (1998).

72   Kleinman, H. K., Philp, D. & Hoffman, M. P. Role of the extracellular matrix in morphogenesis. *Current opinion in biotechnology* **14**, 526-532, doi:10.1016/j.copbio.2003.08.002 (2003).

73   Sokic, S. & Papavasiliou, G. FGF-1 and proteolytically mediated cleavage site presentation influence three-dimensional fibroblast invasion in biomimetic PEGDA hydrogels. *Acta biomaterialia* **8**, 2213-2222, doi:10.1016/j.actbio.2012.03.017 (2012).

74   DeLong, S. A., Moon, J. J. & West, J. L. Covalently immobilized gradients of bFGF on hydrogel scaffolds for directed cell migration. *Biomaterials* **26**, 3227-3234, doi:10.1016/j.biomaterials.2004.09.021 (2005).

75   Martino, M. M., Briquez, P. S., Ranga, A., Lutolf, M. P. & Hubbell, J. A. Heparin-binding domain of fibrin(ogen) binds growth factors and promotes tissue repair when incorporated within a synthetic matrix. *Proc Natl Acad Sci U S A* **110**, 4563-4568, doi:10.1073/pnas.1221602110 (2013).

76   Sakiyama-Elbert, S. E. & Hubbell, J. A. Development of fibrin derivatives for controlled release of heparin-binding growth factors. *Journal of Controlled Release* **65**, 389-402 (2000).

77   Hudalla, G. A. & Murphy, W. L. Biomaterials that regulate growth factor activity via bioinspired interactions. *Advanced functional materials* **21**, 1754-1768, doi:10.1002/adfm.201002468 (2011).

78   Jha, A. K. *et al.* Enhanced survival and engraftment of transplanted stem cells using growth factor sequestering hydrogels. *Biomaterials* **47**, 1-12, doi:10.1016/j.biomaterials.2014.12.043 (2015).

79   Cai, S., Liu, Y., Zheng Shu, X. & Prestwich, G. D. Injectable glycosaminoglycan hydrogels for controlled release of human basic fibroblast growth factor. *Biomaterials* **26**, 6054-6067, doi:10.1016/j.biomaterials.2005.03.012 (2005).

80   Martin-Belmonte, F. & Mostov, K. Regulation of cell polarity during epithelial morphogenesis. *Curr Opin Cell Biol* **20**, 227-234, doi:10.1016/j.ceb.2008.01.001 (2008).

81   O'Brien, L. E., Zegers, M. M. P. & Mostov, K. E. Opinion: Building epithelial architecture: insights from three-dimensional culture models. *Nature reviews. Molecular cell biology* **3**, 531-537 (2002).

82   Mroue, R. & Bissell, M. J. Three-dimensional cultures of mouse mammary epithelial cells. *Methods Mol Biol* **945**, 221-250, doi:10.1007/978-1-62703-125-7_14 (2013).

83   McAteer, J. A., Evan, A. P., Vance, E. E. & Gardner, K. D. MDCK cysts: An in vitro model of epithelial cyst formation and growth. *Journal of tissue culture methods* **10**, 245-248, doi:10.1007/bf01404485.

84   Sancho-Martinez, I. & Belmonte, J. C. I. Stem cells: Surf the waves of reprogramming. *Nature* **493**, 310-311 (2013).

85   Polo, J. M. *et al.* A molecular roadmap of reprogramming somatic cells into iPS cells. *Cell* **151**, 1617-1632, doi:10.1016/j.cell.2012.11.039 (2012).

86   Caiazzo, M. *et al.* Defined three-dimensional microenvironments boost induction of pluripotency. *Nature materials* **15**, 344-352, doi:10.1038/nmat4536 (2016).

87   Downing, T. L. *et al.* Biophysical regulation of epigenetic state and cell reprogramming. *Nat Mater* **12**, 1154-1162, doi:10.1038/nmat3777 (2013).

88   Thomson, J. A. *et al.* Embryonic Stem Cell Lines Derived from Human Blastocysts. *Science* **282**, 1145-1147, doi:10.1126/science.282.5391.1145 (1998).

89   Takahashi, K. *et al.* Induction of Pluripotent Stem Cells from Adult Human Fibroblasts by Defined Factors. *Cell* **131**, 861-872, doi:10.1016/j.cell.2007.11.019 (2007).

90   Takahashi, K. & Yamanaka, S. A developmental framework for induced pluripotency. *Development* **142**, 3274-3285, doi:10.1242/dev.114249 (2015).

91   Fox, I. J. *et al.* Stem cell therapy. Use of differentiated pluripotent stem cells as replacement therapy for treating disease. *Science* **345**, 1247391, doi:10.1126/science.1247391 (2014).

92   Robinton, D. A. & Daley, G. Q. The promise of induced pluripotent stem cells in research and therapy. *Nature* **481**, 295-305, doi:10.1038/nature10761 (2012).

93   Huch, M. *et al.* Long-term culture of genome-stable bipotent stem cells from adult human liver. *Cell* **160**, 299-312, doi:10.1016/j.cell.2014.11.050 (2015).

94   Clevers, H. Modeling Development and Disease with Organoids. *Cell* **165**, 1586-1597, doi:10.1016/j.cell.2016.05.082 (2016).

95   Dekkers, J. F. *et al.* A functional CFTR assay using primary cystic fibrosis intestinal organoids. *Nat Med* **19**, 939-945, doi:10.1038/nm.3201 (2013).

96   Dekkers, J. F. *et al.* Characterizing responses to CFTR-modulating drugs using rectal organoids derived from subjects with cystic fibrosis. *Science Translational Medicine* **8**, 344ra384-344ra384, doi:10.1126/scitranslmed.aad8278 (2016).

97   Wells, J. M. & Spence, J. R. How to make an intestine. *Development* **141**, 752-760, doi:10.1242/dev.097386 (2014).

98   Spence, J. R. *et al.* Directed differentiation of human pluripotent stem cells into intestinal tissue in vitro. *Nature* **470**, 105-109, doi:10.1038/nature09691 (2011).

99   Hughes, C. S., Postovit, L. M. & Lajoie, G. A. Matrigel: A complex protein mixture required for optimal growth of cell culture. *PROTEOMICS* **10**, 1886-1890, doi:10.1002/pmic.200900758 (2010).

100   Gjorevski, N. *et al.* Designer matrices for intestinal stem cell and organoid culture. *Nature* **539**, 560-564, doi:10.1038/nature20168 (2016).

101   Wickström, S. A., Radovanac, K. & Fässler, R. Genetic Analyses of Integrin Signaling. *Cold Spring Harbor Perspectives in Biology* **3**, a005116, doi:10.1101/cshperspect.a005116 (2011).

102   Hoffman, M. P. *et al.* Laminin-1 and laminin-2 G-domain synthetic peptides bind syndecan-1 and are involved in acinar formation of a human submandibular gland cell line. *J Biol Chem* **273**, 28633-28641 (1998).

103   Emsley, J., Knight, C. G., Farndale, R. W. & Barnes, M. J. Structure of the Integrin α2β1-binding Collagen Peptide. *Journal of Molecular Biology* **335**, 1019-1028, doi:10.1016/j.jmb.2003.11.030 (2004).

104   Finkbeiner, S. R. *et al.* Transcriptome-wide Analysis Reveals Hallmarks of Human Intestine Development and Maturation In Vitro and In Vivo. *Stem Cell Reports*, doi:10.1016/j.stemcr.2015.04.010 (2015).

105   Straight, A. F. *et al.* Dissecting Temporal and Spatial Control of Cytokinesis with a Myosin II Inhibitor. *Science* **299**, 1743-1747 (2003).

106   Uehata, M. *et al.* Calcium sensitization of smooth muscle mediated by a Rho-associated protein kinase in hypertension. *Nature* **389**, 990-994 (1997).

107   McCracken, K. W., Howell, J. C., Wells, J. M. & Spence, J. R. Generating human intestinal tissue from pluripotent stem cells in vitro. *Nat Protoc* **6**, 1920-1928, doi:10.1038/nprot.2011.410 (2011).

108   Dye, B. R. *et al.* A bioengineered niche promotes in vivo engraftment and maturation of pluripotent stem cell derived human lung organoids. *eLife* **5**, e19732, doi:10.7554/eLife.19732 (2016).

109   Dye, B. R. *et al.* In vitro generation of human pluripotent stem cell derived lung organoids. *eLife* **4**, e05098, doi:10.7554/eLife.05098 (2015).

110   Finkbeiner, S. R. *et al.* Generation of tissue-engineered small intestine using embryonic stem cell-derived human intestinal organoids. *Biology Open* **4**, 1462-1472, doi:10.1242/bio.013235 (2015).

111   Gerbe, F., Brulin, B., Makrini, L., Legraverend, C. & Jay, P. DCAMKL-1 expression identifies Tuft cells rather than stem cells in the adult mouse intestinal epithelium. *Gastroenterology* **137**, 2179-2180; author reply 2180-2171, doi:10.1053/j.gastro.2009.06.072 (2009).

112   Leoni, G. *et al.* Annexin A1–containing extracellular vesicles and polymeric nanoparticles promote epithelial wound repair. *The Journal of Clinical Investigation* **125**, 1215-1227, doi:10.1172/JCI76693 (2015).

113   Jang, B. G. *et al.* Distribution of intestinal stem cell markers in colorectal precancerous lesions. *Histopathology* **68**, 567-577, doi:10.1111/his.12787 (2016).

114   Besson, D. *et al.* A Quantitative Proteomic Approach of the Different Stages of Colorectal Cancer Establishes OLFM4 as a New Nonmetastatic Tumor Marker. *Molecular & Cellular Proteomics : MCP* **10**, M111.009712, doi:10.1074/mcp.M111.009712 (2011).

115   van der Flier, L. G., Haegebarth, A., Stange, D. E., van de Wetering, M. & Clevers, H. OLFM4 Is a Robust Marker for Stem Cells in Human Intestine and Marks a Subset of Colorectal Cancer Cells. *Gastroenterology* **137**, 15-17, doi:http://dx.doi.org/10.1053/j.gastro.2009.05.035 (2009).

116   Barker, N. *et al.* Identification of stem cells in small intestine and colon by marker gene Lgr5. *Nature* **449**, 1003-1007, doi:http://www.nature.com/nature/journal/v449/n7165/suppinfo/nature06196_S1.html (2007).

117   Kita-Matsuo, H. *et al.* Lentiviral Vectors and Protocols for Creation of Stable hESC Lines for Fluorescent Tracking and Drug Resistance Selection of Cardiomyocytes. *PLoS ONE* **4**, e5046, doi:10.1371/journal.pone.0005046 (2009).

118   Leslie, J. L. *et al.* Persistence and Toxin Production by Clostridium difficile within Human Intestinal Organoids Result in Disruption of Epithelial Paracellular Barrier Function. *Infection and Immunity* **83**, 138-145, doi:10.1128/IAI.02561-14 (2015).

119   Lelongt, B. & Ronco, P. Role of extracellular matrix in kidney development and repair. *Pediatric Nephrology* **18**, 731-742, doi:10.1007/s00467-003-1153-x (2003).

120   Liu, Y. *et al.* Coordinate integrin and c-Met signaling regulate Wnt gene expression during epithelial morphogenesis. *Development (Cambridge, England)* **136**, 843-853, doi:10.1242/dev.027805 (2009).

121   Lucy Erin, O., Brien, Mirjam, M. P. Z. & Keith, E. M. Building epithelial architecture: insights from three-dimensional culture models. *Nature Reviews Molecular Cell Biology* **3**, 531, doi:10.1038/nrm859 (2002).

122   Lo, A., Mori, H., Mott, J. & Bissell, M. Constructing Three-Dimensional Models to Study Mammary Gland Branching Morphogenesis and Functional Differentiation. *Journal Of Mammary Gland Biology And Neoplasia* **17**, 103-110, doi:10.1007/s10911-012-9251-7 (2012).

123   Sakurai, H., Barros, E., Tsukamoto, T., Barasch, J. & Nigam, S. An in vitro tubulogenesis system using cell lines derived from the embryonic kidney shows dependence on multiple soluble growth factors. *Proceedings of the National Academy of Sciences, USA* **94**, 6279-6284 (1997).

124   Chen, D. *et al.* Differential expression of collagen- and laminin-binding integrins mediates ureteric bud and inner medullary collecting duct cell tubulogenesis. *American Journal of Physiology-Renal Physiology* **287**, F602-F611, doi:10.1152/ajprenal.00015.2004 (2004).

125   Weber, H. M., Tsurkan, M. V., Magno, V., Freudenberg, U. & Werner, C. Heparin-based hydrogels induce human renal tubulogenesis in vitro. *Acta Biomaterialia* **57**, 59-69, doi:https://doi.org/10.1016/j.actbio.2017.05.035 (2017).

126   Montesano, R., Schaller, G. & Orci, L. Induction of epithelial tubular morphogenesis in vitro by fibroblast-derived soluble factors. *Cell* **66**, 697-711, doi:10.1016/0092-8674(91)90115-F.

127   Cruz-Acuña, R. *et al.* Synthetic hydrogels for human intestinal organoid generation and colonic wound repair. doi:10.1038/ncb3632 (2017).

128   Riggins, K. S. *et al.* MT1-MMP-mediated basement membrane remodeling modulates renal development. *Experimental Cell Research* **316**, 2993-3005, doi:https://doi.org/10.1016/j.yexcr.2010.08.003 (2010).

129   Patterson, J. & Hubbell, J. A. Enhanced proteolytic degradation of molecularly engineered PEG hydrogels in response to MMP-1 and MMP-2. *Biomaterials* **31**, 7836-7845, doi:https://doi.org/10.1016/j.biomaterials.2010.06.061 (2010).

130   Turk, B. E., Huang, L. L., Piro, E. T. & Cantley, L. C. Determination of protease cleavage site motifs using mixture-based oriented peptide libraries. *Nature Biotechnology* **19**, 661, doi:10.1038/90273 (2001).

131   Zent, R. *et al.* Involvement of Laminin Binding Integrins and Laminin-5 in Branching Morphogenesis of the Ureteric Bud during Kidney Development.

Developmental Biology **238**, 289-302, doi:https://doi.org/10.1006/dbio.2001.0391 (2001).

132   Zhang, X. *et al.* β1 integrin is necessary for ureteric bud branching morphogenesis and maintenance of collecting duct structural integrity. *Development* **136**, 3357 (2009).

133   de Lemos Barbosa, C. M. *et al.* Regulation of CFTR Expression and Arginine Vasopressin Activity Are Dependent on Polycystin-1 in Kidney-Derived Cells. *Cellular Physiology and Biochemistry* **38**, 28-39 (2016).

134   Pohl, M., Sakurai, H., Bush, K. T. & Nigam, S. K. Matrix metalloproteinases and their inhibitors regulate in vitro ureteric bud branching morphogenesis. *American Journal of Physiology-Renal Physiology* **279**, F891-F900, doi:10.1152/ajprenal.2000.279.5.F891 (2000).

135   Clevers, H. Modeling Development and Disease with Organoids. *Cell* **165**, 1586-1597, doi:http://dx.doi.org/10.1016/j.cell.2016.05.082 (2016).

136   Miller, A. J. *et al.* In Vitro Induction and In Vivo Engraftment of Lung Bud Tip Progenitor Cells Derived from Human Pluripotent Stem Cells. *Stem Cell Reports* **10**, 101-119, doi:10.1016/j.stemcr.2017.11.012 (2017).

137   Lancaster, M. A. & Knoblich, J. A. Generation of Cerebral Organoids from Human Pluripotent Stem Cells. *Nature protocols* **9**, 2329-2340, doi:10.1038/nprot.2014.158 (2014).

138   Nakano, T. *et al.* Self-Formation of Optic Cups and Storable Stratified Neural Retina from Human ESCs. *Cell Stem Cell* **10**, 771-785, doi:10.1016/j.stem.2012.05.009.

139   Takasato, M., Er, P. X., Chiu, H. S. & Little, M. H. Generation of kidney organoids from human pluripotent stem cells. *Nature Protocols* **11**, 1681, doi:10.1038/nprot.2016.098 (2016).

140   Watson, C. L. *et al.* An in vivo model of human small intestine using pluripotent stem cells. *Nat Med* **20**, 1310-1314, doi:10.1038/nm.3737 (2014).

141   Broutier, L. *et al.* Culture and establishment of self-renewing human and mouse adult liver and pancreas 3D organoids and their genetic manipulation. *Nature Protocols* **11**, 1724, doi:10.1038/nprot.2016.097

       https://www.nature.com/articles/nprot.2016.097#supplementary-information (2016).

142   Miyoshi, H. & Stappenbeck, T. S. In vitro expansion and genetic modification of gastrointestinal stem cells in spheroid culture. *Nature Protocols* **8**, 2471, doi:10.1038/nprot.2013.153

https://www.nature.com/articles/nprot.2013.153#supplementary-information (2013).

143   Gjorevski, N. *et al.* Designer matrices for intestinal stem cell and organoid culture. *Nature* **539**, 560-564, doi:10.1038/nature20168 (2016).

144   Weaver, J. D. *et al.* Vasculogenic hydrogel enhances islet survival, engraftment, and function in leading extrahepatic sites. *Science Advances* **3**, doi:10.1126/sciadv.1700184 (2017).

145   Brückner, M. *et al.* Murine Endoscopy for In Vivo Multimodal Imaging of Carcinogenesis and Assessment of Intestinal Wound Healing and Inflammation. *Journal of Visualized Experiments : JoVE*, 51875, doi:10.3791/51875 (2014).

146   Garcia, J. R. *et al.* A Minimally Invasive, Translational Method to Deliver Hydrogels to the Heart Through the Pericardial Space. *JACC: Basic to Translational Science* (2017).

147   Levit, R. D. *et al.* Cellular Encapsulation Enhances Cardiac Repair. *Journal of the American Heart Association* **2** (2013).

148   Gjorevski, N. & Lutolf, M. P. Synthesis and characterization of well-defined hydrogel matrices and their application to intestinal stem cell and organoid culture. *Nature protocols* **12**, 2263 (2017).

149   Lu, P., Takai, K., Weaver, V. M. & Werb, Z. Extracellular Matrix Degradation and Remodeling in Development and Disease. *Cold Spring Harbor perspectives in biology* **3**, 10.1101/cshperspect.a005058 a005058, doi:10.1101/cshperspect.a005058 (2011).

150   Greiner, D. L., Hesselton, R. A. & Shultz, L. D. SCID Mouse Models of Human Stem Cell Engraftment. *STEM CELLS* **16**, 166-177, doi:doi:10.1002/stem.160166 (1998).

151   Noble, J. E. & Bailey, M. J. A. in *Methods in Enzymology* Vol. 463 (eds Richard R. Burgess & Murray P. Deutscher) 73-95 (Academic Press, 2009).